Linking Canopy Reflectance and Plant Functioning through Radiative Transfer Models

Zur Erlangung des akademischen Grades eines

Doktors der Naturwissenschaften

von der Fakultät für Bau-, Geo- und Umweltwissenschaften

des Karlsruher Institut für Technologie (KIT)

genehmigte

Dissertation

von

Teja Kattenborn

aus Freiburg

Karlsruhe, 2018

Tag der mündlichen Prüfung:	06. Dezember 2018
Referent:	Prof. Dr. Sebastian Schmidtlein
Korreferent:	Prof. Dr. Carsten Dormann

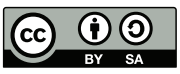

Acknowledgements

At first, I would like to express my gratitude to those people that inspired and supported me along my scientific career and thereby provided the elementary foundation for this thesis, amongst others Barbara Koch, Gerd Hildebrandt, Wolf Forstreuter, Angela Paredes, Fabian Fassnacht, Hans Heese, Sophie Reinecke and Claus-Peter Gross.

Regarding the preparation of this thesis I want to express my special gratitude to Sebastian Schmidtlein and Carsten Dormann. Sebastian Schmidtlein not only introduced me to the field of plant functioning, strategies and traits, the main foundations of this thesis, but also taught me the importance of performing thorough scientific work (contrasting the 'publish or perish' trend). Carsten Dormann introduced me to the the realm of statistics and environmental modelling and was always prepared to provide essential ecological and statistical advice.

Furthermore, I wish to thank the professors who spent their valuable time as members of my thesis defence commission, namely Hannes Feilhauer and Stefan Hinz.

Many thanks to the vegetation group of the Institute of Geography and Geoecology for fruitful conversations and discussions about scientific and everyday topics and the very pleasant environment. Many thanks to Rita Seith for preserving me from as many administrative tasks as possible. Likewise, I am very obliged for the support of Reiner Gebhardt regarding lab-analysis, instruments and IT-hardware. A large part of the data analysed within the framework of this thesis could not have been acquired without the generous support of Prof. Peter Nick and the employees of botanical garden of the Karlsruher Institute for Technology (KIT), who for two years regularly and carefully looked after my 120 potted weeds. In this regard special thanks to Christine Beier for sharing her profound knowledge on plant cultivation. A big thanks goes to the students who helped acquiring and analysing the enormous amount of trait data,

especially to Florence Gerard, Felix Schiefer, Denis Debroize, Jorge Petry, Daniel Ensslin and Sonja Hilpert.

In memory of productive and inspiring research activities including conference visits, field trips and summer schools, I would like to express my gratitude to the graduate school GRACE, in particular to Andreas Schenk, for financial and logistic support. Relating thereto I want to thank all the people that made these trips that exciting, including Jaime Hernandez, Tobias Schmidt, Javier Lopatin, Rocio Araya, Michael Ewald, Jana Eichel, Daniel Draebing, Çağlar Küçük, Herve Damlamian, Mereoni Ketewai, Julian Carbezas, Susan Wiser and Larry Burrows. I also wish to thank Jaennine Cavender-Bares, Anna Schweiger, Pieter Beck, Pablo Zarco-Tejada and Guido Schmuck for the very inspiring and fruitful research visits at the University of Minnesota (USA) and the JRC (Italy), respectively.

The biggest debt of gratitude goes to my parents, who never commanded me what career to choose, but instead always supported me on the path I chose. Last but not least, I want to give my infinite thanks to Anna Kranzer who accompanied and supported me during the highs and lows of my doctoral studies and beyond.

Contents

Summary

From tropics to tundra plant life diversified on the basis of adaptations to the local environmental conditions. These adaptations are manifested in the functioning of plants, which among others includes growth, reproduction, competitive abilities or persistence. Plant functioning not only directly relates to community assembly, but also to large scale processes, such as biosphere-atmosphere interactions or nutrient cycles. Accordingly, many research efforts have been devoted to further understand and characterize plant functioning, e.g. by developing universal models describing plant functioning or to assess the potential of individual plant traits as proxies for plant functions.

Despite recent scientific advances a complete picture of earth's plant functional diversity, in terms of geographic and functional coverage, is missing. This is fundamentally owed to the complexity and logistic constraints to measure plant functioning in the field. To complete this picture optical earth observation data is ascribed a high potential. Optical earth observation sensors measure the solar radiance reflected by plant canopies, which is affected by various biochemical and structural plant traits (onwards 'optical traits', e.g. leaf chlorophyll content or leaf angles). Interception and absorption of solar radiation by canopies is the foundation for a plants metabolism, which implies that the relevant optical traits directly relate to plant functioning. However, optical traits have not been systematically linked to plant functioning and likewise the relationship between plant functioning and canopy reflectance is not yet fully understood. The physical basis of light interacting with optical plant traits is formulated in radiative transfer models (RTM) of plant canopies. RTM can be considered as process-based models which can model the directional reflectance of a plant canopy as a function of several plant traits, the soil background and the sun-sensor geometry. The aim and innovative point of this thesis was to use

RTM to understand and harness the causal links between canopy reflectance and plant functioning. It was shown that that bridging canopy reflectance and plant functioning through radiative transfer models provides several merits to the field of remote sensing of plant functioning:

Firstly, RTM enable to map differences in plant functioning. In a case study it was shown that a RTM inversion using hyperspectral data can be used to generate maps of optical traits without requiring field data for calibration. The trait maps are in agreement with trait expressions from independent data bases and reflect the ecological gradients measured in the field. This suggests that RTM inversions can be considered as a highly transferable technique to produce spatial maps of traits as proxies for differences in plant functioning. Yet, the implementation of RTM inversions is complex and requires in-depth knowledge about the principles of radiative transfer and the vegetation characteristics under study.

Secondly, RTM allow to assess the causal links between plant functioning and canopy reflectance. Here, simulated canopy spectra derived from a RTM were used to assess the contribution of the optical traits to the spectral differences among plant functional types and the relevant spectral features. The results revealed the dominant plant traits and the respective spectral features that allow to spectrally discern differences in plant functioning. Moreover, it was demonstrated that simulations based on RTMs can overcome limitations of case studies and allow to gain universal knowledge on the interrelationships of plant functioning, plant traits and canopy reflectance. Such knowledge provides the basis to develop and improve sensors and algorithms for the remote sensing of plant functioning.

Thirdly, RTM and the optical traits incorporated therein expand our possibilities to understand and quantify differences in plant functioning. Using in-situ measured trait expressions it was shown that the traits incorporated in RTM are causally linked to primary plant functions. This in turn implies that canopy reflectance directly relates to plant functioning (‘reflectance follows function’). Moreover, it was found that the optical trait space partly shows comparable or even higher correlations to the assessed plant functional gradients than those plant traits that are commonly used in plant ecology. Accordingly, RTM provide an alternate perspective and a set of traits to characterize and quantify differences in plant functioning. These traits can thus serve as an valuable supplement or even alternative to traits commonly used in plant ecology.

In summary, this thesis demonstrates that RTM can increase capabilities to understand, quantify and monitor earth's functional diversity and points out the potentials for future research.

Zusammenfassung

Von den Tropen bis zur Tundra hat sich die Pflanzenwelt durch Anpassungen an lokale Umwelteinflüsse diversifiziert. Diese Anpassungen sind in der Funktionsweise der Pflanzen manifestiert, welche unter anderem Wachstum, Fortpflanzung, Konkurrenzfähigkeit oder Ausdauer beinhalten. Pflanzenfunktionen haben nicht nur direkten Einfluss auf die Artenzusammensetzung, sondern auch auf großräumige Prozesse wie Bio- und Atmosphäreninteraktionen oder Stoffkreisläufe. Folglich wurden viele Forschungsanstrengungen unternommen um Pflanzenfunktionen weiter zu verstehen und zu erfassen, z.B. darauf abzielend generalisierende Modelle von Pflanzenfunktionen zu entwickeln oder individuelle Pflanzenmerkmale als Indikatoren für Pflanzenfunktion zu identifizieren. Trotz der wissenschaftlichen Fortschritte fehlt ein vollständiges Bild der Funktionsvielfalt der Pflanzenwelt, sowohl in geographischer als auch funktioneller Hinsicht. Dies ist im Wesentlichen auf die Komplexität und die logistischen Einschränkungen bei der Messung von Pflanzenfunktionen im Feld zurückzuführen. Um dieses Bild zu vervollständigen wird insbesondere optischen Erdbeobachtungsdaten ein hohes Potenzial zugeschrieben. Optische Erdbeobachtungssensoren erfassen das vom Kronendach reflektierte Sonnenlicht. Letzteres wird durch verschiedene biochemische und strukturelle Pflanzenmerkmale (im Folgenden optische Merkmale) beeinträchtigt (z.B. Blattchlorophyllgehalt oder Blattinkel). Das Abfangen und Absorbieren von Sonnenlicht ist die Grundlage des pflanzeneigenen Metabolismus und folglich liegt es Nahe, dass diese optischen Merkmale direkt mit Pflanzenfunktionen zusammenhängen. Der Zusammenhang dieser optische Merkmale mit Pflanzenfunktionen wurde jedoch noch nicht systematisch untersucht, und ebenso ist der Zusammenhang zwischen Pflanzenfunktion und Kronendachreflektion noch nicht vollständig untersucht.

Die physikalischen Interaktionen von Licht und optischen Pflanzenmerkmalen sind bereits hinreichend verstanden und in Strahlungstransfermodellen (RTM) für Vegetationskronendächer formuliert. RTM können als prozessbasierte Modelle betrachtet werden, die die Reflektion des Kronendachs in Abhängigkeit von optische Merkmalen, dem Bodenhintergrund und der Sonnen-Sensorgeometrie modellieren. Das Ziel und die Innovation dieser Dissertation war die kausalen Zusammenhänge zwischen Kronendachreflektion und Pflanzenfunktion mittels RTM zu verstehen und zu nutzen. Es wurde gezeigt, dass für die Fernerkundung von Pflanzenfunktionen die Kopplung von Kronendachreflektion und Pflanzenfunktionen durch RTM mehrere Potentiale bietet:

Erstens, ermöglichen RTM die Kartierung von Pflanzenmerkmalen. Innerhalb einer Fallstudie wurde gezeigt, dass eine Inversion von RTM mit hyperspektralen Daten eine Kartierung von optischen Merkmalen erlaubt, für die keine Felddaten zur Modellkalibrierung benötigt werden. Die kartierten Merkmale zeigten eine hohe Übereinstimmung mit Merkmalsausprägungen aus unabhängigen Datenbanken und spiegelten die im Feld gemessenen ökologischen Gradienten wider. Dies deutet darauf hin, dass RTM-Inversion als äußerst übertragbare Methode betrachtet werden kann, um räumliche Karten von Pflanzenmerkmalen zu erstellen, die als Proxies für Pflanzenfunktionen dienen können. Allerdings erfordert die Implementierung von RTM Inversionen fundierte Kenntnisse über die Prinzipien der Strahlentransfermodellierung und der zu untersuchenden Vegetationscharakteristiken.

Zweitens, ermöglichen RTM die Untersuchung von Zusammenhängen zwischen Pflanzenfunktion und der Kronendachreflektion. In der vorliegenden Thesis wurden simulierte Kronendachspektren aus einem RTM verwendet, um den Beitrag der optischen Merkmale zu den spektralen Unterschieden zwischen Pflanzenfunktionstypen zu erfassen. Die Ergebnisse zeigten die dominanten Pflanzenmerkmale und die entsprechenden spektralen Charakteristiken die für eine fernerkundliche Unterscheidung der Pflanzenfunktion von großer Relevanz sind. Darüber hinaus wurde gezeigt, dass RTM-basierte Simulationen Einschränkungen von Fallstudien kompensieren und Kenntnisse über die Zusammenhänge von Pflanzenfunktionen, Pflanzeneigenschaften und Kronendachtreflektion erweitern können. Diese Kenntnisse bilden die Grundlage

für die Entwicklung und Verbesserung von Sensoren und Algorithmen zur Fernerkundung von Pflanzenfunktionen.

Drittens, erweitern RTM und die darin enthaltenen optischen Merkmale unsere Möglichkeiten Unterschiede in der Pflanzenfunktion zu verstehen und zu quantifizieren. Mit Hilfe von in-situ gemessenen Merkmalsausprägungen konnte gezeigt werden, dass die in RTM enthaltenen optischen Merkmale kausal mit primären Pflanzenfunktionen zusammenhängen. Dies wiederum bedeutet, dass die Reflexion des Kronendachs unmittelbar mit den primären Funktionen der Pflanze zusammenhängt ('Reflektion folgt Funktion'). Darüber hinaus wurde festgestellt, dass optische Merkmale vergleichbare oder sogar höhere Korrelationen mit den verwendeten pflanzlichen Funktionsgradienten aufweisen als die in der Pflanzenökologie üblich verwendeten Merkmale. Entsprechend bieten RTM sowohl eine alternative Perspektive als auch ein Set von Pflanzenmerkmalen mit denen Unterschiede der Pflanzenfunktion charakterisiert und quantifiziert werden können. Diese Merkmale können somit als wertvolle Ergänzung oder Alternative zu den in der Pflanzenökologie üblichen Merkmalen dienen.

Zusammengefasst zeigt diese Thesis, dass RTM unsere Möglichkeiten erweiterten können die funktionelle Vielfalt der globalen Vegetationsbedeckung weiter zu verstehen und zu erfassen und führt zukunftsrelevante Forschungspotentiale auf.

List of Publications

1. Kattenborn, T., Fassnacht, F. E., Pierce, S., Lopatin, J., Grime, J. P. & Schmidtlein, S. (2017). Linking plant strategies and plant traits derived by radiative transfer modelling. *Journal of Vegetation Science*, 28(4), 717-727.

2. Kattenborn, T., Fassnacht, F. E. & Schmidtlein, S. (2018). Differentiating plant functional types using reflectance: which traits make the difference? *Remote Sensing in Ecology and Conservation*.

3. Kattenborn, T. & Schmidtlein, S. (submitted). Radiative transfer modelling reveals why canopy reflectance follows function. *Nature Communications*.

4. Kattenborn, T., Schiefer, F., Zarco-Tejada, P. & Schmidtlein, S. (in review). Remote sensing leaf photosynthetic pigments as concentration [%] is flawed and should be quantified as content [µg/cm^2] instead. *Remote Sensing of Environment*

The content and structure of the included publications were kept in the form of the original publications or submissions, respectively.

List of Figures

List of Tables

Acronyms and Abbreviations

ALA	Average Leaf Angle
Ant	Leaf anthocyannin content
Appx	Appendix
BMWi	German Federal Ministry of Economics and Technology
Cab	Leaf chlorophyll content
Car	Leaf carotenoid content
Cbrown	Brown pigment content (PROSPECT coefficient)
Cm	Leaf dry matter content, synonymous to Leaf Mass per Area (LMA)
CSR	Competitor, Stress-tolerator, Ruderal plant strategy theory (Grime 1988)
Cw	Equivalent water thickness, synonymous to leaf water content
DLR	German Aerospace Center
EnMap	German Hyperspectral satellite mission by DLR (Stuffler et al. 2007)
fAPAR	fraction of Absorbed Photosynthetic Active Radiation
FLIGHT	Radiative transfer model for tree canopies (North 1996)
GAM	Generalized Additive Models (Wood 2003)
HyspIRI	US Hyperspectral satellite mission by NASA (Roberts et al. 2012)
hot	hot spot parameter (Kuusk 1991)
INFORM	Radiative transfer model for tree canopies (Atzberger 2000)
JRC	Joint Research Centre of the European Commission
LAI	Leaf Area Index
LES	Leaf Economic Spectrum (Wright et al. 2004)
LiDAR	Light Detection and Ranging

LIDF	Leaf Angle Distribution Function
LUT	Lookup table
MRPP	Multi Response Permutation Procedure
N / N_{meso}	Mesophyll structure coefficient
NIR	Near-Infrared wavelengths
NRMSE	Normalized Root Mean Squared Error
PAR	Photosynthetic Active Radiation
PCA	Principal Component Analysis
PFT	Plant Functional Type
PLSR	Partial Least Squares Regression
PROSPECT	Leaf radiative transfer model (Feret et al. 2017)
PROSAIL	Canopy radiative transfer model coupling PROSPECT and SAIL
psi	Relative azimuth angle
RADAR	RAdio Detection And Ranging
R	Coefficient of determination
r	Pearson's / Spearman's correlation coefficient
RF	Random Forest algorithm (Breiman 2001)
r/K	r-K selection model, including rate (r) and capacity (K) (MacArthur et al. 1972)
RMSE	Root Mean Squared Error
RTM	Radiative Transfer Model
SAIL	Scattering by Arbitrary Inclined Leaves (Verhoef and Bach 2007)
SAR	Synthetic Aperture RADAR
SLA	Specific Leaf Area
SVM	Support Vector Machines
SWIR	Short Wave Infrared wavelengths
tts	Sun zenith angle
tto	Sensor zenith angle
VIS	Visible spectrum wavelengths

1 Introduction and Motivation

1.1 Generalizations of plant functioning through traits, types and strategies

Of all the possible pathways of disorder, nature favors just a few.

(James Gleick, 1987)

Throughout evolution plants diversified as a result of adaptations to abiotic environmental factors, e.g. nutrient availability, temperature or solar radiation, as well as biotic interactions, e.g. competition, herbivory or pests (Darwin and Wallace 1858; Grime 1988). This diversity of adaptations is reflected through a wide spectrum of functional differences among plants, affecting transpiration, photosynthesis, reproduction, maintenance or growth. Various independent research groups tried to identify general features and major tendencies among the various plant functions in order to understand properties and dynamics of natural ecosystems and how they relate to abiotic and biotic environmental factors. Early attempts to characterize species and vegetation communities by their functioning include their classification into plant functional types (or groups), including life-form categories or guilds (von Humboldt 1806; Braun-Blanquet et al. 1932; Raunkiaer 1934; Root 1967). Until today various PFT schemes were developed to generalize variations in plant functions, whereas their degree of complexity and layout depends on the purpose at hand (Díaz and Cabido 1997; Lavorel et al. 1997). The basis for the allocation of species towards such groups are often differences in physiological (e.g. C3, C4 or CAM metabolism), morphological (e.g. growth form) or phenological (e.g. decideous vs. evergreen) plant characteristics. PFT classifications are widely used in biogeographical models to

assess the distribution and dynamics of plant functioning as well as in earth system models to paramtrize biosphere-atmosphere interactions (Sellers et al. 1997; Smith et al. 1997; Kucharik et al. 2000; Dormann and Woodin 2002). However, it was argued by several authors that PFT schemes do not adequately represent the patterns and functional variability of natural vegetation communities, due to inter alia the following reasons: 1) Patterns of plant communities are often characterized by gradients rather than discrete boundaries. 2) PFT classifications do not necessarily account for intra-specific variation of functional characteristics (e.g. plasticity). 3) Information on species or functional diversity within PFT classes is lost (Dormann and Woodin 2002; Reich 2014; van Bodegom et al. 2014; Reichstein et al. 2014; Wullschleger et al. 2014). Correspondingly, characterizing plant functioning on a continues scale rather than by discrete classes attracted increasing attention during the last decades (Hodgson et al. 1999; Wright et al. 2004; McGill et al. 2006 Reich 2014; Díaz et al. 2015; Pierce et al. 2013; Pierce et al. 2017). Various rather inductive attempts were based on the global collection of extensive data sets compromising plant trait expressions of thousands of species and their subsequent statistical analysis. This rests on the fact that plant functions are expressed and controlled through differences in various biochemical and structural traits (Reich et al. 1997, Grime et al. 1997), which can thus be used as surrogates for the plant function of interest. Accordingly, these traits are commonly referred to as 'functional traits'. Yet, plant functions usually cannot be derived from individual trait expressions, as functions are usually a product of multiple coordinated traits. For instance the photosynthetic rate of a leaf depends inter alia on the rubisco content, chlorophyll content, CO_2 diffusion, internal water conduction, light interception of the leaf surface and light scattering within the leaf (Tucker and Sellers 1986; Field 1991; Guo et al. 2018). Accordingly, such data-driven approaches frequently assessed a broad range of plant traits, which were assumed to be most relevant to differentiate functional differences and patterns within and among species and across environmental gradients. Traits most frequently assessed include Specific Leaf Area (or its inverse Leaf Matter per Area, LMA), leaf nitrogen and phosphorus content (or concentration), nitrogen-phosphorus ratio, leaf photosynthetic capacity, dark respiration rate, Leaf Dry Matter Content (LDMC), Leaf Area, seed mass, seed size and canopy height. One of the most prominent studies resulting from these efforts is the Leaf Economic

Spectrum (LES, Wright et al. 2004), which was based on an ordination of various trait expressions derived from global observations reflecting leaf resource investments (such as mentioned above) in terms of nutrients, proteins and carbohydrates. The results indicate that these traits are highly correlated on a single axis (LES), ranging from fast and acquisitive growth (low resource investment) to slow and conservative growth (high resource investment and slow returns). The results were found to be relatively independent of growth form (herbs, graminoids, shrubs and trees) and latitude. Díaz et al. (2015) performed a similar but extended analysis, incorporating traits which not only represent leaf characteristics (such as in the LES), but also incorporating 'whole-plant traits', which reflect the size of plant organs such as leaf area, canopy height or seed size. The results of this analysis i.e. the 'Global Spectrum of Plant Form and Function', firstly confirmed the presence of the LES and secondly identified a further major axis of functional differences among species corresponding to the size of whole plants and their organs.

Besides such data-driven approaches, which are initially not based on a priori ecological theory, (Pierce and Cerabolini 2018), various authors developed conceptual and theoretical models to describe plant functional gradients in a rather deductive fashion. A landmark event was the formulation of the r/K selection (Pianka 1970; MacArthur et al. 1972) as a conceptual model for life history strategies aiming to describe the causes and effects of variation of life cycles among organisms. In brief, the r/K selection describes the trade-off among traits facilitating on the one hand a fast reproduction and growth and on the other hand traits enabling a long life expectancy and persistence (broadly speaking an analogous gradient to the Leaf Economic Spectrum found three decades latter based on extensive trait observations; Wright et al. 2004). The r/K dichotomy was inter alia used to conceptualize succession of plant communities, starting from colonization (r-selected species) and ending with climax vegetation (K-selection). The model assumes a gradient of increasing competition, were the carrying capacity (K) is defined by a density saturation. However, plants are not only selected by their competitive abilities, but also by their ability to maintain in the presence of abiotic pressures, which in turn decreases competition. Accordingly, J.P. Grime proposed the 3-dimensional CSR plant strategy theory (Grime 1974; Grime 1977). The latter assumes that competitive abilities (C) are selected on sites with optimal conditions for plant growth, which favour plants that can preempt resources through fast

vertical and lateral growth to overtop neighbours. Stress tolerant abilities (S) are advantageous in sites with high environmental pressures, e.g. low nutrient availability or extreme temperatures. In such conditions selection favours plants with robust tissues, slow and conservative growth. Ruderals abilities (R) are selected on sites with frequent disturbance events or biomass removal, as they feature a rapid completion of the life-cycle through fast and acquisitive growth and quick germination to ensure reproduction.

In early stages the CSR theory was frequently criticized as being non-transparent and hardly testable (Tilman 1985; Westoby 1998). Meanwhile, an alternate theory to describe resource competition was proposed by D. Tilman (resource-ratio hypothesis, Tilman 1985; Tilman 1988), resulting in a longstanding debate with Grime, as both authors had a very different perception and semantic of processes involving selection and community assembly (Grace 1991). Accordingly, increasing and longlasting efforts were made to validate and operationalize the CSR theory, including an intensive screening of 67 traits in 43 species of the British flora to validate the primary CSR axis (Grime et al. 1997). Hodgson et al. (1999) provided a more operational methodology to allocate CSR-scores of plant species based on 7 plant traits (e.g. canopy height, LDMC or lateral spread), which was tested across a wide range of the European herbaceous flora. These plant traits were selected as they are relatively easy to measure and as they were considered to be key traits for biophysical processes. Using a more extensive and global dataset consisting of grassland, shrub and tree species ,Pierce et al. (2017) demonstrated that CSR-scores can be quite accurately allocated by means of an ordination of only 3 traits, i.e. Leaf Area, Leaf Dry Matter Content (LDMC) and Leaf Mass per Area (LMA). The method was published together with a ready-to-use tool (‘strate-fly’), which enables to allocate CSR scores for a plant species or community by defining these 3 trait expressions. The fact that all procedures to allocate species to the CSR axis (Grime et al. 1997; Hodgson et al. 1999; Pierce et al. 2013; Pierce et al. 2017) incorporated firstly leaf resource investments (e.g. Leaf Dry Matter Content and Leaf Mass per Area) and secondly organ size (e.g. Leaf Area), suggests that the CSR model, which was initially based on ecological theory, and the data-driven global spectrum of plant form and function (Díaz et al. 2015) both explain the same fundamental gra-

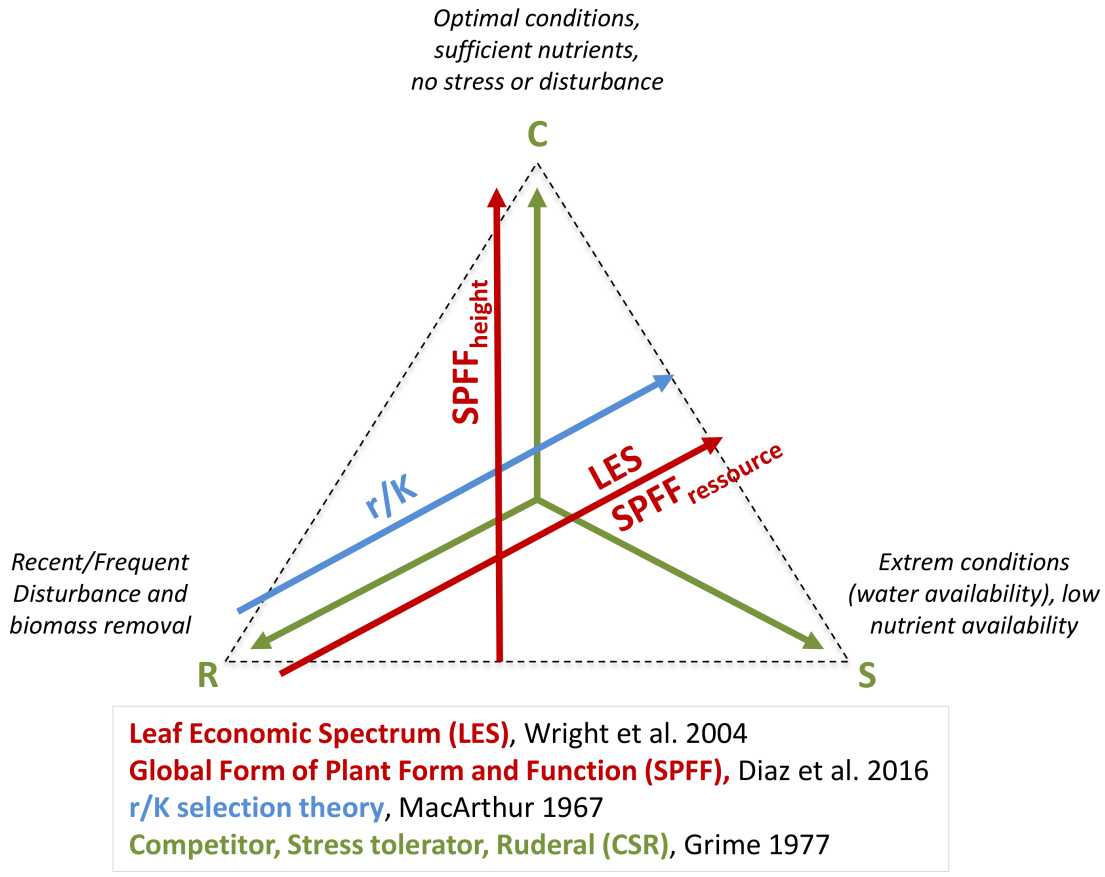

Figure 1.1: Schematic representation of the different functional schemes

dients in functioning (Fig. 1.1), i.e. leaf resource economics and plant size (Díaz et al. 2015; Pierce and Cerabolini 2018).

In summary, plant functioning reflects how plants are adopted to biotic and environmental factors. Various plant traits can be used as proxies for individual plant functions. Multiple plant functions and thus traits feature a coherence to two major functional axis, i.e. resource investments and plant size attributes (Fig. 1.1). Independent research groups generated vast progress identifying these patterns through both data-driven and theoretical models. This knowledge has direct implications for different fields of research, including earth system modelling such as biosphere atmosphere interactions, material and nutrient cycles, and ecological dynamics such as community assembly (Diaz and Cabido 2001; Lavorel and Garnier 2002; Bonan et al. 2002; Violle et al. 2014; Wright et al. 2004; Reichstein et al. 2014). Accordingly, there is a high demand on data of earth's functional diversity, not least because of accelerating global chance and respective monitoring efforts. However, in-situ measurements of plant functions or functional

traits are usually spatially restricted to point observations, are impaired by accessibility and involve enormous field and laboratory work. These constraints are further enhanced as most plant functions and traits show a strong variation within a plants phenology (Rathcke and Lacey 1985; Grime 2006). In-situ observations are therefore barely generalizable in a spatial context or scalable to large regional or global extents (Bini et al. 2006; Brito 2010; Kattge et al. 2011). In order to overcome these limitations various authors highlighted the capabilities of remote sensing from earth observation platforms (unmanned aerial vehicles, airplanes or satellites) to identify spatial and temporal patterns of plant functioning.

1.2 Remote sensing of plant functioning

Remote Sensing is ascribed a high potential for vegetation characterization, as it allows to characterize various physical properties of the earth surface, ranging from passive sensors systems using solar radiation as light source (within 400-2500 nm) to active systems such as SAR (Synthetic Aperture radars, typically in the microwave domain between 1 mm-1 m) or LIDAR data (typically 1000-1550 nm)(Hildebrandt 1996). Most potential towards mapping plant functioning from earth observation data is ascribed to satellite-based passive optical sensors, i.e. multispectral or hyperspectral sensors (Ustin and Gamon 2010; Homolová et al. 2013; Jetz et al. 2016). These sensors measure the reflected solar radiance [W/m^2] that is reflected from the earth surface. The measured radiance is typically normalized to reflectance [%], using simultaneously measured solar radiance or using a reference surface with known reflection. The ascribed potential of optical remote sensing for applications targeting plant functioning is based on two reasons. Firstly, satellite-based optical remote sensing sensors enable to track the optical reflectance of the earth's vegetation with a relatively high spatial and temporal resolution, which enables a spatially continuous characterization of plant canopies through time. Secondly, the reflectance of plant canopies is directly linked to structural and biochemical traits which determine light harvesting and thus the metabolism of a plant (Ustin and Gamon 2010).
Optical earth observation data for vegetation analysis is mainly restricted to 400-2500 nm. Below 400 nm solar irradiance (UV radiation) is strongly absorbed by Ozone (O_3), whereas above

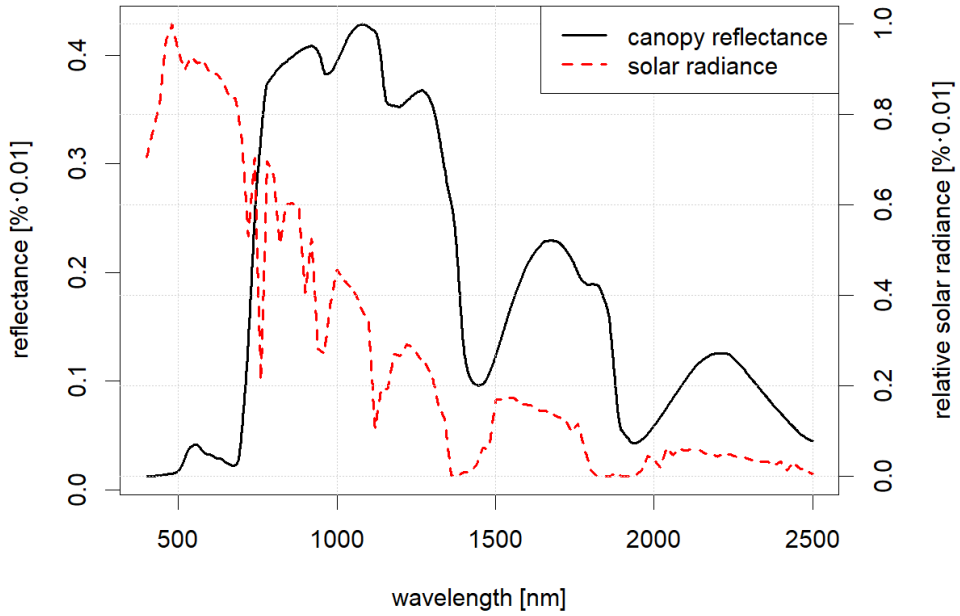

Figure 1.2: Exemplary canopy reflectance spectrum and relative solar radiance across the 400-2500 nm range.

2500 nm solar irradiance is very small and barely measurable (Fig. 1.2). Plants generally feature very characteristic reflectance signatures across 400-2500 nm, which is mainly shaped by the biochemical constituents of the leaves. In the visible range (VIS, 400-700 nm) the overall low reflectance is caused by pigments such as chlorophyll, carotenoids or anthocyanins absorbing the major part of the incident radiation. In near-infrared range (NIR, 700-1300 nm) absorption by leaf constituents is low and hence a large part of the radiation is reflected by the canopy components. In the shortwave infrared (SWIR, 1400-2500 nm) light is predominantly absorbed by dry matter constituents (proteins, lignin, carbohydrates and waxes) and water content. Water absorption is most strongest around 1400-1600 nm and 1800-2100 nm, which makes these regions less useful for vegetation analysis based on earth observation data, as the atmosphere is subject to short-term changes in water content.

The characteristic effects of biochemical and structural plant properties on the spectral properties of vegetation canopies hence allows to map patterns of plant traits, functions or PFT using remote sensing data. The most common approach for such tasks is the use of empirical models, including calibrated indexes (simple band ratios), regressions models or complex machine

learning algorithms (Baret and Guyot 1991; Haboudane et al. 2004; Baret and Buis 2008; Ustin and Gamon 2010; Homolová et al. 2013). Empirical approaches aim to establish statistical relationships between the retrieved spectral signal and vegetation characteristic of interest. Various studies reported accurate results for retrieving a wide range of plant traits, including nutrients (e.g. nitrogen or phosphorus concentrations), pigment contents and concentrations (e.g. chlorophyll content, carotenoids), leaf dry matter constituents (lignin, cellulose, carbohydrates), water content or Leaf Area Index (Homolová et al. 2013). Despite these promising capabilities, the application of empirical models for mapping plant functioning and traits has some clear limitations:

- With regard to mapping plant functions and PFT knowledge gain on the underlying processes is confined when using empirical models with canopy reflectance data. As described above canopy reflectance is the product of various optically relevant plant traits acting in overlapping wavelength regions. Empirical models can therefore hardly decouple the effects of these traits and thus do not disclose why it is actually possible to differentiate the functions or PFT at hand, i.e. what optical traits actually cause the differences in canopy reflectance (Van Cleemput et al. 2018).

- Not all of the above mentioned plant traits directly affect canopy reflectance (e.g. nitrogen, phosphorus or lignin), meaning that their retrieval relies on indirect correlations with those traits that in turn directly affect the radiative transfer (Grossman et al. 1996; Knyazikhin et al. 2013b; Knyazikhin et al. 2013a). This has important implications for the transferability and operationalization of such mapping procedures, as these indirect correlations may only exists in certain plant types, environmental conditions or phenological stages.

- The transferability and robustness of empirical algorithms largely depend on the representativeness and accuracy of the training data (commonly in-situ observations), which implies that a empirical model is presumably only robust for the extent of the sampled variation and the respective species or communities included in the training data (Dorigo et al. 2007). As mentioned in the previous chapter, the acquisition of in-situ data is

generally impaired by logistic constrains (costs, accessibility). This limitation is further exacerbated by differences in the spatial scale and reference of in-situ data (commonly discrete point observations) and remote sensing data (continuous representation of the landscape by often large sized pixels) (Turner 2014; Leitão et al. 2018).

- The transferability of remote sensing procedures based on empirical models is generally limited, as these models are also impaired by peculiarities of the remote sensing data, such as the sensor configuration (band designations) or the sun-sensor geometry during the data acquisition (Grossman et al. 1996; Colombo et al. 2003; Dorigo et al. 2007).

A promising alternative for empirical models with their above mentioned limitations is to link plant functioning and canopy reflectance through canopy radiative transfer models (RTM). RTM can be considered as physical or process-based models which describe the radiative transfer from the sun to the sensor as a function of those plant traits which explicitly affect absorption, transmission and scattering processes.

1.2.1 Bridging plant functioning and canopy reflectance through radiative transfer modelling

Canopy RTM were developed to model the physical processes of the radiative transfer, that is in brief the travel of direct solar radiation and diffuse radiation (light scattered within the atmosphere) within the plant canopy and to the sensor. The processes that determine the radiative transfer in the canopy are absorption (e.g. through photosynthetic pigments and other leaf constituents such as water), transmission (e.g. light travelling through the leaf) and scattering (e.g. reflection at the leaf surfaces or the ground) (Fig. 1.3). The signal that is measured with optical earth observation sensors is the solar radiation that is scattered towards the sensor.

The radiative transfer of plant canopies is commonly modelled by coupling two components, i.e. a leaf RTM and a canopy RTM (Fig. 1.5). The most widely used leaf RTM is PROSPECT (Jacquemoud and Baret 1990; Feret et al. 2017) which is based on the ‘plate model’ (Allen et al. 1969), that assumes a plant leaf as transparent plate composed of parallel surfaces. These parallel surfaces mimic the cellular arrangement in the mesophyll, in which a diffuse and isotropic

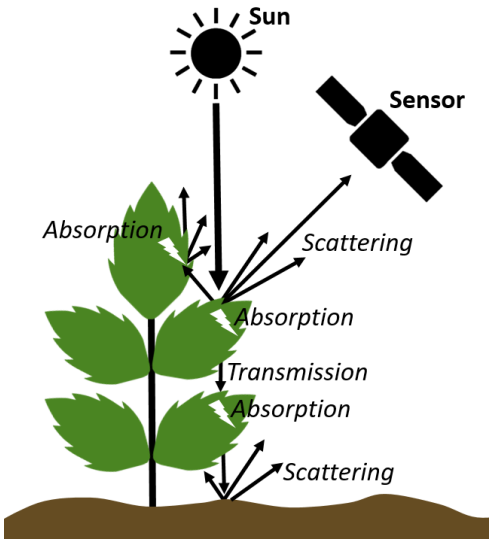

Figure 1.3: Scheme visualizing the fundamental processes of radiative transfer in plant canopies, i.e. transmission, absorption and scattering.

scattering of light is assumed (Mie-scattering). Increased thickness (i.e. number of surfaces) of the mesophyll layer (N) hence increases scattering within the leaf and thereby the chance of light being absorbed by leaf constituents which in turn reduces transmission. Absorption within the leaf is defined by multiple leaf constituents, i.e. pigments (chlorophylls, carotenoids, anthocyanins), water and dry matter, whereas each constituent is implemented by specific absorption coefficients in the wavelengths of 400 to 2500 nm (Fig. 1.4). The specific absorption coefficients were calibrated using 4 experimental datasets, i.e. LOPEX (Hosgood et al. 1995); CALMIT (Gitelson et al. 1998; Gitelson and Merzlyak 1998); ANGERS (Jacquemoud et al. 2003a); HAWAII (Asner and Martin, unpublished data).

The canopy RTM simulates the bidirectional reflectance distribution function (BRDF), which integrates the relative orientation of the sun, of the sensor and of the canopy, including its structural characteristics and leaf optical properties (e.g. derived from a leaf RTM). The most widely used canopy RTM is 4SAIL (from Scattering by Arbitarily Inclined Leaves, Verhoef 1985), which was validated in several studies, including the RAdiation transfer Model Intercomparison (RAMI-3, Widlowski et al. 2007) by the Join Research Centre (JRC, Ispra). 4SAIL represents the canopy as a turbid medium, assuming a homogenous distribution of identical and flat leaves, which act as perfect Lambertian diffusors with random azimuth angles (Verhoef 1985). The fraction of the irradiance being intercepted or scattered by leaves is determined by

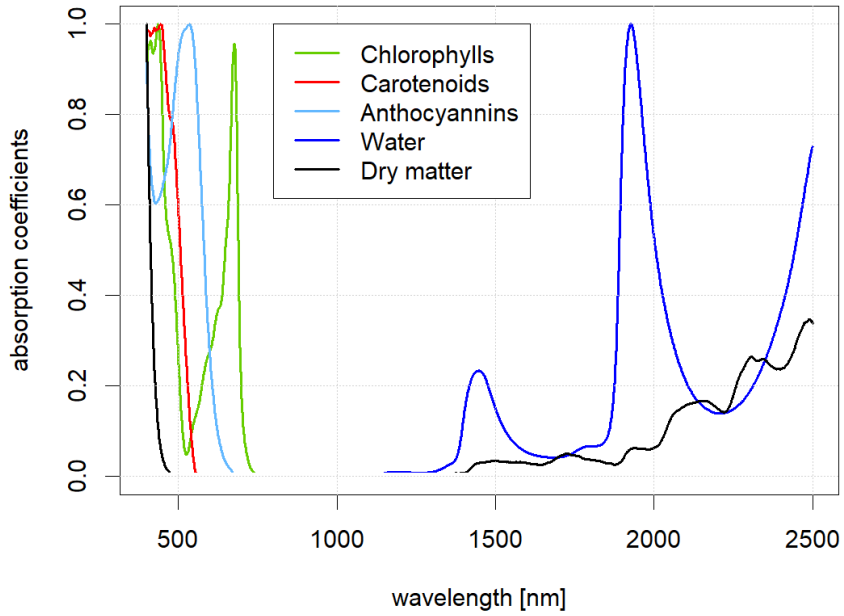

Figure 1.4: Absorption coefficients of leaf chlorophyll content [µg/cm^2], carotenoid content [µg/cm^2], anthocyanin content [µg/cm^2], leaf mass per area [g/cm^2], water content [g/cm^2]. For visualization purposes all absorption coefficients were scaled between 0-1.

the parametrization of the canopy, which is defined by Leaf area Index (LAI), Leaf Inclination Distribution Functions (LIDF) and was further supplemented with the hot spot effect (Kuusk 1991). The soil optical properties are incorporated through default soil reflectance spectra and can be exchanged with custom soil spectra (e.g. retrieved from a spectrometer). Given the assumptions in 4SAIL, its applicability is most robust for homogeneous canopies with one vegetation layer. As the analyses of this thesis are focused on homogeneous canopies, PROSAIL was considered as most appropriate. Heterogeneous canopy structures with variations in crown cover, structure and shape are considered in more complex canopy RTM such as in INFORM (Atzberger 2000) or FLIGHT (North 1996).

Coupling the leaf RTM PROSPECT and the canopy RTM 4SAIL, i.e. using leaf reflectance and transmittance from PROSPECT as input for 4SAIL, is commonly referred to as PROSAIL.

During the last decades PROSAIL was applied in hundreds of studies, covering a wide range of different applications (Jacquemoud et al. 2009; Berger et al. 2018). In various scientific contributions PROSAIL was used in 'forward mode', that is simulating vegetation reflectance

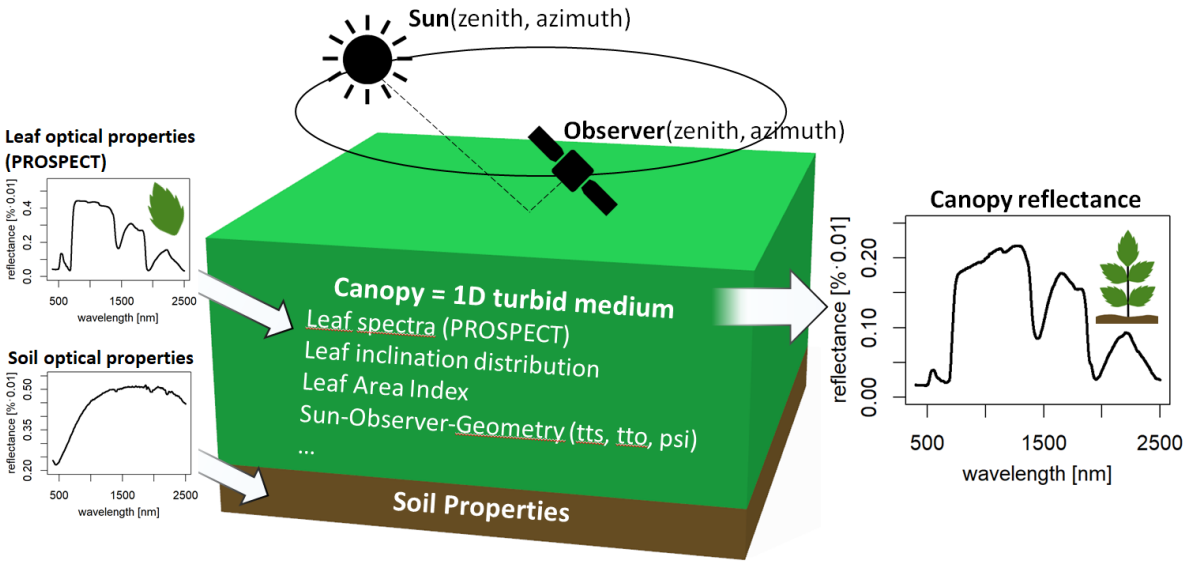

Figure 1.5: Scheme of PROSAIL, coupling the leaf RTM PROSPECT and the bidirectional reflectance model SAIL. Summaries of the PROSPECT and 4SAIL parameters are given in Tab. 1.1 and 1.2.

by defining the incorporated parameter space (Tab. 1.1 and 1.2). As described above canopy reflectance is the integrated product of various spectrally relevant factors (biophysical variables and sun-sensor geometry) which affect the radiative transfer in overlapping spectral regions. PROSAIL allows decoupling the effects of these factors on the canopy reflectance. Respective sensitivity analyses advanced the understanding on how the incorporated biophysical variables contribute to the variability in canopy reflectance. An important example are pioneering works on how LAI and chlorophyll contents shape the 'red edge' (the characteristic transition area from the visible red to near-infrared wavelengths (Baret et al. 1992; Broge and Leblanc 2001). PROSAIL advanced the development of several vegetation indexes, including indexes for the canopy gap fraction (Baret et al. 1995), chlorophyll content (Haboudane et al. 2002; Zarco-Tejada et al. 2004) and fuel moisture and water content (Zarco-Tejada et al. 2003; Bowyer and Danson 2004).

In contrast to the 'forward mode', PROSAIL was also frequently applied in the 'inverse mode', which is commonly referred to as 'inversion'. The rationale of this application is to use PROSAIL to estimate expressions of the incorporated plant traits from measured spectra (e.g. derived from an airborne or spaceborne platform), by comparing the measured spectra to simulated spectra derived from PROSAIL. In principle the inversion thus relies on simulating arti-

Table 1.1: Overview of the PROSPECT parameter space

Parameter	**Abbrev**	**Source and Description**
Chlorophyll a+b [µg cm^{-2}]	Cab	Pigments for photosynthesis
Carotenoids [µg cm^{-2}]	Car	Pigments for photosynthesis and photoprotection
Anthocyanins [µg cm^{-2}]	Ant	Pigments for photosynthesis and pathogen defence;
Equivalent water thickness [g cm^{-2}]	Cw	Leaf water content
Dry matter content [g cm^{-2}]	Cm	Proteins such as lignin, carbohydrates; in ecology referred to as Leaf Mass per Area (LMA) or its reciprocal Specific Leaf Area (SLA)
Mesophyll structure coefficient [ ]	N	Coefficient determining the thickness of the mesophyll layer
Brown pigment content [ ]	Cbrown	Parameter defining leaf content of woody debris and polyphenols (e.g. tannins)

Table 1.2: Overview of the 4SAIL parameter space

Parameter	**Abbrev**	**Source and Description**
Leaf Area Index [m^2 m^{-2}]	LAI	Projected area of leaf surfaces per area
Leaf Angle Distribution Function [ ]	LIDF	Distribution of leaf inclinations in the canopy, defined through either two parameters, i.e. LIDFa specifying the average slope and LIDFb the distribution bimodality or through one parameter, i.e. Average Leaf Angle (ALA)
Hotspot size [m m^{-1}]	hot	Describes the illumination variation determined by the relative alignment between sun and observer angle and the canopy structure; approximated through the ratio of leaf size to canopy height
Solar Zenith angle [°]	tss	Vertical angle between sun, canopy and the horizon
Observer Zenith angle [°]	tso	Vertical angle between sensor, canopy and the horizon
Relative Azimuth angle [°]	psi	Horizontal angle between sun, canopy and the sensor
Soil spectral properties	soil	Soil reflectance spectra or soil BRDF model

ficial spectra with a close correspondence to the measured spectra, whereas the estimated trait expressions equal to the parametrization of these simulations. Inversions procedures can be performed using several approaches, including lookup tables, iterative numerical optimization (e.g. through neural networks) or hybrid approaches, e.g. where a non-parametric non-linear regression model is calibrated using PROSAIL simulations and applied on measured reflectance data (Verrelst et al. 2016; Feilhauer et al. 2017; Berger et al. 2018). The different approaches differ in computation time, complexity and robustness. Most studies use the lookup table approach given its straight forward implementation, overall robustness and computation time (Berger et al. 2018).

Several studies inverted PROSAIL with multi- and hyperspectral remote sensing data to map the plant traits incorporated in PROSAIL (onwards also referred to as 'optical traits'), including inter alia chlorophyll content, LAI, canopy water content (LAI · Cw), leaf water content, dry matter content, foliar biomass (LAI · Cm) (Darvishzadeh et al. 2008; Atzberger et al. 2015; Trombetti et al. 2008; Casas et al. 2014; Feilhauer et al. 2017; Feilhauer et al. 2018). The retrieval of these parameters firstly depends on the complexity of the vegetation under investigation. Increasing variability of the plant traits increases the ill-posed problem, as multiple parametrizations of PROSAIL can result in very similar reflectance spectra. Secondly, the retrieval of the PROSAIL trait space depends on the magnitude of the spectral variability caused by a trait. It can for instance be assumed that chlorophyll content or LAI can be retrieved relatively accurate from inversions, whereas those leaf constituents that cause a comparably low spectral variability are less accurately retrieved (Feilhauer et al. 2017; Berger et al. 2018).

1.3 Aims and structure of the thesis

As summarized above, RTM and in particular PROSAIL have been widely applied to understand interactions between plant traits and canopy reflectance as well as to derive spatially continuous maps of these traits through model inversions and optical earth observation data. Accordingly, various authors suggested a high potential of RTM for functional plant ecology (Jacquemoud et al. 2009; Ustin and Gamon 2010; Homolová et al. 2013). However, until now RTM have received little attention in the context of established ecological theories, i.e. plant strategies, plant functional types or primary gradients of plant functioning (Chapter 1.1).

At the same time various functions of aboveground plant organs are directly designed and tailored to ensure and maximize the energy acquisition from solar radiation throughout a plants life. As described above RTM model this very process, i.e. the travel of light within the canopy as well as light leaving the plant canopy which potentially carries information on the canopy properties. Accordingly, linking plant functions and RTM might firstly increase our understanding of underlying ecological processes (e.g. plant growth, competition for light) and secondly

increase our abilities to improve and harness algorithms and sensors to track earth's functional diversity using earth observation data.
Accordingly, the present thesis tackles the following primary research gaps:

- Can gradients of plant functioning and strategies be revealed by trait maps derived from an inversion of radiative transfer models?
- Which plant traits affecting radiative transfer help to spectrally separate plants of different functioning?
- What are the causal associations between optical plant traits and plant functioning and can these extend our understanding of plant functioning?

These research gaps are addressed within four independent studies (Chapter 2 to 5). At present two studies are published in peer-reviewed international journals. The third and fourth study are currently under review:

- The first study (*Linking radiative transfer models and plant strategies*, Chapter 2) is a proof of concept of assessing plant functional gradients with trait maps derived from a RTM inversion. The study assesses if mapped plant traits derived from an inversion of PROSAIL and hyperspectral airborne data correlate with plant strategies measured in-situ in a raised bog. The plant strategies were defined based on the CSR scheme of Grime (Chapter 1.1). Using the same test site and hyperspectral data Schmidtlein et al. (2012) successfully mapped plant strategies with empirical models (partial least squares regression). However, it was not clear why this is actually possible, that is what is causing differences in canopy reflectance between the different plant strategies? It was thus expected that the RTM inversion not only presents are more transferable approach compared to empirical approaches, but also provides increased knowledge gain.
- The second study (*Differentiating plant functional types using reflectance: Which traits make the difference?*, Chapter 3) assesses which optical plant traits are most relevant to differentiate a wide spectrum of plant functional types using hyperspectral reflectance.

Various plant traits non-linearly affect canopy reflectance spectrum in partly overlapping regions. As such it is complex to attribute spectral differences among plant functional types to single traits. Knowledge on which optical traits are firstly most different among plant functional types and secondly cause measurable differences in canopy reflectance is crucial for designing and harnessing sensors and mapping algorithms. Although the first study assessed the ecological relevance and methodological potential of RTM inversions for assessing plant functional gradients, the results of this case study are only representative for one vegetation type (raised bog vegetation), one point in time and a limited set of traits. Accordingly, the second study considered a broad spectrum of plant functioning using 38 cultivated plants of different plant functional types in which the traits incorporated in PROSAIL were measured insitu across an entire growing season. The measured trait expressions are used to simulate canopy reflectance of the different plant functional types using forward simulations of PROSAIL. Subsequently the contributions of each trait to differentiate plant functional types based on canopy reflectance are compared.

- The third study (*Radiative transfer modelling reveals why canopy reflectance follows function*, Chapter 4) assesses if and how plant functions and strategies are causally expressed through optical traits. Thereby the study addresses the fact that PROSAIL (and RTM in general) are initially developed to model radiative transfer in plant canopies without taking into account the ecological relevance of the model and the parameter space therein. In order to apply RTM in an ecological context it is thus crucial to understand how the trait space incorporated in RTM relates to plant functions. Accordingly, this study compares expressions of those traits implemented in PROSAIL with well-established schemes of plant functioning, i.e. the Leaf Economic Spectrum and CSR plant strategies. Thus, whereas the first and second study assess the link between canopy reflectance and functioning from a remote sensing perspective, the third study focuses on causal and ecological relationships between optical traits and plant functioning.

- The fourth study (*Remote sensing leaf photosynthetic pigments as concentration [%] is flawed and should be quantified as content [µg/cm^2] instead*, Chapter 5) evolved from

the third study, in which among other traits the functional role of pigments was assessed on two scales; i.e. as area-based content [µg/cm^2] and as mass-based concentration [%]. These two metrics are fundamentally different in terms of their relevance for plant functioning, their retrievability from remote sensing observations and their scalability from leaf- to the canopy-scale. However, a consensus on which metric to use appears to be inconclusive as both metrics are referred frequently used in different studies with similar objectives. This study thus firstly clarifies the differences between pigment content and concentration. Secondly, it is demonstrated that for statistical reasons and principles of plant physiology and radiative transfer, the remote sensing of pigments as concentration [%] is unsubstantial and should be assessed as content [µg/cm^2] instead.

2 Linking plant strategies and plant traits derived by radiative transfer modelling

---

This chapter has been published as: *Kattenborn, T., Fassnacht, F. E., Pierce, S., Lopatin, J., Grime, J. P., & Schmidtlein, S. (2017). Linking plant strategies and plant traits derived by radiative transfer modelling. Journal of Vegetation Science, 28(4), 717-727.*

2.1 Abstract

Question: Do spatial gradients of plant strategies correspond to patterns of plant traits obtained from a physically based model and hyperspectral imagery? It has been shown before that reflectance can be used to map plant strategies according to the established CSR scheme. So far, these approaches were based on empirical links and lacked transferability. Therefore, we test if physically-based derivations of plant traits may help in finding gradients in traits that are linked to strategies.

Location: A raised bog and minerotrophic fen complex, Murnauer Moos, Germany.

Methods: Spatial distributions of plant traits were modelled by adopting an inversion of the PROSAIL radiative transfer model on airborne hyperspectral imagery. The traits are derived from reflectance without making use of field data but only of known links between reflectance and traits. We tested whether previously found patterns in CSR plant strategies were related to the modelled traits.

Results: The results confirm close relationships between modelled plant traits and C, S and R strategies that were previously found in the field. The modelled plant traits explained different

dimensions of the CSR-space. Leaf Area Index (LAI) and the reciprocal of Specific Leaf Area appeared to be good candidates for reproducing CSR scores as community traits using remote sensing. LAI has not been used in previous studies to allocate plant strategies.

Conclusions: Combining RTM and the CSR model is a promising approach for establishing a robust link between airborne or spaceborne imagery and plant functioning. The demonstrated potential to map traits with close relation to CSR gradients using only our understanding of the relation between traits and reflectance is a step forward towards an operational use of the CSR model in remote sensing.

2.2 Introduction

Optical remote sensing has established itself as an efficient tool for the retrieval and monitoring of terrestrial vegetation properties in time and space (Ustin and Gamon 2010; Asner and Martin 2015). In remote sensing, these plant attributes are most frequently extracted using statistical models based on prior acquired field samples. However, despite precision and ease of implementation, statistical models lack portability as they are largely affected by sensor and site conditions (Schmidtlein et al. 2012; Vuolo et al. 2013). A physically-based alternative is given by radiative transfer models (RTM), which simulate the interactions of remotely sensed reflectance and plant properties using cause-effect relationships. RTM model the spectrum of a leaf or a plant canopy based on a given set of plant properties (e.g. Leaf Area Index, pigment content, leaf water content, etc.). By inverting RTM, these plant properties can be estimated based on the spectrum measured by a terrestrial, airborne or spaceborne spectrometer. RTM are often applied in agriculture (Meroni et al. 2004; Duan et al. 2014) while canopies exhibiting greater architectural and physiological complexity have rarely been investigated. Exceptions include a small number of studies using RTM inversions in grasslands (Vohland and Jarmer 2008; Darvishzadeh et al. 2011; Si et al. 2012) and forests (Gastellu-Etchegorry et al. 1996; Kötz et al. 2004; Laurent et al. 2011). These studies used RTM inversions to obtain a range of plant properties and reported acceptable accuracies. The transferability of RTM and the positive

findings of these studies promise the widespread utility of RTM inversions in vegetation remote sensing.

Ecologists have employed chemical and structural plant traits to model the leaf economic spectrum (Wright et al. 2004) or to group species into plant functional types (Lavorel et al. 1997). One of the most established concepts with implications for the relationship of plant traits and vegetation functioning is the CSR-model of Grime (1988). The CSR-model posits the existence of three major axes of plant strategies, namely competitiveness (C; characterised by traits that facilitate outcompeting of neighbours), stress-tolerance (S; traits supporting metabolism in harsh abiotic conditions) and ruderality (R; traits facilitating regeneration of the population in habitats characterised by frequent lethal disturbance events). The CSR model suggests that plants evolve strategies that optimise allocation between resource capture, resource conservation, space occupancy, longevity and dispersal (Grime et al. 1997).

Originally the CSR scheme was a classification to assign species to the three primary types (C,S,R) or secondary and tertiary intermediates using plant traits (Grime 1988). Hodgson et al. (1999) used seven readily measurable traits as proxies and regression models to derive CSR scores. Based on the assumption that there should be some links between CSR strategies and visible traits, Schmidtlein et al. 2012 mapped CSR scores of peatland vegetation using airborne imaging spectroscopy. This mapping exercise was based on field reference data, hyperspectral imagery and on statistical models (partial least square regression) that linked both sources of information. Schweiger et al. (2017) transferred this approach to another area. The fact that these attempts were successful implied strong evidence for a causal relation between plant strategies and reflectance spectra, but - as always with statistical models - the causal links could only be hypothesised. In contrast, radiative transfer models, by integrating structural and physiological traits of the canopy, build upon mechanistic understanding of the relationships between physical and biotic aspects of the environment. Here, we make use of these models to test whether the previously found patterns can be confirmed by mapping plant traits with a relation to CSR strategies derived from RTM inversions. These traits are derived from reflectance without making use of field data, but only of known links between reflectance and traits. Knowing the links between mapped strategies and modelled traits would help to make the CSR model more oper-

ational in remote sensing.

The most established RTM for vegetation is PROSAIL, a model of directional reflectance that integrates structural traits of the canopy as well as biochemical leaf traits. For example, PROSAIL was used in the above-cited grassland studies (Vohland and Jarmer 2008; Darvishzadeh et al. 2011; Kötz et al. 2004). Although the set of optically relevant plant traits in PROSAIL is different from the set used by Hodgson et al. (1999) to allocate CSR-scores, some PROSAIL traits are potential alternatives for the allocation of CSR-scores using remote sensing.

Leaf area has a strong association with CSR-scores (Cerabolini et al. 2010b; Pierce et al. 2013), and at least one small-scale study has determined that Leaf Area Index (LAI) of herbaceous communities reflects the range and character of CSR strategies present (Cerabolini et al. 2010a). Reason exists for assuming that this local-scale link between LAI and CSR strategies could reflect a general relationship: LAI is also closely correlated to primary production and thus strongly related to nutrient supply (Asner et al. 2003), and the productivity of the habitat is directly correlated with CSR strategies (Kelemen et al. 2013; Cerabolini et al. 2016). Thus it is reasonable to assume that, within stands with comparable disturbance dynamics, the extent of leaf coverage and thus LAI values should be closely related to the competitive abilities of plant species while low values indicate lower abundance of competitors. At the leaf level, PROSAIL accounts for two traits that are directly linked to photosynthesis, namely leaf carotenoid (CAR) and chlorophyll a+b (CAB) content. According to the leaf economic spectrum (Wright et al. 2004) it can be expected that competitors and ruderals invest the majority of their resources in productive leaf compartments, i.e. photosynthetic activity. Stress-tolerators on the other hand rather invest in strategic measures (e.g. enzymes, wax layers), or in mechanisms to cope with low nutrient availabilities. In a raised bog, stress-tolerator for example buffer their metabolism against environmental levels and changes by stocking nutrients and carbohydrates in extensive storage parenchyma tissues, and thereby cannot invest as much resources directly in photosynthetic machinery (Grime and Pierce 2012).

Further relevant traits at the leaf level are equivalent water thickness (EWT) and the reciprocal of Specific Leaf Area (SLA), which is called dry matter content (LMA) in PROSAIL (Jacquemoud et al. 1996). For definitions of individual traits in PROSAIL see Table 2.2. SLA, i.e. the

area of leaf deployed for each unit of biomass, is a key trait in the global leaf economic spectrum (Wright et al. 2004) and was also used by Hodgson et al. (1999) to allocate CSR-scores. EWT strongly correlates with SLA (Féret et al. 2011; Weiher et al. 1999). Both traits are in strong association with relative growth rate and are important indicators for competitive ability, ruderal strategy and stress tolerance (Grime 1988; Poorter and Garnier 1999). Thus, stress-tolerators, characterised by low SLA (or high EWT), invest in high robustness and low leaf palatability, in order to maximise the overall nutrient residence time. Competitors and especially ruderals are in contrast characterised by high SLA, which is coupled with fast growth rates and decreased vulnerability to energy and resource losses, e.g. biomass removal or disturbance (Grime et al. 1997).

We expect that RTM such as PROSAIL link the spectral reflectance of vegetation canopies with several traits that are directly or indirectly related to the plant strategy types proposed by Grime (Grime 1988). Based on their relatively accurate retrieval reported in previous studies we focus on the traits LAI, CAB as well as SLA and EWT (Colombo et al. 2008; Darvishzadeh et al. 2008, Rivera et al. 2013; Casas et al. 2014). By spatially modelling these traits using RTM we should be able to characterize CSR gradients in the landscape without the need for training data. This would not only allow to assess the relation of the derived traits to CSR-scores, but also explain why it was possible to predict CSR-scores using hyperspectral data and empirical models (Schmidtlein et al. 2012). Thus, going beyond black-box models and using a more generalizable approach of mapping plant functioning would be a big step forward towards remote sensing based monitoring systems that take into account our knowledge about ecosystems.

2.3 Methods

We estimated traits with relevance for Grime's plant strategies using an inversion of PROSAIL and airborne hyperspectral imagery of a wetland area in Bavaria, Germany. To assess the match between estimated plant traits and occurring strategies, we retrieved CSR-scores from field-records of species composition and compared the scores with the distributions of traits.

Table 2.1: Basic statistics for the observed CSR strategy scores. Avg (CI) = average including 95 confidence intervals.

Score	Min	Avg (CI)	Max	Var
C	-0.04	0.08 (0.04 to 0.12)	1.06	0.06
S	-1.22	0.09 (0.14 to 0.05)	0.04	0.07
R	-2.00	1.97 (1.98 to 1.97)	-1.68	0.01

2.3.1 Field data and allocation of CSR-scores

The study site, a wetland area of 20.5 ha, is located in the Murnauer Moos (47.65N, 11.15E, Bavaria, Germany) and has been a test site for CSR mapping before (Schmidtlein et al. 2012). It comprises rich fens along a rivulet, poor calcareous fens and a raised bog. The floristic composition is mainly driven by nutrient availability and by the contrast between wetland soils rich in calcium carbonate on the one hand and acidic peatland on the other hand. Water is in excess throughout the area. Nutrient supply in the acidic raised bogs largely depends on atmospheric deposition or local decomposition of peat and is further hampered by selective cation binding of peat mosses. The raised bog features species such as *Eriophorum vaginatum* or *Andromeda polifolia* which can withstand extreme conditions (low nutrient availability, acidic conditions and frequent soil water saturation). The minerotrophic fens are rich in carbon but still nutrient-poor apart from a zone of influence of a small rivulet that imports nutrients. This zone is accessible to plants adapted to more favourable conditions.

The species distribution was sampled using a rectangular grid of 44 nested plots (Fig. 2.1). To investigate the homogeneity in species composition, each plot consisted of three circular subplots with a surface of 4 m^2. The plot homogeneity was quantified using Bray-Curtis distances between subplots. Four plots were excluded from further analysis due to heterogeneity. A more detailed description of the field data acquisition and processing is given in Schmidtlein et al. (2012). CSR strategies scores were assigned based on the table provided by J.G. Hodgson (Hodgson et al. 1999) and supplemented for 5 further species as described in Schmidtlein et al. (2012) using Hodgson's regression method (Hodgson et al. 1999). A species is characterised by three strategy scores, i.e. competitiveness (C), stress tolerance (S) and ruderality (R), with

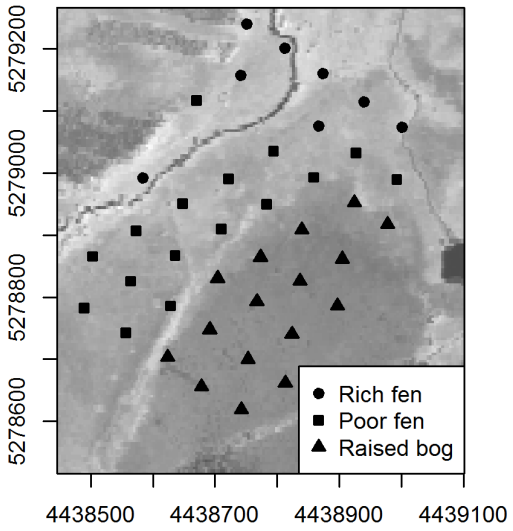

Figure 2.1: Near Infrared representation of the HyMap data (band 22) and vegetation classes for each field plot. Vegetation classes are based on the isopam clustering algorithm (Schmidtlein et al. 2010) and log-transformed species data.

scores ranging from -2 (no affinity) to 2 (high affinity). For each plot the CSR-scores of the single species were averaged using the untransformed percentage species cover values as weights. In the area of investigation, C and S scores exhibited the largest variation (-0.38 to 0.76 and -1.22 to 0.04, respectively). The R scores were all negative (-2.00 to -1.68), indicating a small proportion of species with ruderal strategies inside the plots (Table 2.1). According to Grime's CSR concept and the results of Schmidtlein et al. (2012) we can describe the area as follows: competitive species (C strategists) are primarily present in the richest sites along the rivulet. Stress-tolerant species (S strategists) mainly occupy the raised bog. Ruderal species (R strategists) are largely absent but there is a tendency towards relatively ruderal conditions along the rivulet and in managed fen areas.

2.3.2 Remote sensing data and processing

The remote sensing data were acquired using a HyMap airborne hyperspectral imager in July 2003. It is assumed that at this time most species reached maturity within their phenological cycle, showing most distinct differences in canopy and leaf characteristics. The sensor measures incoming radiation in the spectrum of 430-2480 nm, with channels featuring a bandwidth of 15-20 nm. In the standard HyMap processing chain of the German Aerospace Center (DLR),

the data set with a spatial resolution of 6 m · 4 m and 126 spectral bands was georeferenced with submeter accuracy (RMSE 0.66 m) using an orthoimage (0.4 m resolution). Absolute reflectance was derived using the atmospheric correction routine ATCOR. Erroneous bands (2421-2480 nm) were removed prior to further analysis.

2.3.3 RTM Inversion and mapping of plant traits

The RTM PROSAIL links the leaf reflectance model PROSPECT- 5 (Feret et al. 2008) and the canopy reflectance model 4SAIL (Verhoef and Bach 2007). In the forward mode PROSAIL simulates spectral processes on the basis of plant properties and sun-observer geometry. An inversion of PROSAIL (backward mode) allows for an estimation of plant properties based on measured spectra. Accordingly, for each pixel of the HyMap scene, PROSAIL was inverted using a lookup table (LUT) approach. Based on different parameter combinations the LUT is used to randomly simulate various spectra, which are compared to the measured spectra. Simulated spectra with a close correspondence to the measured spectra are used to identify the most plausible combination of PROSAIL parameters (here plant traits). This minimization method is readily implemented, unbiased by local minima (unlike neural networks) and less affected by spectral disparities between measured and modelled spectra (Atzberger et al. 2015). Following the recommendations of Weiss et al. (2000) and Richter et al. (2009) the LUT size was set to 100,000, featuring a good compromise between computation time and accuracy.

The ill-posed problem of model inversion can be substantially alleviated using prior information of the possible parameter space (Combal et al. 2003). Therefore, sun azimuth, zenith and observer angle were fixed for each pixel according to the logs of the HyMap campaign. In consideration of the broad mixture of species, a spherical distribution of leaf angles (ALA parameter in PROSAIL) was chosen. Fixed values and ranges of the other parameters were selected based on the literature (Darvishzadeh et al. 2011; Atzberger et al. 2015) and available trait data from the TRY database (Kattge et al. 2011; compare appx. 1.1). The values for the non-fixed variables in the LUT were randomly sampled from a uniform distribution (n = 10,000) within the specified range. The parameter settings of the LUT considered for the simulation of LUT spectra are summarized in Table 2.2.

Table 2.2: Ranges or fixed values for each input parameter for the generation of the LUT.

Parameter	**Abbreviation**	**value / range**
Chlorophyll a+b [µg cm^{-2}]	CAB	10-60
Carotenoid [µg cm^{-2}]	CAR	3-15
Equivalent water thickness [g cm^{-2}]	EWT	0.01-0.03
Dry matter content [g cm^{-2}]	LMA	EWT / 3.2-4
Leaf structure parameter	N	1.9
Leaf Area Index [m^2 m^{-2}]	LAI	0.2-6
Average leaf angle [°]	ALA	55, spherical
Brown pigment content	Cbrown	0-0.3
Hot-spot size [m m^{-1}]	HOT	0.05
Solar Zenith angle [°]	SZ	35.5
Observer Zenith angle [°]	SO	6.5
Relative Azimuth angle [°]	RA	98.6
Soil brightness parameter	soil	0.2

Previous studies demonstrated that wavelet analysis improved the parameter retrieval of RTM inversions (Blackburn and Ferwerda 2008; Cheng et al. 2011; Banskota et al. 2013). The latter decomposes the hyperspectral signature into frequency components at different spectral scales, which facilitates the retrieval of the spectral features and thus plant traits. Therefore, LUT spectra with the closest correspondence to the HyMap spectra were identified using a prior transformation in continuous wavelets. The difference of Gaussians (second derivative) was used as kernel function, since the shape of spectral absorption features can be described by multiple Gaussian functions (Le Maire et al. 2004). The wavelets were calculated using the R package 'wmtsa' (settings: number of scales = 6, scale range = 1-12). The wavelets of scales 1 and 2 (the two smallest of the six scales) were excluded as they explain primarily noise and artefacts present in the original spectra. To identify the closest match between the wavelet transformations of LUT and airborne spectra, the RMSE was used as cost function (eq. 2.1), which is reported to deliver robust results (Rivera et al. 2013):

$$RMSE = \sqrt{\frac{1}{n}\sum_{i=1}^{n}(r^i_{measured} - r^i_{simulated})^2} \tag{2.1}$$

where r is the absolute reflectance for the respective band i. The final estimates for each trait (T_{fin}) were derived by selecting the 1% of the LUT entries that resulted in the smallest RMSE.

As proposed by Vohland et al. (2010), the trait values of these LUT entries where weighted according to their RMSE value and subsequently averaged:

$$T_{fin} = \sum_{i=1}^{n} \left(\frac{1/RMSE_i}{\sum_{i=1}^{n} 1/RMSE_i} T_i \right) \tag{2.2}$$

where n is the number of selected LUT entries (i.e. 1000), T_i the value of trait T for LUT-entry i. The overall goodness of fit for each inverted hyperspectral pixel was determined by calculating the absolute deviance of the measured spectra and the weighted average of the corresponding LUT spectra.

The sensitivity of PROSAIL towards LMA is overshadowed by constituents with a high absorption (e.g. chlorophyll and water; Feret et al. 2008). Hence, compared to EWT, the accuracy of estimating LMA by the inversion of PROSAIL is relatively low (Botha et al. 2007). For this reason Weiss et al. (2000) and Combal et al. (2003) recommend a coupling of LMA and EWT as long as plants are growing under well-watered conditions such as those encountered in our sites. Vohland and Jarmer (2008) even observed an increased accuracy of LAI and CAB estimates following this procedure. Accordingly, LMA and EWT values were coupled for the LUT generation. As fixed factors of 4 and 3.2 have been reported (EWT/factor = LMA), we decided to sample a random factor within that range for each LUT entry.

The suitability of radiative transfer models has already been demonstrated for single-layered vegetation as grassland and heathland sites (Vohland and Jarmer 2008; Darvishzadeh et al. 2011; Si et al. 2012). We therefore assume that these results can be safely transferred to raised bogs and fens dominated by grasses and herbs. Yet, to review the overall plausibility of the model implementation and functioning, the absolute values of the estimated traits were compared to studies relating to similar ecosystems (see appx. 1.1).

2.3.4 Relating PROSAIL output to CSR scores

For each sample point (Fig. 2.1) the plant traits estimated by the model inversion (LAI, CAB, etc.) were extracted for each subplot and subsequently averaged. As we expected non-linear monotonic relationships between plant traits and strategies (CSR-scores), the correlations were

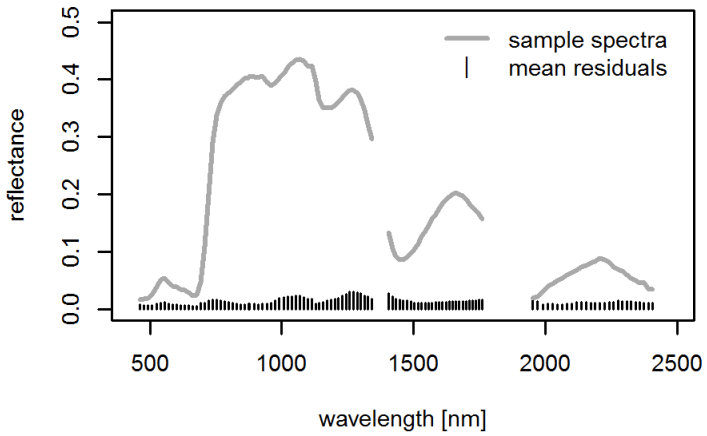

Figure 2.2: Mean absolute error for all field plots between measured (HyMap) spectra and modelled spectra (LUT) for each spectral band. The mean absolute error for all bands is 0.0131 reflectance units.

quantified using Spearman's rank correlation coefficient r_s. The general relationships between plant traits and CSR axes were visualized using ternary diagrams (R-package 'ggtern', v. 2.1) so-called 'trade-off triangles' (Pierce et al. 2013). Therein, plant traits (response) were plotted in relation to C, S and R scores (predictors) using Generalized Additive Models (GAM) with cubic splines.

2.4 Results

The average goodness of fit of the modelled spectra at the plot locations amounts to 0.0133 absolute reflectance units (ranging from 0 to 1). Overall, modelled spectra and HyMap spectra did not show striking mismatches in specific spectral regions (Fig. 2.2), which implies the overall suitability of the LUT settings and the inversion procedure. This is further indicated by the noise-free and smooth patterns of the retrieved trait maps for LAI, SLA and chlorophyll (Fig. 2.3), which correspond to the previously observed floristic gradients (Fig. 2.1).

All assessed traits showed significant correlations with CSR scores. The highest correlations between CSR scores and plant traits were found for modelled LAI (see Table 2.3). The latter correlated positively with C (r_s: 0.86) and R scores (r_s: 0.51), whereas S scores decreased with higher LAI values (r_s: -0.87). Similar trends were observed for CAB and SLA, whereas overall CAB showed higher correlation with plant strategies than SLA. Broadly speaking, for

Table 2.3: Spearman's r_s among modelled plant traits and CSR- scores (*** P $\leq$ 0.001 **P $\leq$ 0.01).

Parameter	min	mean	max	C	S	R
LAI; Leaf Area Index [m^2 m^{-2}]	0.55	1.55	3.92	0.86***	-0.87***	0.51***
CAB; Chlorophyll cont. [µg cm^{-2}]	32.2	43.2	49.0	0.76***	-0.76***	0.44**
SLA; Specific Leaf Area [m^2 kg^{-1}]	12.8	15.3	21.3	0.59***	-0.59***	0.50**

each plant trait the relationship with S scores was contrary to C and R scores. In accordance with their low variation in the field data, R scores showed lower correlations with plant traits (Tab. 2.3).

Analogous trends were observed in the ternary plots (Fig. 2.3). The gradient of CAB was more closely related to the C-S than to the R-S axis. The highest LAI values were predicted in intermediate positions of C and R. A similar gradient could be found for the modelled relationship with SLA. The distance between gradient lines in the ternary plots varied along the range of CSR scores, which indicates non-linear relationships.

2.5 Discussion

2.5.1 Linking plant traits to strategies

The relationships between modelled plant traits and ground-sampled C, S and R strategies were found to be relatively close considering the fact that the CSR system itself is a model, with scores derived from other variables than the investigated traits. The weakest correlations were generally found for R scores. In the same study area, analogous patterns have been found (Schmidtlein et al. 2012) for the relationship between reflectance and observed plant strategies. This can be readily explained by the low abundance of ruderal species (compare Table 2.1), resulting from a relative lack of disturbance throughout the study site. Therefore, results and extrapolations based on R scores should be interpreted with caution, and future work including a larger range of disturbed habitats would be useful.

The LAI shows the highest correlation with the plant strategies, and plots with high LAI have a relatively strong affinity towards competitive and ruderal strategies (Fig. 2.4). Overall, these findings are well in line with results of previous studies (Asner et al. 2003), showing that LAI is

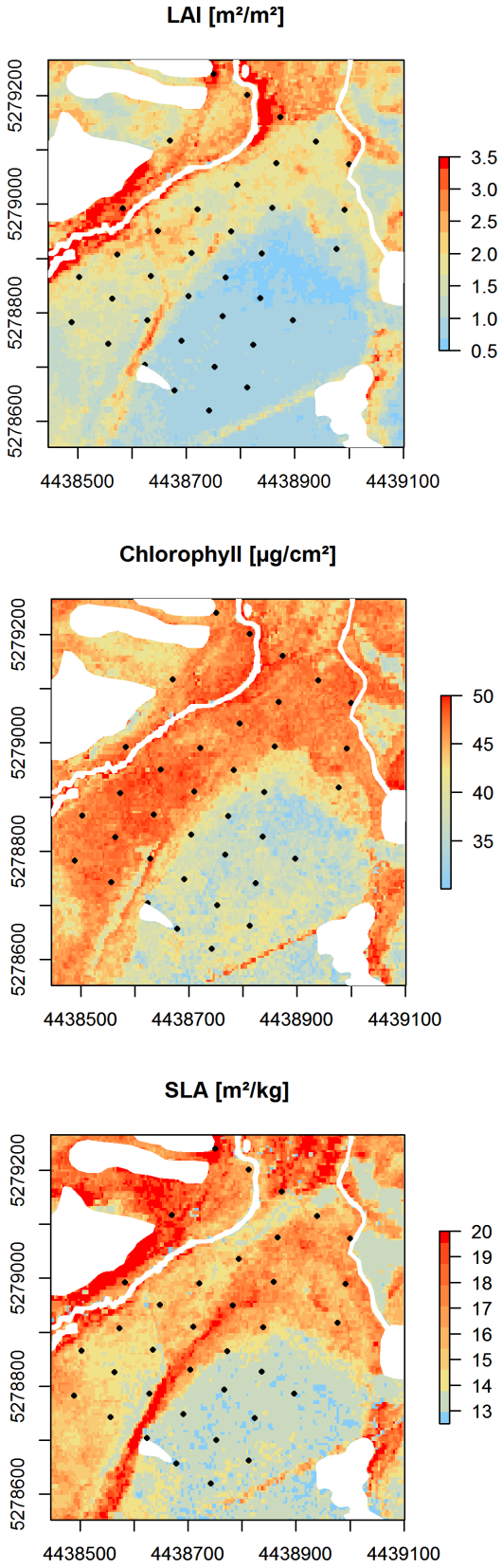

Figure 2.3: Maps of estimated plant traits derived from the inversion of PROSAIL including locations of the field plots. Forest patches and surface waters are masked. Geographical units (xy) are given in meters (EPSG: 31468).

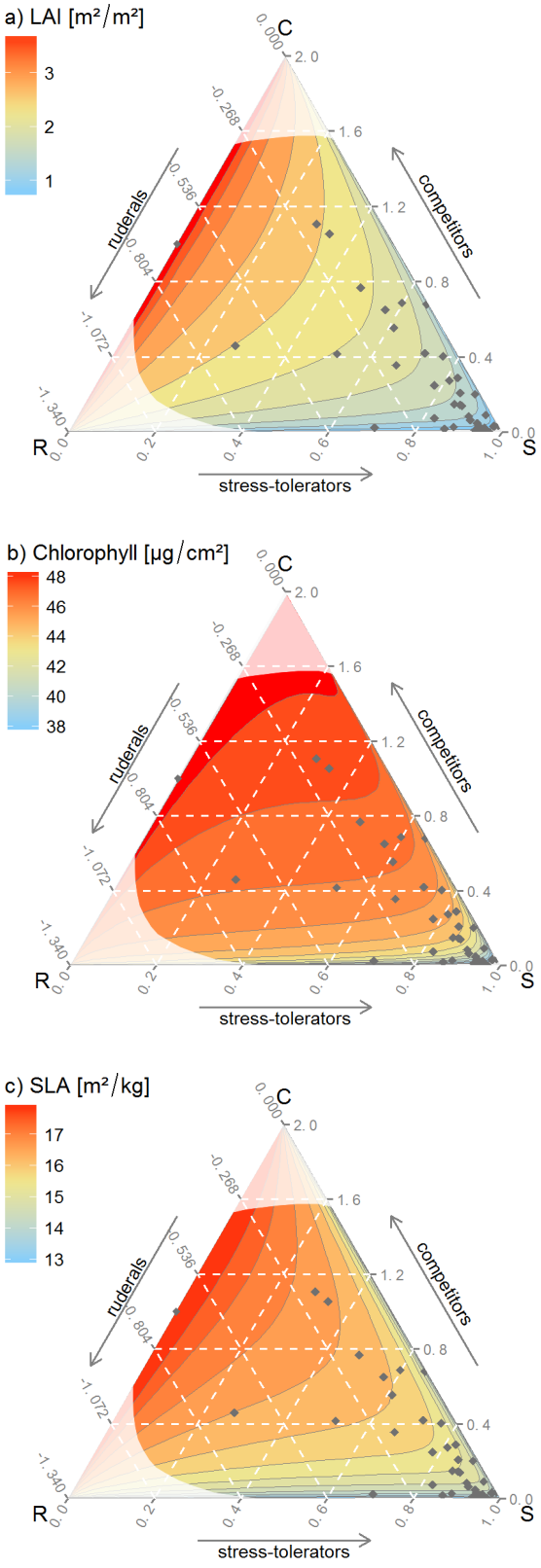

Figure 2.4: Ternary plots showing measured CSR strategies and extrapolated gradients of plant traits as obtained from a GAM. Regions with absence of field samples with respective CSR strategies have been faded.

a sound proxy for plant productivity. Previous research to directly link LAI to CSR scores did so in comparison of two contrasting herbaceous communities (Cerabolini et al. 2010a). Yet their results are hardly comparable, as the study aimed at comparing LAI and the variance of CSR scores, and not the strategy per se. LA, the average leaf area of single leaves, has frequently been used to allocate CSR scores of individual plants (Grime et al. 1997; Hodgson et al. 1999; Pierce et al. 2013). In contrast to LA, LAI is derived as an integrated canopy attribute. Therefore, LAI is a dimensionless quantity that complies with the spatial constraints of Earth Observation data (Asner et al. 2003) and can be mapped across a range of spatial scales with relatively high accuracy (Garrigues et al. 2008; Zheng and Moskal 2009). For these reasons and due to the demonstrated high explanatory power, LAI can be considered a valuable trait to derive average plant strategies using remote sensing. It can be assumed that LAI needs to be complemented by SLA in order to distinguish certain lush, ruderal stands from stands with many competitors.

For chlorophyll content a similar relationship can be observed, where higher leaf chlorophyll content clearly corresponds to increased competitive ability (C scores) as well as increased nutrient availability. The fact that the chlorophyll gradient is rather directed to C than R scores is well in line with our expectations, i.e. short-lived R strategists invest fewer resources into leaf pigments than C strategists. An acceptable accuracy of chlorophyll retrieval from the inversion of PROSAIL has been shown before (Darvishzadeh et al. 2008; Atzberger et al. 2013), so we suggest chlorophyll content as being important for plant strategies.

The modelled gradient of SLA, which follows the C-S (competitiveness) as well as the R-S axis (ruderality), reflects well-known relationships among resource allocation and plant strategies (Garnier 1992; Hodgson et al. 1999; Wright et al. 2004). Yet, among the mapped plant traits SLA exhibits comparably lower correlations with the CSR scores (Tab. 2.3). As SLA was derived by inverting PROSAIL's dry matter content parameter (sensu Jacquemoud and Baret 1990), we assume that this lower correlation is caused by the relatively lower sensitivity for dry matter content during the PROSAIL inversion (Botha et al. 2007), which is inter alia caused by low specific absorption coefficients and overshadowing through water absorption at the relevant wavelengths. To minimize these effects, dry matter content was coupled with equivalent water thickness, which is based on a broad spectral range between 800 and 2500 nm (Jacquemoud

and Baret 1990). Yet, as the correlations with plant strategies are explicit and significant, SLA proves to be an important predictor for the remote sensing of CSR gradients. In particular, because in addition to the leaf surface-related traits, SLA extends the dimensionality of leaf information, as it pools information related to leaf density and therefore resource investment.
As shown by the distribution of traits in the ternary plots (Fig. 2.4), the degree of linearity in the relationship between traits and CSR scores varies. This emphasizes that for some ranges of the CSR feature space, a certain trait might explain more variation than another trait with a generally similar relationship.
All modelled traits relate to some extent to the variation in the sampled CSR feature space. Thus the observed relationships between plant traits and strategies comply with established ecological findings. In particular, the variation along the C-S axis could be explained to a large extent. The results also underline the possibility of mapping R scores, despite the low variation in the latter throughout the study area. Hence, we assume that especially a combination of several traits can largely explain CSR gradients in natural landscapes. PROSAIL takes into account further plant traits such as carotenoid content or mesophyll thickness, which are likely to be closely related to plant strategies. However, the accuracy of their retrieval using a RTM inversion is known to be significantly lower and we therefore refrained from directly linking these traits to CSR scores. Slightly higher deviances between modelled and HyMap spectra were found in the areas of the NIR shoulder (750-1350 nm) and likely are artefacts of atmospheric effects and their correction, respectively. This region is mostly sensitive to variations in LAI. Yet, the low relative deviance is not likely to largely affect the retrieved LAI values and even less likely to influence the overall LAI pattern. The range of modelled trait values is in agreement with the range of values found in comparable areas (see appx. 1.1).

2.5.2 RTM and CSR in applied remote sensing

The results confirm that spatial gradients of plant strategies can indeed be rediscovered in gradients of traits obtained from a physically based model and hyperspectral imagery. Inverting PROSAIL has great potential to spatially map plant traits, which in turn could, in future, be used to allocate CSR scores (we do not take this step in the current paper). Processes of ecosystem

change are often directly linked to plant functioning, and one candidate model for summarizing plant functioning are plant strategies. Their use for global applications is discussed in Pierce et al. (2013) and Pierce et al. (2017), and imaging spectroscopy has already been identified as a promising technology for tracking ecosystem changes (Jetz et al. 2016). We expect that combining RTM and plant strategies will prove a viable option to explicitly link remote sensing concepts and plant functioning at a range of scales.

While statistical models can be used to derive relationships, physically based models allow insight into the processes leading to the observed phenomena. Hence, in contrast to the 'black box' functioning of statistical models, RTM follow physical concepts, which can substantially improve the understanding of the underlying processes. Moreover, in using RTM-based remote sensing, no calibration data are needed, which enhances the transferability across landscapes. Despite the demonstrated merits of inverting RTM, landscapes can feature a vast array of strategy related attributes that are not addressed in models such as PROSAIL (e.g. multi-layered canopies, flowering, complex mosaics of canopies and non-vegetated surfaces). Hence, for application in broad-scale assessments RTM must be further refined. In view of the global variation in leaf and canopy traits, inversion techniques must be further improved, e.g. by considering trait constraints based on covariance of optical leaf traits (Roth et al. 2016). Both models, CSR and PROSAIL, are based on quantifiable plant traits, which allows the direct linkage of principles of optical remote sensing and plant ecology. PROSAIL reproduced patterns of traits related to plant strategies using only knowledge of the effects of these traits on reflectance. The fact that gradients in CSR-related traits can be mapped using only reflectance is a step forward towards operational use of the CSR model in remote sensing.

2.6 Outlook

The present study assessed whether Grime's plant strategies observed in the field correspond to plant traits derived by the inversion of PROSAIL using airborne imaging spectroscopy data. We demonstrate that the plant traits derived from inverse modelling indeed feature significant correlations with spatial patterns of measured C, S and R scores. This is consistent with our

expectations regarding the role of these traits. The evidenced potential of combining RTM and the CSR model encourages further research in this direction. The relationships between plant strategies with canopy and leaf traits have to be further understood and generalized using extended data sets in terms of spatial coverage and range of plant strategies. Moreover, remote sensing allows the physical quantification of further plant traits, which we will address in future research. One of these traits is canopy height, which has been identified as one of the most descriptive traits to allocate CSR scores (Grime et al. 1997; Hodgson et al. 1999). Canopy height can be mapped using LiDAR, photogrammetry or RADAR interferometry (Kattenborn et al. 2015). Furthermore, time and life-history traits should be taken into consideration. This includes assessing the seasonal variation of relevant plant traits to further understand and characterize their relationship to plant strategies and to determine the optimal timing for hyperspectral imaging. Moreover, we assume that phenology and plant development are important predictors of strategies, which can be assessed using multi-seasonal remote sensing data. So far, the quality of spaceborne hyperspectral data has been rather limited for an application of RTM such as PROSAIL. Yet, with the upcoming imaging spectrometer missions, e.g. EnMap (Stuffler et al. 2007), PRISMA (Labate et al. 2009) or HyspIRI (Roberts et al. 2012), compatible data for the demonstrated approach will be readily available. Thus, we expect that in the future the inversion of RTM using image spectroscopy will play an important role for ecosystem and habitat assessments at multiple scales. The Group on Earth Observations Biodiversity Observation Network (GEO BON) proposes species traits and ecosystem composition by functional type as Essential Biodiversity Variables (EBV) for monitoring biodiversity from space (Skidmore and Pettorelli 2015; Paganini et al. 2016). A reduction of trait dimensionality such as that induced by major strategies may facilitate this use.

Acknowledgements

This study was funded by the German Science Foundation (DFG, project: Remote sensing of vegetation boundaries, SCHM 2153/1-1) and by the German Aerospace Centre (DLR) on behalf of the Federal Ministry of Economics and Technology (BMWi), FKZ50EE1347. The project

is part of the preparation for the EnMAP satellite mission. We would like to thank Stefanie Holzwarth (DLR) for the atmospheric correction of the hyperspectral data. The University of Bayreuth provided funding for the imagery, thanks to C. Beierkuhnlein. We also thank U. Friedel, C. Weiß and P. Zimmermann for their fieldwork.

3 Differentiating plant functional types using reflectance: Which traits make the difference?

This chapter has been published as: *Kattenborn, T., Fassnacht, F. E. & Schmidtlein, S. (2018). Differentiating plant functional types using canopy reflectance: Which traits make the difference? Remote Sensing in Ecology and Conservation*

3.1 Abstract

Abiotic ecosystem properties together with plant species interaction create differences in structural and physiological traits among plant species. Certain plant traits cause a spatial and temporal variation in canopy reflectance that enable the differentiation of plant functional types using earth observation data. However, it often remains unclear, which traits drive the differences in reflectance between plant functional types, since the spectral regions in which electromagnetic radiation is influenced by certain plant traits are often overlapping. The present study aims to assess the relative (statistical) contributions of plant traits to the separability of plant functional groups using their reflectance. We apply the radiative transfer model PROSAIL to simulate optical canopy reflectance of 38 herbaceous plant species based on field measured traits such as leaf area index, leaf inclination distribution, chlorophyll content, carotenoid content, water and dry matter content. These traits of the selected grassland species were measured in an outdoor plant experiment. The 38 species differed in growth form and strategy types according to Grime's CSR model and hence represented a broad range of plant functioning. We determined the relative (statistical) contribution of each plant trait for separating plant functional groups

via reflectance. Therein we used a separation into growth forms, that is graminoids and herbs, and into CSR strategy types. Our results show that the relative contribution of plant traits to differentiate between the examined PFT groups using canopy reflectance depend on the PFT scheme applied. Plant traits describing the canopy structure were more important in this regard than leaf traits. Accordingly, LAI and leaf inclination showed consistently high importance for separating the examined PFT groups. This indicates that the role of canopy structure for spectrally differentiating PFT might have been underestimated.

3.2 Introduction

Structural, physiological and phenological characteristics of a plant (hereafter traits) determine its performance in terms of growth, reproduction and survival. Environmental gradients of climate, topography or soil properties together with species interaction drive the variation in traits among plant species (Grime 1988; Wright et al. 2004). Species can thus be assigned to plant functional types (PFT) that group species with common functional traits (Lavorel et al. 1997). Even coarse map products of PFT distributions can be of high value as input for dynamic ecosystem models (Smith et al. 2001; Sitch et al. 2003) and earth system models (Poulter et al. 2011) as they provide a direct link to physiological plant properties. The Group on Earth Observation's Biodiversity Observation Network (GEO BON) regards functional types as essential for monitoring biodiversity from space (Paganini et al. 2016). Hyperspectral earth observation (EO) data is ascribed a high potential to determine the spatial distribution of PFT and thus ecosystem properties as multipleplant traits exhibit a trackable this spectral response is driven by the relationship of these plant traits and electromagnetic radiation, i.e. absorption and scattering processes within the canopy. Hyperspectral EO-sensors measure the reflected electromagnetic radiation and hence indirectly optically relevant plant traits. On this basis, previous studies used hyperspectral EO-data and empirical models to produce continuous maps of the spatial distribution of PFT (Schmidtlein et al. 2012; Feilhauer et al. 2016). However, it often remains unclear, why this actually works, i.e. which traits help us to differentiate between PFT. Several authors (Ustin and Gamon 2010; Jetz et al. 2016; Asner and Martin 2009) list plant traits (e.g. pigment,

dry matter, nitrogen or phosphorus content), which are supposedly important to optically differentiate plant functioning. However, knowledge about the physical contribution of these traits for differentiating PFT by reflectance remains limited. One reason for this is that most approaches using hyperspectral data are data-driven and based on complex statistical algorithms to exhaust the information content and to cope with the high data dimensionality. However, the 'black-box' nature of such empirical approaches generally cannot show causal relationships between the remotely sensed signal, plant traits and functioning. Assessing the contribution of individual traits is challenging as the canopy reflectance represents the integrated effects of various optical traits (Kokaly et al. 2009; Ollinger 2011). Thus, the reflectance at a given wavelength is driven by multiple plant traits. For instance, chlorophylls, which are fundamental for light harvesting, are known to absorb light in the spectral region between 400 and 700 nm. However, reflectance in these regions is also influenced by other traits such as total leaf area, leaf orientation or mesophyll structure (Jacquemoud et al. 2009). Thus, the contribution of a trait to discriminate plant functional types might be optically overshadowed by other traits acting in the same spectral region. Accordingly, relationships between multiple plant traits, plant functioning and canopy reflectance might not be traceable using statistical or machine learning models which do not explicitly consider known interactions between individual plant traits. In other words, a high importance of the visual part of the spectrum for separating between two plant functional types found by a data-driven model is not automatically a consequence of differing plant pigments compositions.

A possibility to improve our understanding of the spectral response of different PFT is given by canopy radiative transfer models. Canopy radiative transfer models integrate established knowledge on how plant traits interact with electromagnetic radiation into a process-based model. They are hence suitable to describe in a mechanistically oriented way how traits trigger reflectance. This provides an alternative, disentangled view on the origins of differences in reflectance between PFTs, with a better chance to identify causal links between canopy reflectance, plant traits and PFT. The currently most established radiative transfer model for vegetation canopies is PROSAIL (Jacquemoud et al. 2009), which couples two models addressing different origins of variability in reflectance: PROSPECT modelling the optical properties of

single leaf surfaces and 4SAIL which accounts for variability in canopy reflectance caused by differences in leaf orientation and foliage content of a plant canopy as well as its relation to sun and sensor. PROSAIL can be used to simulate the hyperspectral reflectance of plant canopies (e.g. as measured by an airborne or spaceborne spectrometer) as a function of defined plant traits. The incorporated plant traits are restricted to those, which could be implemented with acceptable accuracy during the development of 4SAIL and PROSPECT and are hence likely to be the optically most relevant traits. The incorporated plant traits that can be linked to plant functioning include two traits characterizing the canopy architecture. First, the leaf area index (LAI) relating leaf area to the corresponding surface area on the ground, which is a proxy for net primary productivity (Bondeau et al. 1999; Asner et al. 2003). Second, the variation of leaf angles, characterized by the leaf inclination distribution function (LIDF), controlling inter alia the light harvesting efficiency, leaf temperature and transpiration (Niinemets and Valladares 2004; Niinemets 2010). The other traits define foliage properties, such as pigments for photosynthesis and photoprotection, i.e. chlorophyll a+b (Cab), carotenoid content (Car) and brown pigment content (Cbrown) which relates to tannins and woody debris. Dry matter content per area (Cm) aggregates cellulose, lignin, and other structural carbohydrates and indicates leaf resource investments and tissue properties. Dry matter content is a frequently used proxy to characterize plant economics and strategies (Grime et al. 1997; Wright et al. 2004). Water content per leaf area (Cw) or equivalent water thickness can indicate drought resistance and flammability (Lawlor and Cornic 2002; Zarco-Tejada et al. 2003). The thickness of the spongy mesophyll is characterized by a mesophyll structure coefficient (N).

The knowledge on the optical properties of these traits as formulated within PROSAIL thus allows us to link plant canopy reflectance with plant traits and functioning in order to address the question: Which traits mechanistically drive the difference in canopy reflectance among PFT (we used types related to growth forms and plant strategies)? That is, what is the relative (statistical) contribution of plant traits included in PROSAIL for differentiating these PFT using hyperspectral data?

3.3 Methods

The present study assesses how canopy structural and leaf traits affect the differentiation of herbaceous PFT using canopy reflectance. This reflectance was simulated in order to understand in depth how traits contributed to this reflectance. The simulation was accomplished using the radiative transfer model PROSAIL parametrized using trait data acquired from outdoor cultivated plants.

3.3.1 Selection and cultivation of PFT

The trait data used to parametrize our models were acquired within an outdoor cultivation in the botanical garden of the Karlsruhe Institute of Technology (KIT). 38 herbaceous species belonging to different PFT were cultivated. As one scheme for allocating the PFT we used the CSR scheme (Grime 1988), which is one of the most established concepts of plant grouping by function (Hodgson et al. 1999; Pierce et al. 2017). The CSR-model posits the existence of three major dimensions in plant strategies, namely competitiveness (C; characterised by traits that facilitate outcompeting neighbours), stress-tolerance (S; characterised by traits supporting metabolism in harsh abiotic conditions) and ruderality (R; traits facilitating regeneration of the population in habitats characterised by frequent destructive disturbance events). The CSR model suggests that plants evolve strategies that optimize allocation between resource capture, resource conservation, space occupancy, longevity and dispersal (Grime et al. 1997). Our selection of species comprised competitive, stress tolerant, ruderal and intermediate species of both grasses and herbs from central Europe. Competitive species (C) are typically characterized by higher canopies and large leaves to pre-empt light resources. Stress tolerant (S) species often feature lower canopy heights and fewer but more robust leaves with low pigment concentrations. Ruderals (R) are fast growing species with a short lifespan and thus lower persistent resource investments, i.e. in dry matter (Grime and Pierce 2012). Intermediate species (CSR) have no affinity to the aforementioned strategies and hence feature intermediate trait expressions.
In addition to the CSR scheme we classified the species into growth forms, i.e. graminoids (g)

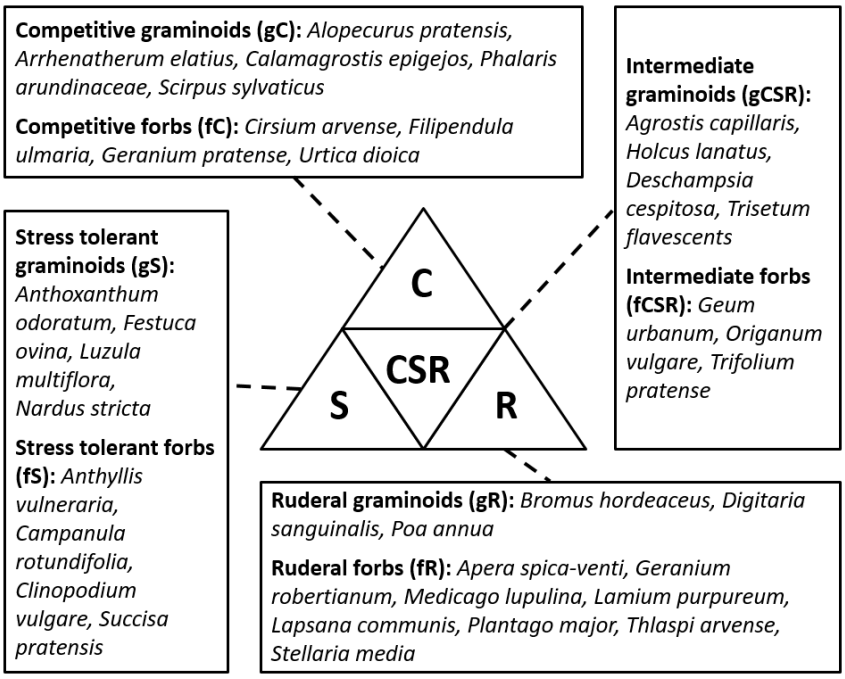

Figure 3.1: PFT scheme and respective species cultivated to derive the trait data.

and forbs (f). Figure 3.1 displays the described PFT scheme and the respective species of the experiment. The discernibility of PFT was hence assessed for three PFT schemes groupings:

1. growth forms, i.e. forbs and graminoids (f,g)
2. CSR strategies among graminoids, i.e. competitive, stress tolerant, ruderal and intermediate graminoids (gC, gS, gR, gCSR)
3. CSR strategies among forbs, i.e. competitive, stress tolerant, ruderal and intermediate forbs (fC, fS, fR, fCSR).

Propagation of the seedlings was performed indoor in March. When the plants reached a sufficient size, they were moved outdoor for a week of acclimatization. Afterwards they were planted out in four repetitions in separate pots with a size of 0.4 m · 0.4 m and 30 l volume filled with a standardized substrate. All pots were fertilized, weeded and regularly irrigated.

3.3.2 Acquisition of trait data

To reproduce a representative temporal variability the traits of all species were repeatedly measured on a weekly basis from May to November following a standardized procedure. Whenever

leaves had to be sampled, a set of sunlit leaves which best corresponded to the overall state of the plant was selected. The acquisition of leaf samples and leaf spectra was restricted to leaflets and thus did not consider petioles or rachis.

To measure **dry matter content** per area and **water content** per area approximately 10 g of whole leaves without twig were plucked. To limit the destructive impact, these measurements were performed on a species rather than a pot basis, by extracting leaf material equally from the four repetitions. The extracted leaf samples were immediately weighted on site after extraction and sealed in plastic bags containing a water saturated tissue. Within 24 hours the total leaf area of the extracted samples was derived using a flatbed scanner (Canon LiDE 70). Following the protocol by Pérez-Harguindeguy et al. (2013), the samples were oven-dried at 70°C for at least 72 h and subsequently weighted to derive the average leaf dry mass per area [g/cm^2]. Water content [g/cm^2] was derived by subtracting Leaf dry mass per area from Leaf fresh mass per area.

Chlorophyll content, **carotenoid content**, **mesophyll structure** and **brown pigment content** were derived using an inversion of leaf spectra and the PROSPECT-D model (Féret et al. 2017). Traditional measurement approaches for chlorophyll and carotenoid contents, such as the spectrophotometer method by Lichtenthaler (1987), were not applicable considering the high number of measurements per week (approx. 500) and limited resources. Leaf spectra were acquired using the ASD FieldSpec III (ASD, Inc. Boulder, CO, USA) equipped with a plant probe and a leaf clip. Five measurements of independent leaves were recorded for each individual pot and thus 20 measurements per species. A special treatment was applied for species with leaves not wide enough for the opening of the plant probe (2 cm diameter). The leaves were seamlessly and without overlapping placed side by side on an adhesive tape, covered with a microscope slide and subsequently scanned. The inversion of PROSPECT-D was performed using wavelet transformations and a lookup table approach (Blackburn 2006; Blackburn and Ferwerda 2008; Cheng et al. 2011; Ali et al. 2015; Li et al. 2018). Details on the inversion and its validation are given in appx. 2.1.

Leaf inclination distributions were derived using leveled digital photographs. For each species not less than 50 Individual leaf angles were measured using leaves oriented parallel to the view-

Table 3.1: Overview of the traits measured in situ and the method used for their retrieval.

Trait	Unit	Abbrev	Method
Chlorophyll content	[µg cm^{-2}]	Cab	Inversion of leaf spectra (PROSPECT-D)
Carotenoid content	[µg cm^{-2}]	Car	Inversion of leaf spectra (PROSPECT-D)
Leaf Area Index	[m^2 m^{-2}]	LAI	Leaf ceptometer (AccuPAR LP-80)
Dry matter content	[g cm^{-2}]	Cm	Dry weight / leaf area
Water content	[g cm^{-2}]	Cw	(Fresh weight - Dry weight) / leaf area
Leaf inclination distribution	[°]	LIDF	Horizontal photographs (Ryu et al. (2010))
Brown pigment content	-	Cbrown	Inversion of leaf spectra (PROSPECT-D)
Leaf structure parameter	-	N	Inversion of leaf spectra (PROSPECT-D)

ing direction using the public domain processing software ImageJ (http://rsbweb.nih.gov/ij/). For more details on the procedure see Ryu et al. (2010). As this procedure is very time- and labour-consuming the leaf inclination distribution was only measured once (based on photographs of 2-3 different dates).

Leaf Area index was measured using an Accu-PAR LP-80 ceptometer and an external reference sensor to account for the current incoming irradiance. In order to ensure that the LAI measurements are performed at ground level the measurements were taken via 2 lateral holes, which were put in each pot. For each pot 18 measurements were recorded and subsequently averaged. Trait data which correspond to the period of senescence were subsequently excluded in the present study. A statistical summary of the sampled trait data is available in appx. 2.2.

To assess the contribution of each trait to differentiate PFT under possibly varying environmental conditions we aimed at a good coverage of possible combinations of trait expressions. To achieve this, we inflated the number of weekly trait expressions by picking random values around a smoothed time series of measurements. The generated values for the different traits were then combined into 1000 random trait combinations per PFT that entered the simulation of spectra. These random trait combinations are likely to represent the full range of possible statuses within the examined PFT across a full growing season. The details of these pre-processing steps are given in appx. 2.3.

3.3.3 Simulation of species specific reflectance

The resulting combinations of trait expressions were used as input for PROSAIL 5B (Feret et al. 2008; Verhoef and Bach 2007) to simulate canopy spectra in the wavelength range of 400-2500 nm. In order to assess the effect of a given trait we compared the spectra calculated based on realistic trait expressions with spectra calculated based on random trait expressions sampled from the total ranges of values covered by all species.

During all PROSAIL simulations the soil brightness parameter (psoil), which determines the moisture content of the soil, was kept constant at 0.5. The sun angle (tts) was set to 35° and the observer angle (tto) was set to nadir (0°), resulting in a negligible effect of the hotspot size parameter, which was therefore kept constant at 0.01.

In order to comply with the quality of spectral acquisitions under operational conditions power law noise (1/f noise) was added (West and Shlesinger 1990) to simulate radiometric uncertainties caused by effects such as band anomalies, calibration errors or residuals of atmospheric and topographic correction algorithms. The randomly generated noise was added with a magnitude (0.2-2% reflectance, details see appx. 2.4), which corresponds to the standard radiometric uncertainty that is assumed for the hyperspectral satellite EnMAP (Bachmann et al. 2015). This ensures a more realistic view on a spectral separability of PFT as compared to perfectly clear PROSAIL spectra, which are likely to be not fully representative for operational data acquisitions. In view of airborne and spaceborne remote sensing data bands located in water absorption regions were removed prior further analysis (1400-1500, 1880-2000, 2450-2500 nm).

3.3.4 Comparing the contribution of plant traits on the discernability of PFT using MRPP

The (statistical) contribution of each considered plant trait for the separation of PFT (according to the three examined PFT schemes) was compared on the basis of the pre-processed in-situ trait data as well as the simulated plant canopy spectra. By this comparison it was possible to assess to what extent the discernibility provided by a plant trait measured in-situ is actually preserved in the spectral reflectance of a plant canopy. For both levels, i.e. in-situ traits and canopy spectra, the relative contribution of each plant trait was measured using a Multi Response Per-

mutation Procedure (MRPP, Mielke and Paul 1991; McCune et al. 2002). The latter was chosen for its robustness and parsimony. The MRPP is a multivariate non-parametric test of whether there is a significant difference between groups. The MRPP provides a change-corrected group agreement (A) and a significance (P). Similar to a coefficient of determination in a linear model, A ranges from 0 to 1 and maximizes if the discrimination between groups is perfect. Accordingly, a hypothetical A value of 1 would imply that the expression of a trait differs completely among PFT, whereas an A value of 0 implies that the trait does not differ between PFT. For the analysis based on in-situ measured traits, the MRPP was directly applied. That is, we tested for each plant trait its differences among the classes of a PFT scheme (e.g. differences in LAI between C, S, R and CSR forbs).

For the analysis of the canopy reflectance level, A was calculated for each band individually using the previously described simulated reflectances derived from PROSAIL. Hence, for each simulated wavelength we conducted two MRPP analyses to test for differences of the reflectances between the PFT groups of a scheme. The first MRPP was conducted based on canopy reflectances that were simulated using the in-situ measured traits of each species of the to be classified PFT groups (true variation). In contrast, in the second MRPP we replaced the in-situ measurements of one individual trait (e.g. LAI) with random values from the full range of measurements taken across all examined species (randomized trait expression). The values of A for a given wavelength derived from the second MRPP applied to the data set with randomized trait expressions were then subtracted from A values obtained from the first MRPP based on the true variation of all traits (ΔA, compare Fig. 3.2). Resulting positive values for ΔA reveal that the optical discrimination among PFT is enhanced if the variance of that trait (e.g. LAI) was included in the simulation of the canopy spectra. This procedure was repeated for each individual trait and wavelength. This way the band-wise relative contribution of each trait to separate PFT was determined.

As hyperspectral data contain spectrally continuous information across the covered wavelength regions, relevant information may be inherited by the reflectance of individual bands as well as by the shape of a spectrum. The MRPP-based analysis of the canopy spectra was hence not only applied on the reflectance values for each band, but also to the first and second derivative

thereof as these depict the shape of a spectrum.

3.3.5 Comparing the contribution of plant traits on the spectral discernability of PFT using machine learning

An aspect which is not fully considered in the band-wise MRPP-based analysis of the simulated canopy spectra are potential synergies among multiple spectral features. Multiple bands in combination can thus potentially carry more information than individual bands. Accordingly, we complemented the MRPP analysis with an additional analysis based on a machine learning algorithm to assess whether the relative contribution of traits for the spectral differentiation of PFT differs if the information content of the whole spectrum is considered. This analysis was performed using the partial least square (PLS) algorithm, which is commonly used in hyperspectral data analysis. For parameter optimization the PLS models were trained in a model tuning environment (R-package 'caret') using the scaled and centred simulated reflectances and a 5-fold cross validation. Analogously to the MRPP-based analysis a PLS model was created for the reflectance dataset with the variation of all traits and one-by-one, with randomized traits. The contribution of each trait to discern the respective PFT was determined by subtracting the Kappa value (K) based on the data set with a randomized trait from the Kappa obtained from the original variation of traits (ΔK, compare Fig. 3.2). In order to prevent a stochastic bias this procedure was performed for 100 iterations. In each iteration, the input traits (true and randomized variation of traits) were again sampled prior to the simulation of the spectra. The analysis was also carried out using a random forest and a support vector machines algorithm which did not result in notable differences (results not shown).

3.4 Results

3.4.1 Relative contribution of in-situ measured traits

For the separation of growth forms (graminoids vs. forbs) based on in-situ traits, leaf inclination was by far the most important trait, followed by carotenoid and brown pigment content (Fig. 3.3a). Comparably poor differentiation was provided by chlorophyll content, LAI, mesophyll

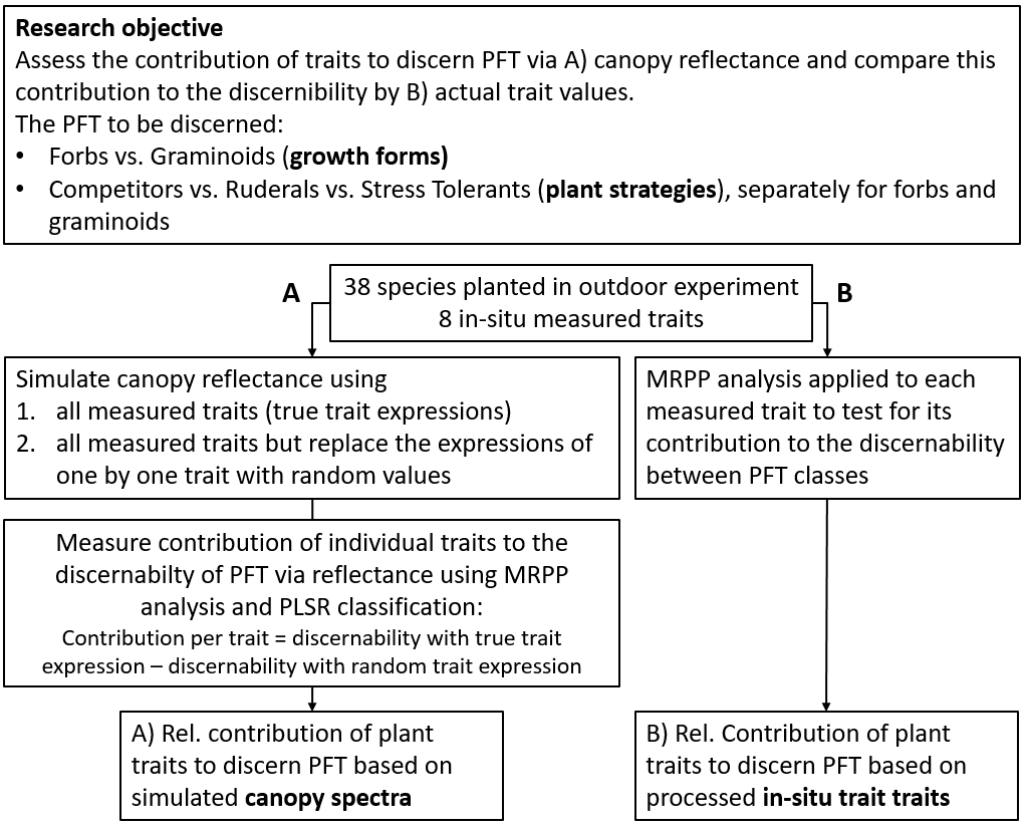

Figure 3.2: Simplified workflow of this study.

structure, dry matter and water content. Regarding the differentiation among graminoid strategies, the traits showed a more diverse contribution, where leaf chlorophyll content, carotenoid content, mesophyll structure coefficient and LAI had a similarly high contribution (Fig. 3.3b). The by far lowest contribution was given by water content. For the separation of forb strategies the contribution of traits is relatively balanced as water content and leaf inclination had the highest contribution, whereas all other traits show a similar modest contribution.

3.4.2 Contribution of traits to the differences between PFT canopy reflectance

Overall, the relative contribution of plant traits to the differentiation of PFT using canopy reflectance differed notably among the PFT groupings, i.e. the discernibility of growth forms, graminoids strategies and forb strategies. For separating growth forms (Fig. 3.4), leaf inclination had by far the highest contribution, especially in the red-edge region, followed by LAI and a notably lower contribution of dry matter and chlorophyll content and LAI. Very low contributions for the spectral differentiation between graminoids and herbs were found for mes-

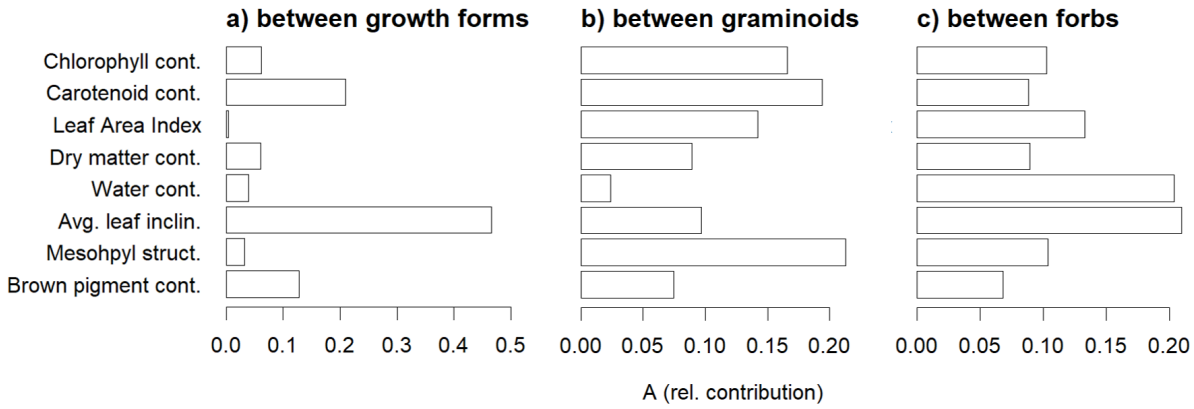

Figure 3.3: Relative contribution (A) of in-situ traits to separate three PFT schemes, i.e. a) growth forms, b) graminoid CSR-strategies and c) forbs CSR-strategies. A is the chance-corrected within group agreement as measured by a multi-response permutation procedure (MRPP).

ophyll structure, carotenoid, water and brown pigment content. Relative to the other traits, LAI showed a clearly increased contribution compared to the analysis of the in-situ measured trait data (Fig. 3.3a). Carotenoid content, brown pigment content and mesophyll structure showed higher contributions than LAI when considering in-situ traits and contrarily a lower contribution than LAI for a discrimination when using canopy reflectance.

The spectral discrimination between graminoid strategies (Fig. 3.5) was highest for LAI in the VIS and SWIR followed by dry matter and water content and leaf inclination in the SWIR. Moderate to low ΔA were found for mesophyll structure, brown pigment, chlorophyll content, and carotenoid content.

The spectral separation among forb strategies was dominated by water content and LAI in the NIR and SWIR region. Moderate contribution could be observed by dry matter content and leaf inclination chlorophyll content. Brown pigment content, mesophyll structure and carotenoid content did not substantially contribute to separate forb strategies.

The results based on the machine learning algorithm PLS are shown in Fig. 3.7. Overall the observed relative contribution shows a high correspondence to the results derived from the MRPP-based analysis. In summary the results of the MRPP (based on individual bands) and the PLS analysis (based on multiple bands) show that, in contrast to the discrimination by in-situ trait data (Fig. 3.3) carotenoid content, brown pigment content and mesophyll thickness did not contribute much to the reflectance-based differentiation of PFT (Fig. 3.4, 3.5, 3.6). The variation

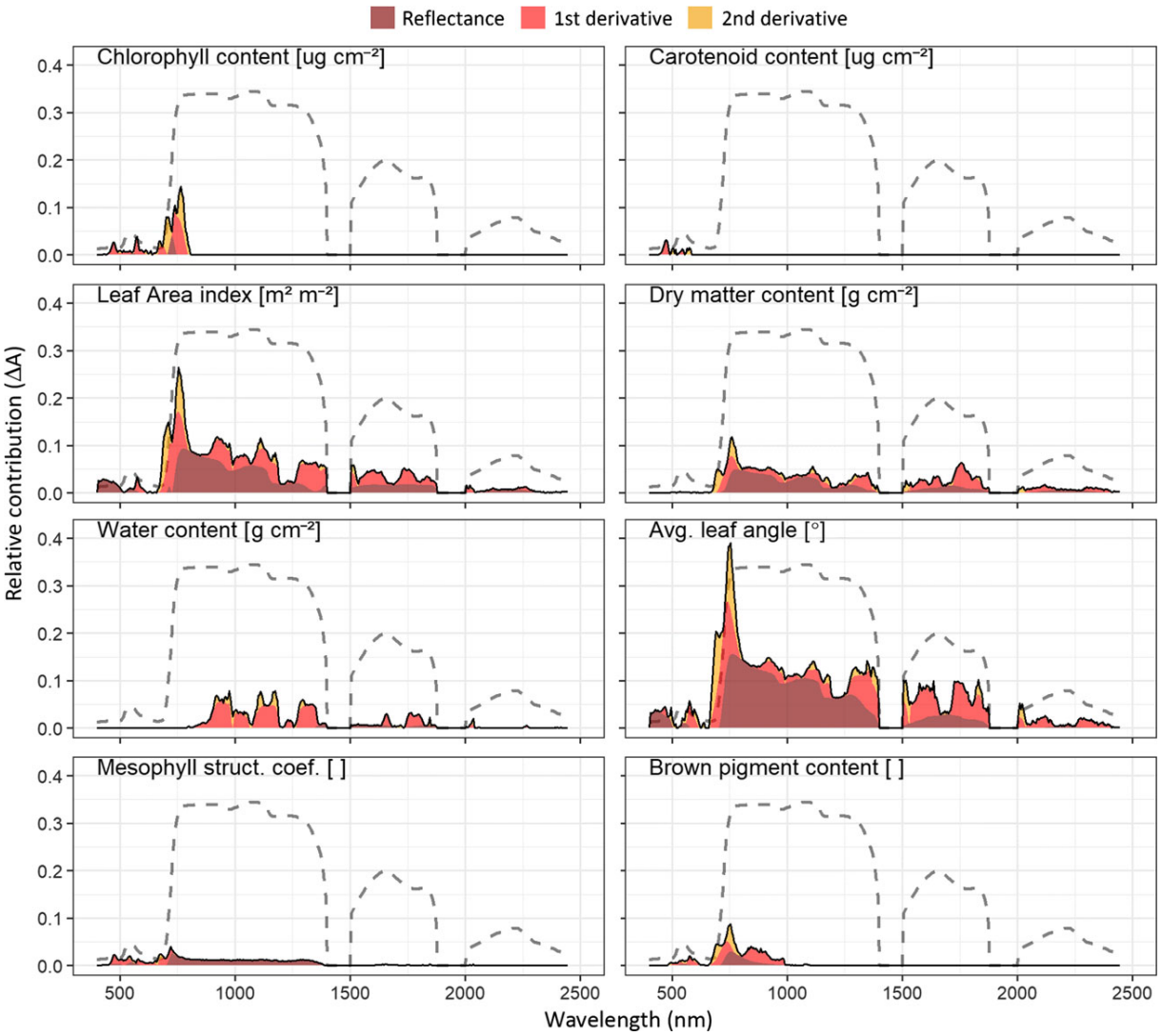

Figure 3.4: Relative contribution (ΔA) of plant traits to the band-wise separation of **growth forms**. For guidance a common vegetation spectrum was added to each panel (dashed line).

in chlorophyll content only resulted in moderate contributions. Dry matter content and water content generally showed a moderate to high contribution for the separation of the considered PFT. The variation of either leaf inclination or leaf area index, which both describe aspects of canopy structure, contributed a large part for the spectral differentiation of the considered PFT schemes.

3.5 Discussion

As expected, different plant functions led to different trait expressions which in turn resulted in different optical properties. Depending on the PFT scheme at hand, i.e. the differentiation of

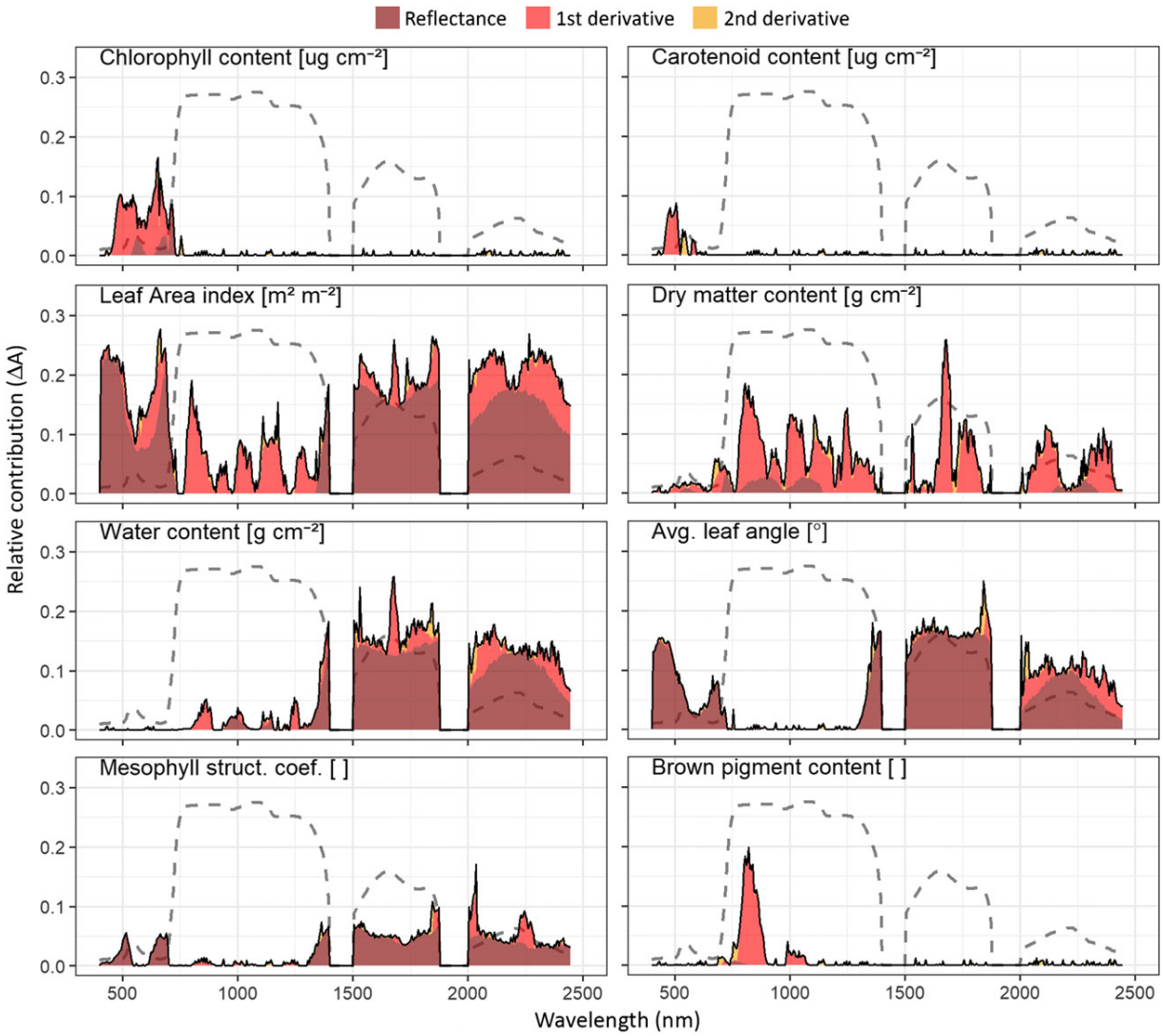

Figure 3.5: Relative contribution (ΔA) of plant traits to the band-wise separation of **CSR strategies among graminoids**. For guidance a common vegetation spectrum was added to each panel (dashed line).

growth forms, forb strategies or graminoid strategies, the relative discriminative power of the traits changed considerably. Yet, we could observe some clear trends:

Our results show that the contribution of in-situ leaf traits to the differentiation of PFT does not necessarily correspond to their discriminative power if it comes to differentiating herbaceous PFT through canopy reflectance, which indicates that not all variation in plant traits can be retrieved using canopy reflectance. Despite the comparatively high contribution of in-situ carotenoid content for discriminating plant strategies and growth forms (Fig. 3.3), the contribution observed at the canopy reflectance level was comparably low (Fig. 3.4, 3.5, 3.6). Mesophyll structure, which showed a comparably high contribution to separate plant strategies on the in-

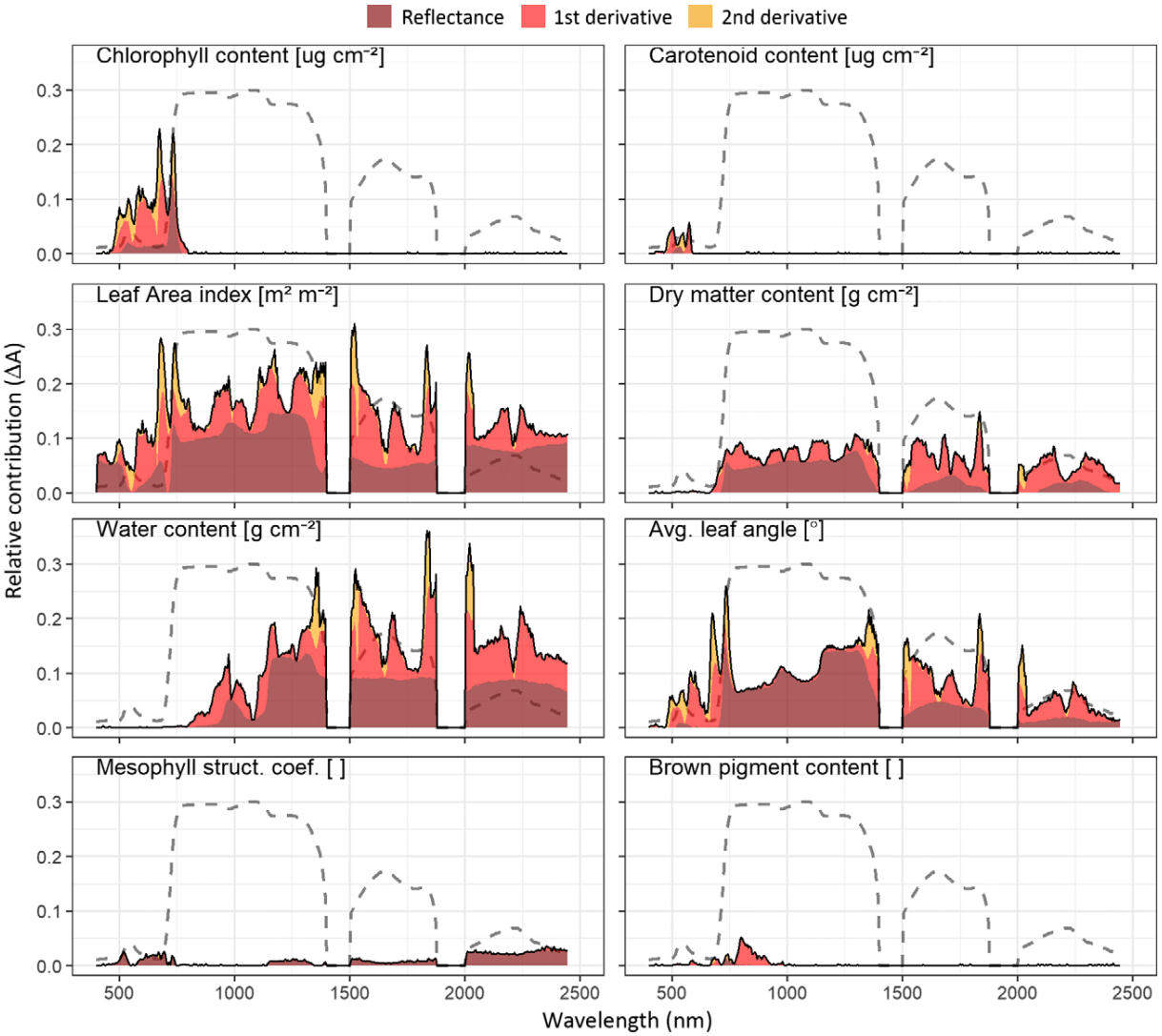

Figure 3.6: Relative contribution (ΔA) of plant traits to the band-wise separation of **CSR strategies among forbs**. For guidance a common vegetation spectrum was added to each panel (dashed line)

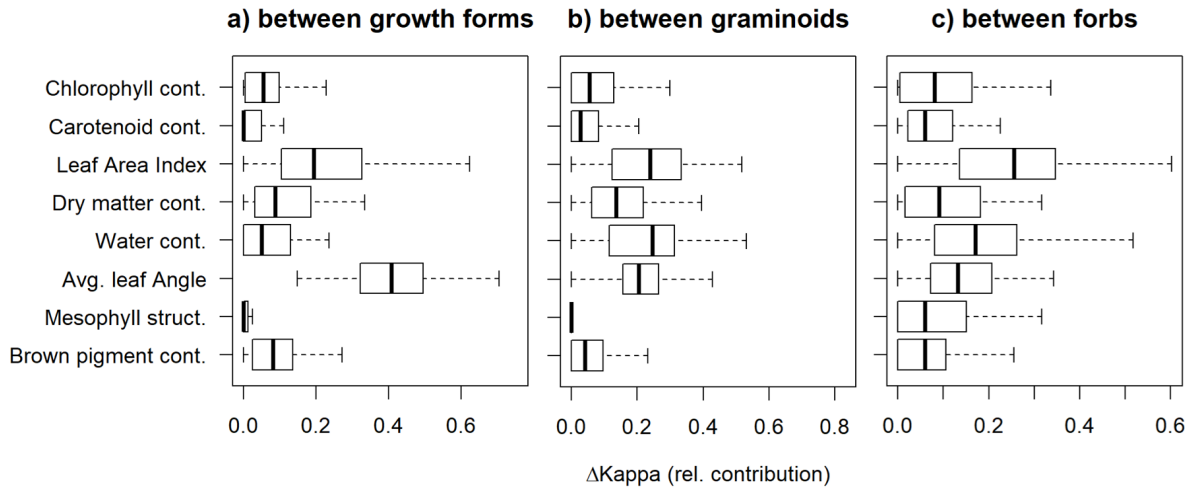

Figure 3.7: Relative contribution (ΔKappa) of plant traits to seperate the three PFT schemes, i.e. a) growth forms, b) graminoid CSR-strategies and c) forbs CSR-strategies based on PLS models.

situ level (Fig. 3.3b, c), showed only a negligible discriminative power at the spectral level (Fig. 3.4, 3.5, 3.6). The only leaf traits which markedly contributed to the spectral separation of the PFT were water and dry matter content. This is well in line with previous studies, which evidenced that water and dry matter content or its inverse SLA is strongly correlated with plant functioning and strategies (Grime et al. 1997; Wright et al. 2004; Weiher et al. 1999).

Traits describing the canopy structure, i.e. LAI and leaf inclination, showed for both the in-situ traits and the simulated canopy spectra a strong discriminative power. This is consistent with established knowledge in vegetation ecology regarding linkages between canopy architecture and plant functioning (Givnish 1984; Craine et al. 2001; Poorter et al. 2006; Niinemets 2010). For the simulated canopy spectra, the contribution of canopy structure was more pronounced, while leaf traits (e.g. pigments) were less important than expected based on earlier studies from the remote sensing community. For instance, Jetz et al. (2016) list six 'key functional plant traits' for remote sensing of functional biodiversity, of which all are leaf traits. Similarly, Asner and Martin (2009) state that the optical reflectance of plant canopies is primarily driven by the leaf biochemistry and propose to utilize EO-data and spectrally derived 'chemical fingerprints' to map plant functioning. The latter study is referring to tropical forest ecosystems and may hence not be directly comparable to our results obtained with herbaceous species. However, it could be assumed that within forest ecosystems, structural traits may play an even more pronounced role as the structural diversity of forests canopies is higher than the one of herbaceous plant canopies. One key-problem of earlier studies conducted in forests may be that accurately measuring structural traits in the field is very challenging and hence earlier studies might have had limited capabilities to adequately disentangle structural and biochemical traits in their analysis (Homolová et al. 2013). Our results suggest that for spectrally differentiating PFT the role of traits describing the canopy architecture might be underestimated in the community. The overall lower contribution of leaf traits at the canopy reflectance level can to a large extent be explained by the confounding effects of canopy architecture (LAI, leaf inclination) affecting the same wavelength regions. This is in line with Knyazikhin et al. (2013b), who physically deduce that canopy structure largely affects the retrievability of leaf properties. These authors evinced that canopy structure is the dominant determinant of the plant spectral response. A direct mea-

surement of absorption through leaf constitutes by means of canopy reflectance is elementarily hampered as a fraction of the non-reflected light is scattered as a function of various canopy structural attributes which hence blur these absorption processes (Curran 1989).

On the other hand, processes taking place at the leaf level, such as photosynthesis or photoprotection are not independent from the leaf arrangement but are tailored concertedly to the overall structure of the canopy (Niinemets 2010). For instance, investments in pigment contents per leaf area are adjusted to the exposure of foliage, which is inter alia governed by the total amount of foliage (LAI) and its inclination (leaf inclination distribution) directed to the beam path of the solar radiation. Accordingly, plant functional gradients of canopy physiology such as fraction of absorbed photosynthetic active radiation (fAPAR) or net primary productivity cannot solely be explained by leaf properties but strongly depend on canopy architecture (Huemmrich 2013a; Middleton et al. 2009). In view of our findings, future studies should include the linkage between plant functioning and structural canopy variables. For example, as LAI is a dimensionless quantity it complies with the spatial constraints of EO-data and can be mapped across a range of spatial scales with relatively high accuracy (Garrigues et al. 2008; Zheng and Moskal 2009). The correlation of LAI with plant strategies has already been indicated (Kattenborn et al. 2017) and LAI was observed to closely correlate to primary production and thus strongly relates to nutrient supply (Asner et al. 2003). With respect to growth forms such as shrubs and trees the crown shape and foliage clumping, which describes the aggregation of foliage within a canopy, might be important additional structural canopy properties relating to plant functioning (Niinemets 2010; Ollinger 2011). The present study did not account for canopy structural attributes such crown shape or arrangement, since PROSAIL assumes a turbid medium and thus homogeneous vegetation canopies. These conditions match fairly well with herbaceous canopies but do not apply for complex forests canopies. Yet, the presented approach can also be transferred to radiative transfer models adapted to forest canopies; e.g. INFORM (Atzberger 2000) which is a modification of PROSAIL and includes further structural traits such as stem density, crown width or canopy height; or FLIGHT (North 1996) which is a more complex 3D radiative transfer model based on Monte Carlo ray tracing.

The relative contribution of the traits derived from the machine learning procedure (PLS)

showed an overall high correspondence to the results of the MRPP-based procedure. Minor divergences exist as the MRPP analysis is based on single bands, whereas the PLS approach accounts for interactions among bands, which is more likely to compensate for effects as scattering by the canopy structure or noise. The advantage of the MRPP-based analysis is an increased parsimony and the opportunity to identify the contributing spectral features across the reflectance spectrum. As such the MRPP-based analysis of the individual bands for separating PFTs showed that all three spectral regions, i.e. VIS, NIR and SWIR contribute for the differentiation of PFT (Fig. 3.4, 3.5 3.6). Although reflectance in the VIS region is to a large extent shaped by the absorption properties of leaf pigments (Ustin and Gamon 2010) we found that a high proportion of the class separability in the VIS region can be attributed to the canopy structural traits LAI and LIDF (Fig. 3.4, 3.5 3.6). This emphasizes that the variation at certain wavelengths cannot be explicitly linked to single traits, since the optical reflectance of plant canopies is a product of both biochemical and structural traits. Thus, caution should be used when interpreting trait-reflectance relationships, such as feature or band selection metrics.

Essential information is often confined in narrow spectral segments across the simulated wavelength range (grey line in Fig. 3.4, 3.5 3.6, 400-2500 nm). The jagged pattern of the bandwise relative contribution (ΔA) varies greatly according to the PFT scheme at hand and shows several local maxima across the spectrum. These findings indicate that optical EO-sensors should ideally meet two criteria for mapping plant functioning; firstly, cover the VIS, NIR and SWIR regions and secondly, feature a high spectral resolution. Future hyperspectral missions such as Hypsiri (Roberts et al. 2012) and EnMAP (Stuffler et al. 2007) meet these criteria and are therefore expected to be of high value for mapping plant functioning.

The fact that canopy architecture features a high contribution to differentiate plant functioning emphasizes the potential of multi-angular remote sensing, which enhances the retrieval of canopy structural characteristics (Widlowski et al. 2004). Similarly, the results encourage a combination of optical with LIDAR or RADAR (e.g. Sentinel-1) data, as the latter two are suitable to retrieve structural information of plant canopies (Disney et al. 2006; Latifi et al. 2012).

Our results largely depend on the functionality and validity of PROSAIL. The latter is a simplification of radiative transfers in natural plant canopies and does not account for all optically

relevant plant properties, such as flowers, which also have a substantial influence on the on canopy reflectance (Feilhauer et al. 2016). Some parameters used in PROSAIL serve as proxies for traits with similar optical response. For instance, dry matter content represents constituents as starch, sugar, cellulose or lignin, whereas chlorophyll content combines chlorophyll a+b. Yet, as these traits have very similar absorption features, it may be unlikely that a separation of these aggregated traits enhances the optical separation of PFT.

The leaf angle distribution was only assessed once, as the applied procedure using digital photographs and manual delineation of leaf angles was time- and labour-consuming. A recently published methodology presented by Müller-linow et al. (2015) allows for a more efficient estimation of leaf angle distributions using a semi-automatic workflow based on photogrammetric 3D reconstruction and close-range RGB images and could be applied in future studies.

The direct transferability of the results to other PFT schemes or ecosystems may be limited. Yet, the presented workflow can be transferred and as such might present a useful blueprint for assessing the relevant optical traits of other PFT schemes. The presented methodology can also be transferred to assess relationships of the electromagnetic spectrum and plant traits which are not strictly related to PFT, but for instance to assess the relevance of traits to map plant species or essential biodiversity variables (Pettorelli et al. 2016).

3.6 Conclusion & Outlook

So what makes the difference between the canopy reflectance of growth forms and plant strategies? The contribution of a trait to spectrally separate PFT does not necessarily correspond to the role that a trait could play to differentiate PFT in the field. The reason is that canopy reflectance is a complex response to multiple traits and these responses are not easy to disentangle with statistical methods. Instead, radiative transfer models (RTM) provide a possibility to untangle the reflectance of a PFT and trace it back to individual traits. RTM provide a transferable scheme to assess the mechanistic interrelationships between optically relevant plant functional traits and their spectral response. Clearly, the relative contributions of the traits vary by PFT scheme. However, canopy structural traits contribute a large part when it comes to spectrally

separating the herbaceous PFT addressed in our study. This indicates that the role of canopy structure might have been undervalued when differentiating PFT using canopy reflectance. It can be assumed that in more complex canopies additional structural traits, such as crown shape or leaf clumping, further contribute to the mappability of plant functioning. A better understanding of these interrelationships requires a systematic assessment of optically relevant plant functional traits across environmental gradients and taxonomic lines.

Our results indicate that for mapping plant functioning an optical sensor ideally covers the VIS, NIR and SWIR regions having relatively narrow bands (hyperspectral). Refining our knowledge about plant functioning and its optical properties can improve our capabilities to configure future EO-systems and harness EO-data.

Acknowledgements

The project was funded by the German Aerospace Centre (DLR) on behalf of the Federal Ministry of Economics and Technology (BMWi), FKZ50EE1347. The project is part of the preparation of the EnMAP satellite mission. We acknowledge support by Deutsche Forschungsgemeinschaft and open access publishing fund of Karlsruhe Institute of Technology. We would like to thank all employees of the botanical garden of the Karlsruher Institute for Technology (KIT), especially Peter Nick and Christine Beier, for their generous support.

4 Radiative transfer modelling reveals why canopy reflectance follows function

---

This chapter is based on a journal article currently under review: *Kattenborn, T. & Schmidtlein, S. (submitted). Why does the reflectance of plant canopies follow function? Nature Communications*

4.1 Abstract

Optical remote sensing is ascribed a high potential to track earth's plant functional diversity. Yet, causal explanations on how and why plant functioning is expressed in canopy reflectance remain limited. Variation in canopy reflectance can be described by radiative transfer models (here PROSAIL), which incorporate plant traits affecting light transmission in canopies (hereinafter 'optical traits'). To establish causal links between canopy reflectance and plant functioning, we compare expressions of these traits with two plant functional schemes, i.e. the Leaf Economic Spectrum (LES) and CSR plant strategies. Various optical plant traits indeed relate to these two plant functional schemes, whereas traits describing leaf properties correlate with the LES. Traits related to canopy structure show no correspondence to the LES, but correlate with CSR plant strategies. Multiple optical traits feature comparable or higher correspondence to the CSR space than traits originally used to allocate CSR scores. This evidences that plant functions and strategies are directly expressed in optical traits and entails that canopy 'reflectance follows function'. This firstly open up new possibilities to understand and describe differences

in plant functioning and secondly increases our capabilities to harness optical earth observation data for monitoring earth's functional diversity.

4.2 Introduction

Through natural selection plants diversified in various functions in order to adapt to environmental conditions, including abiotic factors (e.g. precipitation or nutrient gradients) and biotic interactions (e.g. competition or herbivory) (Darwin and Wallace 1858). Assessing plant functioning and its pattern in space and time are prerequisites for understanding biosphere-atmosphere interactions and ecosystem dynamics, such as community assembly and material and nutrient cycles (Diaz and Cabido 2001; Bonan et al. 2002; Wright et al. 2004; Reichstein et al. 2014; Violle 2014). With accelerated global change the data demand on patterns of plant functioning increased as the latter is heavily affected by anthropogenic impacts (Chapin et al. 1997; Cramer et al. 2001; Ten Brink et al. 2010; Cardinale et al. 2012). However, due to vast temporal and spatial variations in plant functions and the complexity to retrieve the latter in an explicit, consistent and spatially exhaustive way, data of earth's plant functional diversity remain limited (Kattge et al. 2011; Violle et al. 2014). In order to close this gap optical earth observation data is ascribed a high potential (Ustin and Gamon 2010; Homolová et al. 2013). During the recent years various studies demonstrated that optical earth observation data allows to map variations in plant functioning, functional types and strategies (Schmidtlein 2005; Garbulsky et al. 2011; Baret et al. 2007; Hilker et al. 2008, Friedl et al. 2010; White et al. 2009; Schmidtlein et al. 2012; Feilhauer et al. 2016). However, it often remains unclear why we can remotely sense functional differences (Schaepman et al. 2009; Ustin and Gamon 2010; Ollinger 2011). In order to fully harness and improve the potential of earth observation data and available algorithms it is crucial to understand the underlying processes allowing us to monitor plant functioning. The key to such an understanding are the traits that contribute to canopy reflectance.

The mechanistic interactions between solar radiation and plant canopies, including the light that is emitted from plant canopies and thus retrievable from earth observation sensors, is already

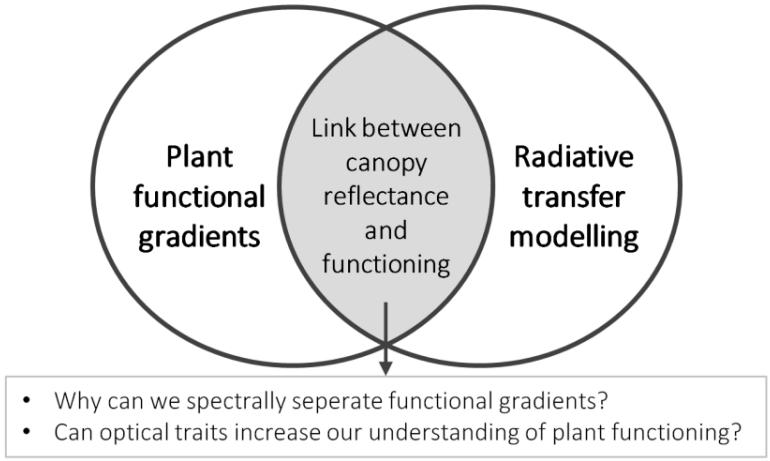

Figure 4.1: Rationale of linking plant functioning with radiative transfer modelling.

well understood and formulated in process based models, i.e. canopy radiative transfer models (RTM). Although radiative transfer is determined by traits with relevance for plant functioning, few studies explicitly linked RTM and plant functioning (Ali et al. 2016; Feilhauer et al. 2017; Kattenborn et al. 2017). We assess the distribution of these traits (hereinafter 'optical traits') along plant functional gradients, because knowing more about the links between optically relevant traits and plant functioning allows for mapping and monitoring plant functions in a more mechanistic way. This could dramatically improve the robustness and transferability of our models. Furthermore, it can be assumed that bridging plant functioning and canopy reflectance with radiative transfer theory can increase our understanding on how environmental factors and biotic interactions shape plant functional diversity (Ustin and Gamon 2010)(Fig.1).

As optical traits we consider those traits that are incorporated in PROSAIL-D (Verhoef and Bach 2007; Jacquemoud et al. 2009; Feret et al. 2017). PROSAIL is the most widely applied RTM for plant canopies and couples two models, firstly PROSPECT modelling the leaf optical properties (e.g. pigment or water content), and secondly 4SAIL which takes into account the structural properties of the canopy (e.g. leaf orientation) and its relative orientation to the sun and sensor (Jacquemoud et al. 2009). We also consider traits that can be directly deduced from the original PROSAIL-D trait space (e.g. leaf pigments by leaf mass or fAPAR). A summary of the traits and assumed links to plant functions is provided in Tab. 4.1.

Table 4.1: The optical trait space considered in the present study and their functions. The trait space consists of traits implemented in PROSAIL and derivates their off.

	Trait / Parameter [unit]	Abbr.	Description / functional role
Traits incorporated in PROSAIL-D	Chlorophyll content [µg/cm²]	Cab_{area}	Leaf pigments chlorophyll a+b; primary molecule for light harvesting (Féret et al. 2017)
	Carotenoid content [µg/cm²]	Car_{area}	Leaf pigments including xantophylls and carotenes; photoprotection and light harvesting (Féret et al. 2017)
	Anthocyanin content [µg/cm²]	Ant_{area}	Leaf pigments of the flavonoid family; photoprotection, protection from pathogens and light harvesting (Close & Beadle 2003; Zarco-Tejada et al. 2018)
	Leaf area index [m²/m²]	LAI	Ratio of total one sided leaf area per unit ground; dominant control of primary productivity and transpiration (Bondeau 1999; Asner 2003; Kattenborn et al. 2017)
	Leaf inclination distribution function [deg.]	LIDF	Variation of leaf angles in the canopy; controls light harvesting efficiency, leaf temperature and transpiration (Niinemets 2004, Niinemets 2010).
	Leaf mass per area [g/cm²]	LMA	Inverse of Specific Leaf Area (SLA), Aggregates leaf constituents such as sugar, starch, cellulose or lignin; well-known proxy for resource allocation and plant strategies (Wright et al. 2004, Pierce et al. 2017,)
	Equivalent water thickness [mg/cm²]	EWT	Water content per leaf area; determines thermal regulation, drought resistance and flammability (Zeiger, 1983, Lawlor & Cornic 2002; Zarco-Tejada et al. 2003).
	Mesophyll structure coefficient [-]	N_{meso}	Artificially designed PROSPECT parameter, relating to the thickness of the mesophyll layer, which affects light harvesting and light transmission as well as CO_2 diffusion. (Jacquemoud & Baret, 1990; Niinemets 2001)
	Brown pigment content [-]	Cbrown	Artificial PROSPECT parameter, relates to polyphenols such as tannins and other secondary metabolites with functions such as UV protection or defensive compounds against herbivory and pathogens (Hättenschwiler & Vitousek 2000; Dormann & Skarpe 2002)
Traits derived from PROSAIL-D trait space	Canopy leaf mass per area [g/m²]	LMA_{canopy}	Total leaf mass per canopy area [m²] calculated as the product of LAI and LMA
	Canopy water content [g]	EWT_{canopy}	Total water content per canopy area [m²] calculated as the product of LAI and EWT
	Chlorophyll conc. [‰]	Cab_{mass}	Chlorophyll mass per leaf dry mass
	Carotenoid conc. [‰]	Car_{mass}	Carotenoid mass per leaf dry mass
	Anthocyanin conc. [‰]	Ant_{mass}	Anthocyanin mass per leaf dry mass
	Fraction of absorbed PAR [%]	fAPAR	Fraction of photosynthetic active radiation (PAR) absorbed in canopy. Integrates absorption by pigments and canopy structural traits (LAI, ALA); reflects gross photosynthetic capacity of the canopy. Simulated using PROSAIL (details sensu appx. 3.3)
	Accumulated absorbed PAR [kWh/m²]	$APAR_{cum}$	PAR absorbed within the growing season; derived from multiplying fAPAR with course of direct and diffuse radiation during species specific growth length (details sensu appx. 3.3)

We assessed the distribution of these optical traits across plant functional gradients using in-situ measurements acquired in an outdoor experimental setting, with plants grown in pots. The species pool comprised 45 herbaceous species from Central Europe and covered a broad functional spectrum (Tab. 4.2). Instead of looking at individual functions such as carbon sequestration or evapotranspiration we referred to more general expressions of plant functioning provided by two well-established schemes: the Leaf Economic Spectrum (LES, Wright et al. 2004) and Grime's CSR model of plant strategy types (CSR, Grime et al. 1997; Pierce et al. 2017). Both are general approximations of principal functional differences between species that bundle many individual functions to metrics characterizing their overall performance towards abiotic and biotic environmental selection pressures. The LES was derived from analyzing various leaf traits (leaf lifespan, leaf mass per area, photosynthetic capacity, dark respiration rate, nitrogen and phosphorus concentration) and describes the spectrum of leaf resource investments ranging from fast and acquisitive (low investment) to slow and conservative growth (high investment) (Fig. 4.2a, Wright et al. 2004). We compare optical traits to the LES, as resource economics in leaves were found to reflect a main axis of functional differences in plants (Wright et al. 2004; Díaz et al. 2015) and can thus be assumed to be directly linked to the optical leaf traits in PROSAIL. The CSR model characterizes plant species by means of three axis, defining their competitive (C), stress tolerating (S) and ruderal abilities (R) (Fig. 4.2b, Grime et al. 1997; Pierce et al. 2017). Competitors are adapted to nutrient-rhich sites and feature rapid growth to large size to preempt resources, stress-tolerators compensate sub-optimal environmental conditions through slow and robust growth, whereas ruderals are small-sized and feature short-lifecycles to counteract events of disturbance and biomass removal. We compare optical traits to the CSR scheme as the latter, in contrast to the LES, further integrates differences in function at the whole plant level (Grime et al. 1997; Pierce and Cerabolini 2018) and thus may be more appropriate for assessing optical traits that are related to the canopy structure.

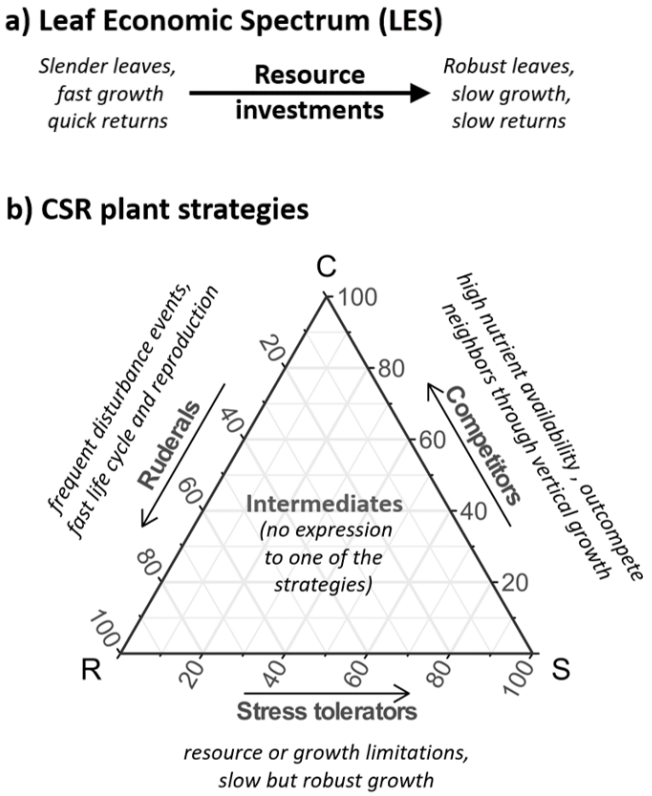

Figure 4.2: Schemes of the plant functional gradients compared to the optical trait expressions derived from the cultivated plants; a) The Leaf Economic Spectrum (LES) and b) CSR plant strategies.

4.3 Results

4.3.1 Optical traits versus Leaf Economic Spectrum

Which role do optical traits play in relation to the LES? The differences in optical-traits (compare Tab. 4.1) can be summarized in a three-dimensional feature space (Fig. 4.3), build by a principal component analysis, with component 1 comprising 28%, component 2 26% and component 3 16% of the total variation. In order to relate the optical traits to the LES, the latter was projected to this 3-dimensional optical trait space. As expected, the optical trait LMA, as one of the original constituents of the LES, correlated the most with the LES (-0.68 Pearson's r). Comparably lower but significant positive correlation ($p<0.05$) existed with pigment contents measured on a mass basis, i.e. Cab_{mass} (r=0.42), Car_{mass} (r=0.53), Ant_{mass} (r=0.52), indicating decreasing pigment concentrations with increasing resource investments. Pigments measured on an area-basis also correlated significantly but negatively with the LES, i.e. Cab_{area} s(r=-0.45), Car_{mass} (r=-0.44), so that pigments contents predominantly increase with slow and

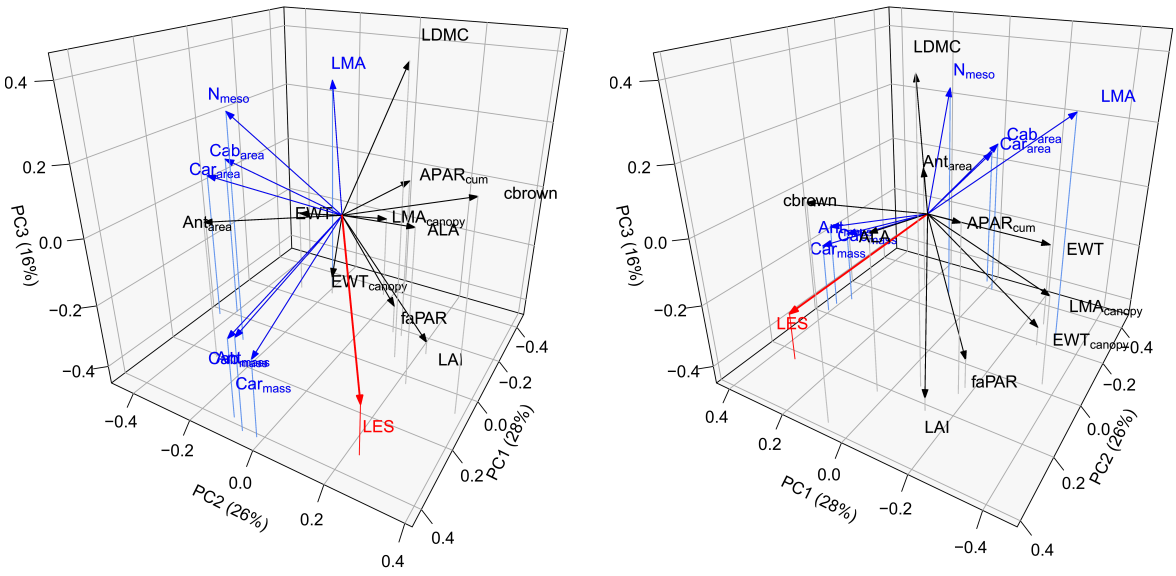

Figure 4.3: Two perspectives of the transformed trait space (principal component analysis) and relation to the Leaf Economic Spectrum (LES, red). Traits that are significantly related to the LES are highlighted in blue.

conservative growth. The artificial proxy for the mesophyll thickness N_{meso} correlates negatively with the LES (r=-0.40) reflecting higher mesophyll thickness with increasing resource investments. Traits linked to leaf water content (EWT, EWT_{canopy}, LDMC) or canopy structure (LAI, ALA, fAPAR, $APAR_{cum}$) were not significantly related to the LES. A table listing all correlations is given in Appx. 3.5.

4.3.2 Optical traits versus CSR plant strategies

The distribution of optical traits within the 3-dimensional CSR scheme of plant strategies was assessed using thin plate regression splines and generalized additive models (GAM, Wood 2003). Neither EWT nor EWT_{canopy} correlated to plant strategies among forbs nor graminoids. In contrast LAI, LMA, LMA_{canopy}, LDMC, $pigment_{mass}$, fAPAR and $APAR_{cum}$ showed significant relationships across forbs and graminoids (Fig. 4.4). $Pigment_{area}$, N_{meso}, Cbrown and ALA exhibited no consistent relationship to CSR plant strategies across growth forms and thus related differently among forb and graminoid strategies (Fig. 4.5, 4.6). A table summarizing the results for all traits is given in Appx. 3.6.

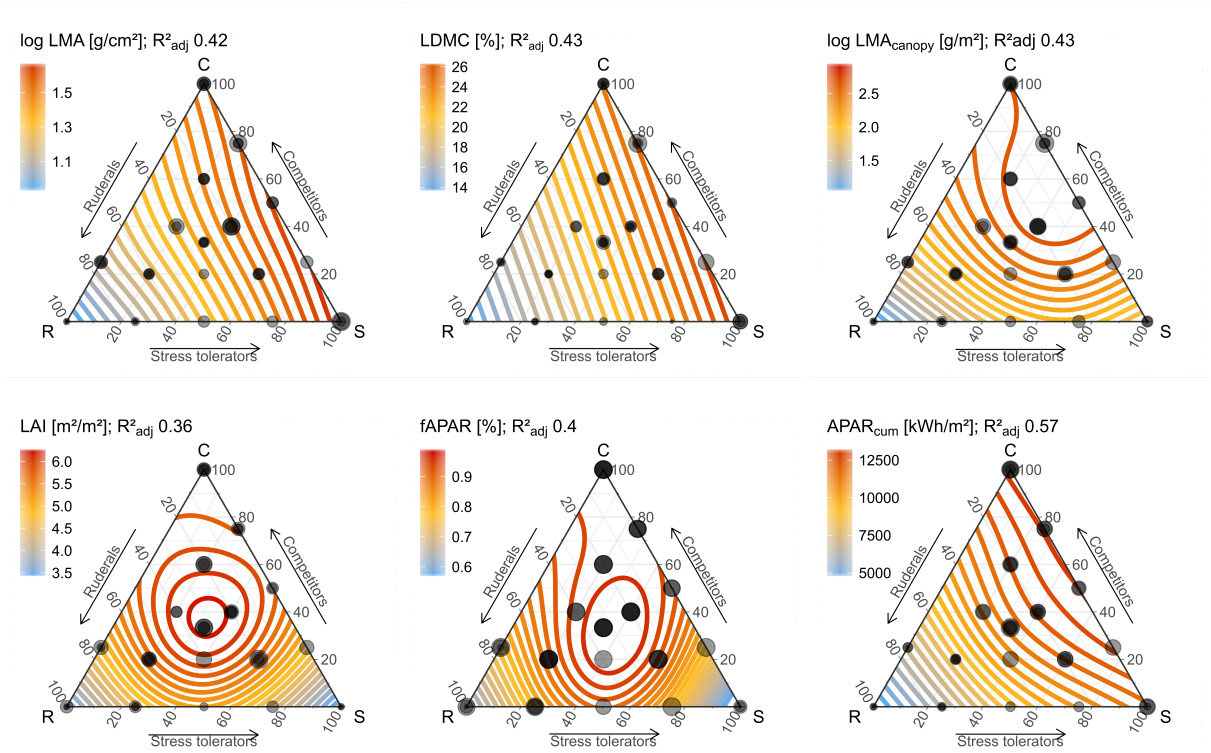

Figure 4.4: Distribution of plant traits in the CSR-feature space of forbs and graminoids based on GAM extrapolations. Observations are displayed as transparent grey dots with a size proportional to the respective trait.

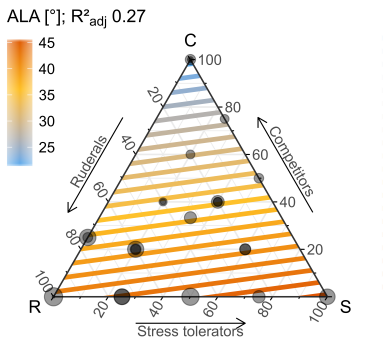

Figure 4.5: Distribution of average leaf angle (ALA) in the herbaceous CSR- feature space based on GAM extrapolations. Observations are displayed as transparent grey dots with a size proportional to the respective trait.

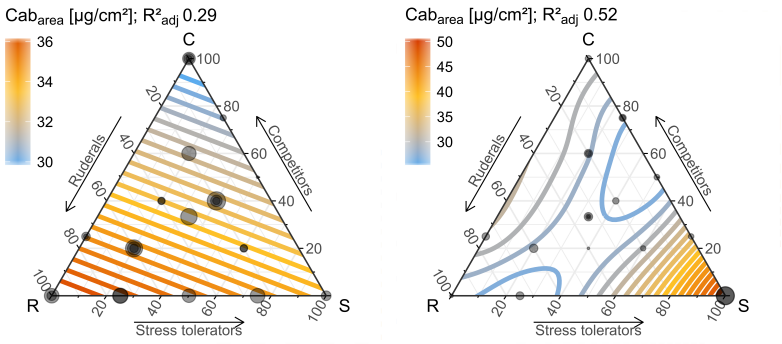

Figure 4.6: Distribution of Cab_{area} for herbaceous (left) and graminoid (right) CSR plant strategies based on GAM extrapolations. Observations are displayed as transparent grey dots with a size proportional to the respective trait.

4.4 Discussion

From a reductionist perspective vegetation canopies can be considered as solar power plant and various functions and traits thereof are coordinated to ensure an efficient energy generation through adaptions to environmental factors (e.g. nutrient availability, temperature) and biotic interactions (e.g. competition) (Ehleringer 1986; Ustin and Gamon 2010). Consequently, our results confirm that plant functions and strategies are expressed through traits which directly affect or are directly related to optical processes in plant canopies and thus determine their reflectance. This interrelationship 'reflectance follows function' firstly provides the physical basis for the retrieval of differences in plant functions by means of optical earth observation data and underlines the potential to track earth's functional diversity. Secondly, linking plant functions and strategies through radiative transfer (and optical traits) provides a different and additional perspective on how environmental factors and biotic interactions shape plant functional diversity.

Why does the reflectance of plant canopies follow function? Our results evidence strong links between optical plant traits and the two schemes that we used as baselines for plant functioning, that is the Leaf Economic Spectrum (LES) and CSR plant strategies. Originally the LES was captured through leaf lifespan, LMA, photosynthetic capacity, dark respiration rate, nitrogen and phosphorus content (Wright et al. 2004). Thus, as being one of the original constituents the variation of the measured LMA shows an obvious correspondence to the LES, whereas we

also found significant correlations with $pigment_{mass}$, and $pigment_{area}$ as these are directly linked to photosynthetic capacity and nitrogen content (essential constituent in chlorophylls inherent Rubisco, Pons et al. 1998). In general it can be assumed that pigments contents ($pigment_{area}$) increase with leaf lifespan, whereas the concentration of pigments ($pigment_{mass}$) decreases. Thus, the investments in leaf tissue proportionally outweigh investments in leaf pigments, which can be explained as with increasing chlorophyll content light absorption follows a saturating curve, since chloroplasts become increasingly stacked in the palisade cells resulting in intraleaf shading (Terashima and Hikosaka 1995; Evans 1996; Evans and Poorter 2001). Accordingly, plants with short leaf lifespan invest fewer pigments to maximize the energy revenue returned. However, the LES reflects only one primary dimension of plant functioning, ranging from quick to slow return on leaf resource investments. Accordingly, traits which integrate the canopy structure (LAI, LMA_{canopy}, ALA, fAPAR or $APAR_{cum}$) show no significant correspondence to the LES, which suggests that these traits are related to other functional axes (compare Fig. 4.3). In the 'global spectrum of plant form and function' (Díaz et al. 2015) identified two major axis of plant functional convergence, with one axis reflecting leaf resource investments (LES) and the other axis reflecting plant and organ size-related traits. We thus assume that optical traits integrating canopy properties correspond to the size-related axis. This is confirmed by significant relationship between these optical traits and the multidimensional CSR space, which characterizes plant functioning in terms of competitive, stress tolerant and ruderal abilities at the whole plant level (Pierce and Cerabolini 2018). Accordingly, multiple traits which do not exhibit coherence to the LES, (e.g. LAI, LMA_{canopy}, or fAPAR) in turn showed a notable correspondence to the CSR space. Our results confirm previous relationships between traits and the CSR space and exhibit gradients which have not been assessed before: In agreement with pivotal formulations of the CSR scheme (Grime et al. 1997) and the allocation by (Hodgson et al. 1999), LMA is lowest for ruderal species and highest for stress tolerators, closely followed by competitors (Fig. 4.4). Leaf mass per canopy area, i.e. LMA_{canopy} (LMA · LAI), which was to our knowledge not compared to CSR strategies before, reflects total leaf carbon assimilation per canopy area. We found highest LMA_{canopy} for competitive species, followed by intermediate LMA_{canopy} for stress tolerators and intermediates and lowest values for ruderals. This gradient

reflects the primary principles of the plant strategies (Grime et al. 1997); stress tolerators feature a conservative growth with a long leaf lifespan resulting in a steady accumulation of dry matter, whereas ruderals are adapted to disturbance events and thus have short lifecycles in which they accumulate few resources. Competitors feature both high productivity and a relatively long lifespan and therefore highest resource accumulation (LMA_{canopy}).

EWT [g/cm^2] nor EWT_{canopy} show a correspondence with plant strategies. In contrast LDMC, which is the ratio of leaf mass and leaf water content (LDMC= LMA/(LMA+EWT)), shows a clear coherence towards plant strategies and was therefore already used by (Hodgson et al. 1999) to allocate CSR scores. This suggests that functional characteristics are rather expressed through the relative water concentration in leaf tissue rather than the absolute leaf water content.

A more complex pattern was determined for LAI, where intermediate species (CSR) have highest LAI values followed by competitors, and lowest LAI values correspond to high S and R scores. We thus assume that intermediate species (CSR) invest a large share of resources in foliage area, whereas competitors, ruderals and stress tolerators invest more resources towards their strategy-specific trait-expressions and functions. Competitors occur primarily in nutrient rich sites, where competition for sun light is most pronounced and triggers increased height growth to overtop neighboring individuals. Increased canopy height in turn requires additional resource investments in support tissues, e.g. in the stem for vertical plant growth itself as well as in enhanced leaf robustness (higher LMA) to compensate for increased exposure to wind (compare LMA gradient, Fig. 4.4, Niinemets 2010). An increased LMA was also found for plants adapted to high light intensities (competitors) through increased palisade parenchyma to maximize photosynthetic capacity and thus quantum yield per unit leaf area and reduce potential light saturation (Björkman 1981; Poorter et al. 2009). This suggests that relative to intermediate strategies, competitors therefore invest fewer resources in the development of total foliage area (LAI). Thus, competition for sun light might enforce a trade-off between the maximization of height growth and the maximization of light interception, which was also found for tropical tree species by (Poorter et al. 2006), who reported that shade tolerant species with smaller canopy heights in turn were observed to accumulate more leaves.

Leaf inclination (ALA) does not show a trivial correspondence to the CSR spectrum, but differs

between growth forms, reflecting generic differences in the canopy architecture of graminoids and forbs. Variation in leaf angles across graminoid strategies shows no explicit pattern. For forb strategies ALA increases from competitive forbs to stress tolerant and ruderal forbs (Fig. 4.5). This agrees with Hikosaka and Hirose (1997) who simulated leaf angle distributions for plant canopies and found lower leaf angles with increasing competition. Competitive forbs, which aim to overtop and shade out the surrounding and competing plants, develop rather flat leaf angles to deplete or scatter most of the light before it is available for rivals. However, a horizontal leaf position requires increased support costs for petioles and branches and is generally less efficient for light absorption as inter alia self-shading and light saturation increases (Niklas 1994, Hikosaka and Hirose 1997). Leaf angles thus increase with decreasing competition to scatter light between leaves and hence distribute light into the lower canopy (Huemmrich 2013b; Hikosaka and Hirose 1997).

As also found for the LES the derived distributions of chlorophylls, carotenoids and anthocyanins across the CSR space are very alike (Appx. 3.8, Fig. A.6)), as pigments are usually highly correlated in mature leaves (Feret et al. 2017). Yet, the relationships differ greatly among pigments measured on an area basis ($pigment_{mass}$) and measured on a mass basis ($pigment_{area}$, Appx. 3.8, Fig. A.4). The relationship between $pigment_{area}$ and CSR strategies further differs between forbs and graminoids (Fig. 4.6), which agrees with (Tjoelker et al. 2005), who found differences in leaf photosynthetic activity between grasses and forbs. For forbs ruderals and intermediates feature highest $pigment_{area}$. Among graminoid strategies $pigment_{area}$ shows a low and inconclusive variation across the CSR space apart from a strong increase for extremely stress tolerant graminoids (*Festuca ovina* and *Nardus stricta*).

Pigments normalized by mass ($pigment_{mass}$) show a very consistent gradient across growth forms (Appx. 3.8), which however almost exclusively mirrors the LMA gradient (r^2 = 0.74, 0.80, 0.85 for Cab_{mass}, Car_{mass}, Ant_{mass}, respectively). This is further confirmed as the modelled $pigment_{mass}$ values across the CSR-space are highly correlated with $pigment_{mass}$ values based on a null-model, in which we sampled random pigmentsarea values that were subsequently divided by LMA and thus mass normalized (r^2 = 0.80, 0.91, 0.64 for Cab_{mass}, Car_{mass}, Ant_{mass}, respectively). Accordingly, we found that $pigments_{mass}$ indeed do not reflect pigment

variation per se, but rather the LMA gradient, which varies in higher magnitudes than traits with photosynthetic function (Osnas et al. 2013; Lloyd et al. 2013). Likewise the strong correspondence between $pigment_{mass}$ and the LES can largely be attributed by the high variation in LMA, as indicated by the null-model (Appx. 3.8). This indicates that contrary to its frequent application (see e.g. Asner and Martin 2009 or Jetz et al. 2016) the characterization of plant canopies through pigments on a mass basis is greatly redundant with LMA therefore appears to be not expedient.

The distribution of simulated fAPAR across the CSR space shows a strong correspondence to LAI (Fig. 4.4), which suggests that variation in light harvesting is particularly determined by LAI (in line with Hikosaka and Hirose 1997; Asner et al. 2003 and Huemmrich 2013a) and therefore highest for intermediate strategies followed by competitors. Yet, fAPAR solely represents the potential energy gain at a point in time (here averaged for the course of a day) and thereby does not consider phenological differences between plant strategies. Accordingly we modelled the accumulated photosynthetic active radiation, i.e. $APAR_{cum}$, which integrates fAPAR and the course of absorbed direct and diffuse radiation (assessed from Helios-3 archives, Espinar et al. 2012) during a plants phenological season (recorded for the cultivated plants). $APAR_{cum}$ thus reflects the accumulated photosynthetic and carbon assimilation during a plant's growth period (Goward et al. 1985). $APAR_{cum}$ showed a very consistent and clear pattern across growth forms; corresponding to their short growth period ruderals feature the lowest $APAR_{cum}$. Intermediate $APAR_{cum}$ is found for stress tolerators which can compensate conditions that limit productivity through robustness and persistence, resulting in a comparably low but prolonged light harvesting. Highest $APAR_{cum}$ is found for competitors, as competitive abilities require long-term investments (e.g. height growth) that are rewarded with long term-returns. These results thus show that the phenology-dependent variation in energy acquisition directly reflects established plant strategies and functions. Moreover, the comparable strong relationship with $APAR_{cum}$ emphasize that gradients in plant productivity are not fully reflected by a single biochemical or structural trait, but relate to the integrated response of pigments, LAI, ALA as well as phenology (Ollinger 2011). This particularly highlights the potential of multitemporal earth observation data for mapping functional gradients. The overall strong correlation between

gradients derived from $APAR_{cum}$ and LMA_{canopy} (r^2 = 0.88) underlines the plausibility of the results, as a large share of the absorbed energy is used for carbon assimilation in leaves (Pons et al. 1998). The minor discrepancy between $APAR_{cum}$ and LMA_{canopy} exists for competitors, where photosynthetic assimilation ($APAR_{cum}$) is highest, but LMA_{canopy} shows a slight bias towards C-CSR, which could result from competitors investing a considerable part of their resources in height growth rather than total leaf tissue.

According to our results Cbrown and N_{meso} do not show a consistent relation to the CSR strategies across growth forms. Both traits only correspond to CSR strategies among graminoids (Appx. 3.7). In agreement with Jacquemoud and Baret (1990) N_{meso} correlates with LMA. The distribution of Cbrown could not be explained in an ecological context. Overall, Cbrown and N_{meso} have a relatively low impact on canopy reflectance (Jacquemoud 1993) and do not greatly contribute to the spectral differentiation of variations in plant functioning (Kattenborn et al. 2018). The trait measurements used in this study were retrieved from plants cultivated under optimum growth conditions. It can be expected that some traits more explicitly express their functional role under certain circumstances. For instance increased leaf anthocyanin content has been observed during pathogen infections (Zarco-Tejada et al. 2018). Furthermore, a plants ability to cope with excess incident radiation can be expressed through developing ample leaf carotenoid content (Feret et al. 2017).

4.5 Conclusion

Optical remote sensing data is ascribed a high potential to track earth's functional diversity. Yet, causal explanations on why plant functioning can be differentiated using canopy reflectance sensed by optical earth observation data remain limited. Our findings demonstrate that bridging ecological theory and canopy reflectance through radiative transfer modelling allows us to identify the causal links between canopy reflectance and plant functioning. These links suggest that canopy 'reflectance follows function', meaning that adaptations of plants to their environment are directly 'reflected' in their optical properties across the visible, near and short wave infrared wavelengths. More specifically, it was found that plant functions and strategies are considerably

expressed through multiple structural, physiological and phenological traits with relevance for canopy reflectance and thus optical earth observation data. This opens up new opportunities for understanding plant functional changes in space and time. As indicated by (Reich 2014) increasing the dimension of relevant traits for an ecological system allows us to more precisely and completely understand and predict ecosystem dynamics and ecological processes such as community assembly. (Kunstler et al. 2016) further suggest trait ecology may lack a sufficient variety of traits to capture dissimilarities and explain competition among species. As shown here optical plant traits depict variations in multiple plant functions and can thus complement the suite of determinable proxies to describe spatial variation in plant functioning and community assembly. This is particularly emphasized as several optical plant traits show comparable or even stronger correlations with CSR plant strategies (LAI, LMA_{canopy}, $APAR_{cum}$) than those traits that were originally used to allocate the CSR space (e.g. LMA or LDMC, Hodgson et al. 1999). Upcoming hyperspectral satellite missions such as EnMAP (Stuffler et al. 2007) or HyspIRI (Roberts et al. 2012) will provide optical reflectance products that are sensitive to the optical plant traits considered in this study. Our results therefore encourage further research to deepen our understanding how plant functioning is expressed through optical plant traits using more extensive trait data and further traits incorporated in more complex radiative transfer models (e.g. crown architecture), such as INFORM (Atzberger 2000) or FLIGHT (North 1996).

Acknowledgements

The project was funded by the German Aerospace Centre (DLR) on behalf of the Federal Ministry of Economics and Technology (BMWi), FKZ50EE 1347. We would like to thank all employees of the botanical garden of the Karlsruher Institute for Technology (KIT), especially Peter Nick and Christine Beier, for their generous support. The study has been supported by the TRY initiative on plant traits (http://www.try-db.org). The TRY initiative and database is hosted, developed and maintained by J. Kattge and G. Boenisch (Max Planck Institute for Biogeochemistry, Jena, Germany). TRY is currently supported by Future Earth/bioDISCOVERY and the German Centre for Integrative Biodiversity Research (iDiv) Halle-Jena-Leipzig.

4.6 Methods

4.6.1 Retrieval of the traits space implemented in PROSAIL

We derived the PROSAIL trait space from in-situ measurements performed in outdoor cultivated plants, including 45 forb and graminoid species covering the full range of the CSR spectrum (Tab. 4.2). We performed the seed propagation in greenhouses and moved the plants outdoor for a week of acclimatization once they were grown to an adequate size. Afterwards the plants were planted out in four repetitions in separate pots with a size of 0.4 m · 0.4 m and 30 l volume filled with a standardized substrate. Fewer repetitions had to be planted for species where seedling propagation was less successful. All pots were regularly fertilized, weeded and irrigated.

For each species we measured the considered traits on a weekly basis for each pot. We determined the species specific trait expressions by averaging the measurements among pots and subsequently calculating the median for the whole season. In the current study we only considered measurements that were performed in non-senescent canopies of adult plants (here defined as plants with closed canopy).

In view of the envisaged amount of measurements per species traditional approaches for pigment retrieval such as the spectrophotometer method by (Lichtenthaler 1987) were not feasible. Furthermore, N_{meso} and Cbrown are specific parameters of PROSPECT. We thus measured leaf chlorophyll content (Cab_{area}), carotenoid content (Car_{area}), anthocyanin content (Ant_{area}), mesophyll structure coefficient (N_{meso}) and brown pigment content (Cbrown) using leaf reflectance spectra and their inversion using the leaf radiative transfer model PROSPECT-D (Feret et al. 2017). We acquired leaf spectra of 5 individual leaves per cultivated pot using an ASD FieldSpec III (ASD, Inc. Boulder, CO, USA) attached with a plant probe and leaf clip. For species with leaves not wide enough for the opening of the plant probe (2 cm diameter) we seamlessly and without overlap placed the leaves side by side on an adhesive tape. The inversion of PROSPECT-D was based on a lookup table approach and wavelets (Blackburn 2006; Blackburn and Ferwerda 2008; Cheng et al. 2011; Ali et al. 2015). Further details on the inversion procedure and its validation are given in Appx. 3.1. We estimated LAI using an Accu-PAR LP-80 ceptometer equipped with an external reference sensor to account for the current photosynthetic

active radiation (PAR). For each pot we recorded and subsequently averaged 18 individual measurements. We measured leaf mass per area (LMA) and equivalent water thickness (EWT) per species rather than per pot in order to limit the destructive impact over time. Samples included only leaflets without petioles and rachis. The fresh mass of around 10 g of whole leaves per species was measured on site. The total leaf area of these leaf samples was retrieved using a flatbed scanner. LMA [g/cm^2] was derived by drying the sample material at 70°C for at least 72 h. EWT [g/cm^2] was derived by subtracting LMA from leaf fresh mass per area.

ALA was retrieved from leaf inclination distributions that we determined using leveled digital photograph and the procedure described by (Ryu et al. 2010). For each species we measured not less than 50 angles of leaves parallel to the viewing direction. The leaf angle distributions and ALA respectively were only retrieved once as this procedure is very laborious.

We deduced additional traits from the PROSAIL traits space to further exploit its information content: leaf dry matter content (LDMC = LMA/(LMA+EWT)); canopy leaf mass per area (LMA_{canopy} = LMA · LAI); canopy pigment content ($pigment_{canopy}$ = $pigment_{area}$ · LAI); fraction of absorbed photosynthetic active radiation (fAPAR) simulated using PROSAIL (Verhoef and Bach 2007, details sensu Appx. 3.3); cumulative absorbed photosynthetic active radiation ($APAR_{cum}$ in kWh/m^2), which corresponds to the total absorbed energy within the growing season of each species. $APAR_{cum}$ was approximated as the product of fAPAR, incoming direct and diffuse irradiance averaged for April-October (data assessed from Helios-3 data, Espinar et al. 2012, details sensu Appx. 3.3) and the length of the growing season, (here defined as the observed number of weeks between begin of adolescence and senescence). A statistical summary of the trait space is given in Appx. 3.2.

4.6.2 Linking the Leaf Economic Spectrum and optical plant traits

(Wright et al. 2004) determined the LES using the first component of a principal component transformation of six leaf traits, i.e. LMA, photosynthetic assimilation $rate_{mass}$, leaf $nitrogen_{mass}$, leaf $phosphorus_{mass}$, dark respiration $rate_{mass}$ and leaf lifespan. From those traits we only measured LMA (or SLA respectively) within the above described plant experiment. We therefore requested the remaining traits from the TRY-database, where sufficient data was

Table 4.2: List of all cultivated species. The number in brackets indicates the number of repetitions per species followed by the allocated CSR strategy.

Graminoids (n=20)	**Forbs (n=25)**
Alopecurus geniculatus (4, R/CSR); *Alopecurus pratensis* (4, C/CSR); *Anthoxanthum odoratum* (4, SR/CSR); *Agrostis capillaris* (4, CSR); *Apera spica-venti* (4, R/SR); *Arrhenatherum elatius* (4, C/CSR); *Brachypodium sylvaticum* (4, S/SC); *Bromus hordeaceus* (3, R/CR); *Calamagrostis epigejos* (4, C/SC); *Deschampsia cespitosa* (4, S/CSR); *Digitaria sanguinalis* (4, R/SR); *Festuca ovina* (4, S); *Holcus lanatus* (4, CSR); *Luzula multiflora* (4, S/CSR); *Molinia caerule*a (2, SC); *Nardus Stricta* (4, S); *Phalaris arundinacea* (4, C); *Poa annua* (4, R); *Scirpus sylvaticus* (4, C/SC); *Trisetum flavescens* (4, CSR);	*Aegopodium podagraria* (4, CR/CSR); *Anthyllis vulneraria* (2, S/SR); *Arctium lappa* (4, C); *Centaurium erythraea* (4, SR); *Cirsium arvense* (4, C); *Cirsium acaule* (3, CS/CSR); *Digitalis purpurea* (4, CR/CSR); *Filipendula ulmaria* (1, C/SC); *Geum urbanum* (4, S/CSR); *Geranium pratense* (4, C/CSR); *Geranium robertianum* (R/CSR); *Plantago major* (4, R/CSR); *Clinopodium vulgare* (4, S/CSR); *Campanula rotundifolia* (4, S); *Lamium purpureum* (4, R); *Lapsana communis* (4, R/CR); *Medicago lupulina* (3, R/SR); *Origanum vulgare* (4, CS/CSR); *Pulicaria dysenterica* (4, CS); *Stellaria media* (4, R/CR); *Succisa pratensis* (3, CS/CSR); *Taraxacum officinale* (4, R/CSR); *Thlaspi arvense* (3, R); *Trifolium pratense* (4, CSR); *Urtica dioica* (4, C);

freely available for 26 of the 45 species (see Appx. 3.4) for a list of the 26 species) and two further traits, i.e. leaf nitrogen$_{mass}$, leaf phosphorus$_{mass}$. We determined the LES for the 26 species using the log10 transformed expressions of these three traits and the loadings reported by (Wright et al. 2004). The LES retrieved this way was compared (projected) to the trait space of PROSAIL through a principal component analysis (PCA). Prior to the PCA the PROSAIL traits were centred and scaled.

4.6.3 Linking CSR plant strategies and optical plant traits

The position of a species in the CSR space is defined by three axis expressing competitive, stress tolerant and ruderal abilities (scores). We used the CSR scores provided by (Hodgson et al. 1999), who allocated CSR strategies for a multitude of European plant species using trait expressions of canopy height, LDMC, flowering period, flowering start, lateral spread, LMA and specific leaf area (Tab. 4.2). For few species we adopted the allocation based on the BIOLFLOR database (Kühn et al. 2004) and expert knowledge. We assessed the relationship between each PROSAIL trait and the CSR space using non-parametric models, i.e. generalized additive models (GAM) and thin plate regression splines (Wood 2003). As input for the GAM we used the first two PCA components (cumulative variance 97%) instead of the raw CSR

scores to facilitate the interpretability of the results. The results were visualized in ternary plots (R-package ‘ggtern’, Hamilton et al. 2016)

5 Remote sensing leaf photosynthetic pigments as concentration [%] is flawed and should be quantified as content [µg/cm^2] instead

---

This chapter is based on a journal article currently under review: *Kattenborn, T., Schiefer, F., Zarco-Tejada, P. & Schmidtlein, S. (in review). Remote sensing leaf photosynthetic pigments as concentration [%] is flawed and should be quantified as content [µg/cm^2] instead. Remote Sensing of Environment.*

5.1 Abstract

Photosynthesis is essential for life on earth as it inter alia determines the composition of the atmosphere and is the driving mechanism of primary production. Photosynthetic capacity is particularly determined by leaf photosynthetic pigments such as chlorophyll, carotenoids or anthocyanins. These pigments absorb the required energy in form of visible solar radiation. Being sensitive to this spectral information optical earth observation sensors evolved as a promising technology to map the spatial and temporal variation of these photosynthetic pigments. Thereby, leaf pigments are either quantified as leaf area-based content [µg/cm^2] or as leaf mass-based concentration [g/g or %]. However, these two metrics are fundamentally different and until now there is neither an in-depth discussion nor a consensus on which metric to choose. This is underlined as approximately a third of the studies do not explicitly differentiate between pigment content and concentration. We therefore clarify the differences between both metrics and thereupon evidence that the remote sensing of leaf pigment concentration [%] is unsubstan-

tial, as firstly pigment concentration primarily reflects variation in leaf mass per area and not pigments itself. Secondly, the radiative transfer in plant leaves is determined by the absolute content of pigments in a leaf and not its relative concentration to other leaf constituents. Thirdly, as being a ratio pigment concentration is an unambiguous metric which further complicates the quantification of leaf pigments at the canopy scale. We thus conclude that remote sensing of leaf pigments should be performed on an area basis [µg/cm^2].

5.2 Significance statement

Photosynthetic leaf pigments indicate a plants physiological status and functioning and are of direct relevance for biosphere-atmosphere interactions and biological cycles. For the temporal and spatial quantification of leaf pigments optical remote sensing became an important technology. However, there is no consensus on how leaf pigments should be quantified, i.e. as area-based content [µg/cm²] or as mass-based concentration [%]. These two metrics are fundamentally different in terms of the remote sensing-based retrieval and their plant physiological relevance. Our paper firstly clarifies the differences between pigment content [µg/cm²] and concentration [%] and demonstrates that for statistical reasons and principles of plant physiology and radiative transfer the remote sensing of pigment concentration [%] is unsubstantial.

5.3 Introduction

Plants on the earth surface are indispensable for the production of oxygen and organic matter through photosynthesis. Photosynthesis is primarily driven by pigments which are hence important links to assess plant stress, plant functioning, biological cycles and biosphere-atmosphere interactions (Nelson and Yocum 2006; Blackburn 2006; Kattenborn et al. 2018). Pigments absorb incident radiation in the visible spectrum, whereas radiation that is not absorbed by the canopy or the ground is scattered. These scattered remnants of the incident radiation constitute the basis for quantifying pigments such as chlorophylls, carotenoids or anthocyanins using optical remote sensing observations (Tucker and Sellers 1986; Jacquemoud et al. 1996; Blackburn 2006; Kattenborn et al. 2017; Zarco-Tejada et al. 2018). Commonly pigments are quantified

on two scales, either as pigment content, i.e. pigment mass per leaf area [µg/cm²] (onwards $pigment_{area}$) or as pigment concentration, i.e. pigment mass per leaf dry mass [g/g or %] (onwards $pigment_{mass}$). Note that content and concentrations are often used interchangeably, while here we use content for per-area and concentration for per-mass. It appears to be inconclusive which quantification method to choose in remote sensing as both are referred to in studies with similar objectives (e.g. Jacquemoud et al. 1996; Zarco-Tejada et al. 2001; Asner and Martin 2009; Jetz et al. 2016). Here, we argue that quantifying $pigment_{mass}$ with remote sensing is unsubstantial as 1) this measure does not explicitly reflect variation in pigments per se, but rather variation in leaf dry matter content, 2) $pigment_{mass}$ is less accurately retrieved than $pigment_{area}$ using optical remote sensing and 3) it is more difficult to up-scale $pigment_{mass}$ to the canopy scale. We deduce that quantifying $pigments_{area}$ is more appropriate in remote sensing, due to its explicit relation to radiative transfer, enhanced scalability and, as explained below, as a more direct expression of plant stress and functioning.

5.4 Pigment concentration primarily reflects leaf mass and not pigment variation itself

Put simply $Pigment_{mass}$ [%] is the ratio of $pigment_{area}$ [µg/cm^2] and the Leaf Dry Mass per Area [g/cm^2] (LMA). Leaf mass is composed of carbohydrates (hemi-cellulose, cellulose, starch), proteins, lignin and waxes, and it generally reflects differences in leaf lifespan resulting from adaptations to environmental factors (Wright et al. 2004). As evinced using global trait databases LMA has a higher variance than leaf traits that are related to photosynthesis (e.g. leaf nitrogen content or photosynthetic capacity, see Wright et al. 2004; Osnas et al. 2013; Lloyd et al. 2013). This is critical as leaf resource investments (e.g. LMA) and leaf traits relating to photosynthesis are largely independent of one another (Osnas et al. 2013; Lloyd et al. 2013; Osnas et al. 2018) and accordingly the division by LMA actually dominates the actual variation of pigments content. Here we demonstrate these relationships for pigment content using a dataset comprising median LMA, $chlorophyll_{area}$, $carotenoid_{area}$ and $anthocyanin_{area}$ values from 45 herbaceous species retrieved in-situ (see supporting information for details).

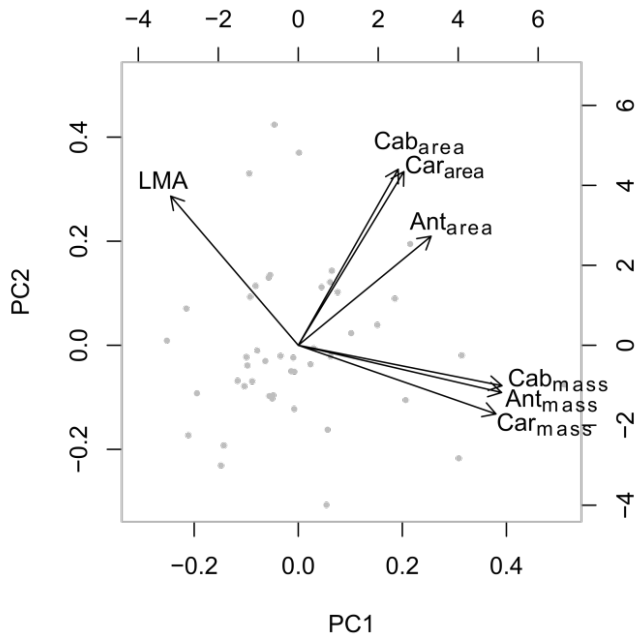

Figure 5.1: Principal component transformation of LMA, chlorophyll$_{area}$, carotenoid$_{area}$, anthocyanin$_{area}$, chlorophyll$_{mass}$, carotenoid$_{mass}$ and anthocyanin$_{mass}$. Pigments$_{area}$ are largely independent from LMA, whereas pigments$_{mass}$ predominantly reflect the variation in LMA.

The coefficient of variation of LMA (38.4 %) clearly exceeds those of chlorophyll$_{area}$ (24.8%), carotenoid$_{area}$ (15.0%), and anthocyanin$_{area}$ (26.1%). Correspondingly, a principal component analysis (Fig. 5.1) of LMA, pigments$_{area}$ and pigments$_{mass}$ (pigment$_{area}$/LMA) reveals that pigments$_{mass}$ primarily reflect the LMA gradient (strong negative correlation). Gradients of pigments$_{area}$ in contrast are largely uncorrelated with LMA. Thus, it can generally be expected that spatial gradients of pigments$_{mass}$ predominantly mirror the variation in LMA, whereas the actual spatial variation of pigments$_{area}$ is severely diluted.

5.5 Remote sensing of pigment content outperforms pigment concentration retrievals

As reported by previous authors the retrieval of leaf constituents is stronger for absolute contents per area than for concentration per mass (Grossman et al. 1996; Jacquemoud et al. 1996; Oppelt and Mauser 2004). This can be explained by the radiative transfer mechanisms. Leaf constituents affect the reflectance properties of a plant canopy through absorption, whereas absorp-

tion increases with increasing contents of the respective constituent (e.g. $pigments_{area}$) and in turn reflectance decreases. The spectral signal is thus determined by the absolute content of the constituent (e.g. $pigments_{area}$) and not by its concentration relative to other constituents (here LMA). Or put differently, concentrations ($pigment_{mass}$) cannot represent the absolute amount of matter interacting with radiation (also see Jacquemoud et al. (1996)). For this reason, pigments in radiative transfer models are parametrized by specific absorption coefficients on an area basis. As $pigment_{mass}$ is the ratio of $pigment_{area}$ to LMA, it further implies that remote sensing of $pigment_{mass}$ (e.g. through empirical models) requires the simultaneous consideration of spectral features corresponding to both $pigment_{area}$ (in the visible range) and LMA (in the short wave infrared range), as illustrated in Fig. 5.2a. However, the retrieval of LMA using optical reflectance is inevitably less accurate than $pigment_{area}$ as the respective spectral features are overshadowed by water absorption (Jacquemoud et al. 1996) and short wave infrared information is generally affected by lower signal to noise ratios (Cocks et al. 1998). Uncertainties in the retrieval of LMA spectral features propagate into errors of $pigment_{mass}$ assessments. Thus, the retrieval of $pigment_{mass}$ is substantially impaired as it requires spectral information of the short wave infrared range (which is not always available) and the generally less accurate retrieval of the LMA variation. In contrast, the retrieval of $pigment_{area}$ only relies on spectral features in the visible range (Fig. 5.2b).

5.6 Pigment concentration is a rather inconclusive proxy with impaired scalability

As being a relative concentration, $pigment_{mass}$ is a rather inconclusive metric: high $pigment_{mass}$ can result from either high $pigment_{area}$ and intermediate LMA or intermediate $pigment_{area}$ and low LMA. It is therefore possible for two leaves or plant canopies to be equal in $pigment_{mass}$, but greatly different in $pigment_{area}$ and LMA. Accordingly, $pigment_{mass}$ does not explicitly indicate if a plant canopy actually has low pigment content, e.g. due to stress or its inherent plant functional properties (compare Fig. 5.3).

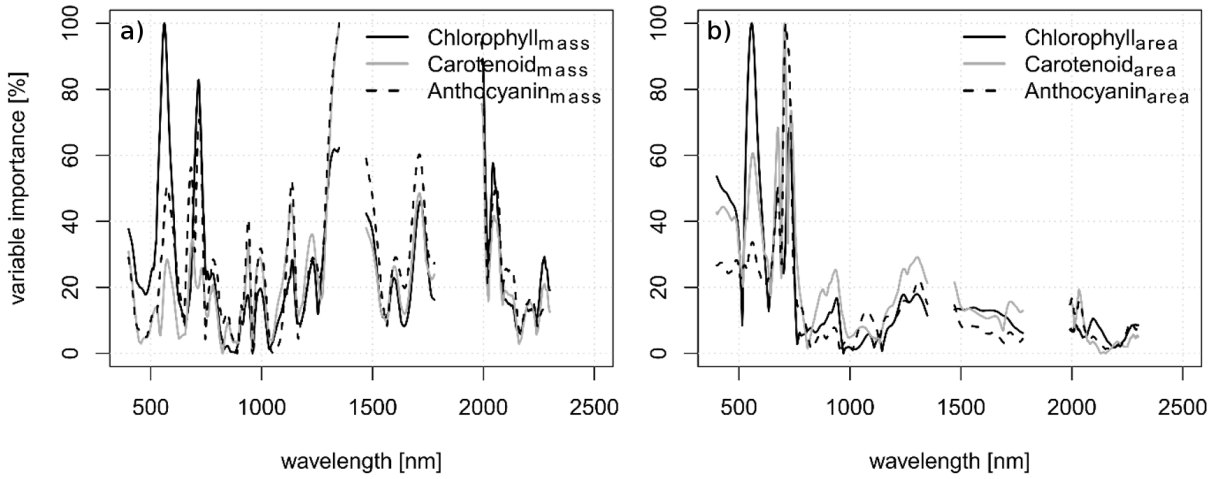

Figure 5.2: Variable importance of partial least square regression models for the retrieval of a) pigment$_{mass}$ and b) pigment$_{area}$ based on 593 canopy spectra of 45 herbaceous species (see supplementary information for details). The variable importance demonstrates that the pigment$_{mass}$ retrieval relies on visible and shortwave-infrared information (pigments and LMA), whereas the retrieval of pigment$_{area}$ solely relies on visible information.

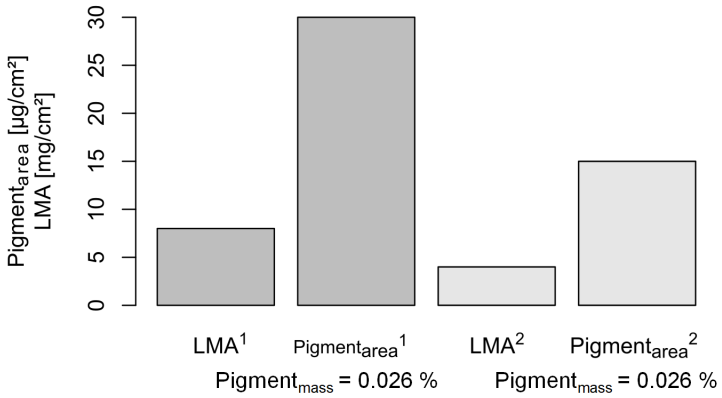

Figure 5.3: Scheme demonstrating equal pigment concentration despite varying LMA and pigment contents of two samples (1,2).

This ambiguity likewise limits the scalability to the canopy level, that is pigment content per canopy surface area (canopy pigment content [g/m^2], onwards pigment$_{canopy}$). Pigment$_{canopy}$ reflects the absolute photosynthetic capacity of a vegetated area and is thus directly relevant for assessing productivity or atmosphere-biosphere interactions (De Pury and Farquhar 1997; Peng et al. 2011). In case of scaling pigment$_{mass}$ to pigment$_{canopy}$ prior knowledge on the total amount of foliage in the canopy surface area is required, i.e. Leaf Area Index [m^2/m^2] (LAI), and the LMA of the foliage (eq. 5.1), whereas as described above the quantification of LMA is generally limited using optical remote sensing (compare Homolová et al. 2013). In contrast, scaling pigment$_{area}$ to pigment$_{canopy}$ solely requires the multiplication with LAI (eq. 5.2) which

can be retrieved from remote sensing data with very acceptable accuracy (Zarco-Tejada et al. 2001; Myneni et al. 2002; Schlerf et al. 2005).

$$pigment_{\text{canopy}} = pigment_{\text{mass}} \cdot LAI \cdot LMA \tag{5.1}$$

$$pigment_{\text{canopy}} = pigment_{\text{area}} \cdot LAI \tag{5.2}$$

5.7 Discussion and Concluding remarks

Based on the above arguments, we strongly advocate to focus on pigment content per area, rather than pigment mass concentration, for the monitoring of vegetation photosynthesis and physiological status. There may be situations conceivable where $\text{pigment}_{\text{mass}}$ provides the information sought, e.g. for plant nutritional quality for herbivores. The studies currently reporting on $\text{pigment}_{\text{mass}}$ (see supplementary data) do so without justification, with substantial implications. We assume that the frequent use of $\text{pigment}_{\text{mass}}$ may firstly be a heritage from plant ecology, where for instance leaf nutrients (e.g. nitrogen or phosphorus) are frequently quantified on a mass basis rather than an area basis (see Wright et al. 2004 or Díaz et al. 2015). However, as indicated above and by Osnas et al. (2013), Lloyd et al. (2013) and Osnas et al. (2018), normalizing traits describing photosynthetic functions on a mass basis introduces severe statistical and conceptual issues, as the variance in leaf resource investments is naturally higher than the variance of photosynthetic traits and leaf resource investments are largely independent from photosynthetic functions. Secondly, from a plant functional perspective one might argue that there is a motivation to map $\text{pigments}_{\text{mass}}$ using remote sensing, as the latter possibly indicates the photosynthetic return per invested dry matter. Following this logic, everything else being equal a plant with low LMA receives higher returns than a plant with high LMA. However, as LMA is highly correlated with leaf lifespan, implies that the eventual return per invested LMA greatly depends on the time span in which the leaf performs photosynthesis. Accordingly, $\text{pigment}_{\text{mass}}$ at a given point in time does not explicitly reveal the photosynthetic return per invested dry matter.

The literature consulted during the preparation of this short communication revealed that re-

garding pigment quantification the terms content and concentration are frequently used interchangeably (in 32% of the studies, see supplementary information). Future studies should make it very explicit what they are quantifying, and why, with per-leaf area-content of pigment or any other leaf constituent as the standard.

Based on the elaborated rationales we conclude that remote sensing of pigments in plants should be performed on an area and not a mass basis. We assume that these rationales also apply for the remote sensing of leaf nitrogen, as pigments and nitrogen are generally highly correlated in leaves.

Acknowledgements

The project was funded by the German Aerospace Centre (DLR) on behalf of the Federal Ministry of Economics and Technology (BMWi), FKZ50EE 1347. We would like to thank all employees of the botanical garden of the Karlsruher Institute for Technology (KIT), especially Peter Nick and Christine Beier, for their generous support.

5.8 Supplementary Information

5.8.1 Material and Methods

The trait data presented in Figure 5.1 was acquired in plants cultivated in pots ($0.3 \cdot 0.3$ m) in the botanical garden of the Karlsruher Institute of Technology (KIT). LMA [g/cm^2] and pigment contents [µg/cm^2] (chlorophylls, carotenoids and anthocyanins) were retrieved on a weekly basis from adolescence to senescence for 45 species including graminoids and forbs which were grown in four repetitions (see Tab. 5.1 for a list of the species). The pigment contents were retrieved using an inversion of PROSPECT and leaf spectra acquired with and ASD FieldSpec III equipped with a plant probe and leaf clip. Further details on the experiment and the trait retrieval are given in (Kattenborn et al. 2018). We calculated pigment concentrations ($pigment_{mass}$) by dividing pigment contents ($pigment_{area}$) with LMA. We calculated medians of the respective traits which were scaled to unit variance prior to the principal component transformation.

The variable importance of the partial least square regression (PLSR) models of $pigment_{mass}$ and $pigment_{area}$ were based on canopy reflectance spectra acquired in the same plant experiment described above. The canopy spectra were derived on a weekly basis from adolescence to senescence using an ASD FieldSpec III (ASD, Inc. Boulder, CO, USA) at a height of 0.75 m above the canopy. The ASD FieldSpec III was calibrated using a reference panel (Spectralon) to acquire absolute canopy reflectance spectra. For each cultivated pot 9 spectra were acquired in nadir at different positions and subsequently averaged, resulting in a total of 593 canopy reflectance spectra. We removed noise from the spectra using a Savitzky-Golay filter and removed spectral regions located in the water absorption bands (1350–1470, 1780–1990, 2300–2500 nm). We calibrated the PLSR models using a 10-fold cross validation with 5 repetitions and extracted PLSR internal variable importance.

Table 5.1: List of all cultivated species XXX (remove CSR!).

Graminoids (n=19)	**Forbs (n=26)**
Alopecurus geniculatus, *Alopecurus pratensis*, *Anthoxanthum odoratum*, *Agrostis capillaris*, *Arrhenatherum elatius*, *Brachypodium sylvaticum*, *Bromus hordeaceus*, *Calamagrostis epigejos*, *Deschampsia cespitosa*, *Digitaria sanguinalis*, *Festuca ovina*, *Holcus lanatus*, *Luzula multiflora*, *Molinia caerulea*, *Nardus Stricta*, *Phalaris arundinacea*, *Poa annua*, *Scirpus sylvaticus*, *Trisetum flavescens*	*Aegopodium podagraria*, *Anthyllis vulneraria*, *Arctium lappa*, *Apera spica-venti*, *Centaurium erythraea*, *Cirsium arvense*, *Cirsium acaule*, *Digitalis purpurea*, *Filipendula ulmaria* , *Geum urbanum*, *Geranium pratense*, *Geranium robertianum*, *Plantago major*, *Clinopodium vulgare*, *Campanula rotundifolia*, *Lamium purpureum*, *Lapsana communis*, *Medicago lupulina*, *Origanum vulgare*, *Pulicaria dysenterica*, *Stellaria media*, *Succisa pratensis*, *Taraxacum officinale*, *Thlaspi arvense*, *Trifolium pratense*, *Urtica dioica*

Table 5.2: Consulted literature in preparation of the presented manuscript. Concise terminology indicates if studies used pigment content and concentration interchangeability.

ID	**Publication**	**$pigment_{mass}$ or $pigment_{area}$**	**approach**	**Concise terminology**
1	Asner, G. P., Martin, R. E., Anderson, C. B., & Knapp, D. E. (2015). Quantifying forest canopy traits: Imaging spectroscopy versus field survey. Remote Sensing of Environment, 158, 15–27. https://doi.org/10.1016/j.rse.2014.11.011	mass	empirical	
2	Gitelson, A. A., & Merzlyak, M. N. (1996). Signature analysis of leaf reflectance spectra: algorithm development for remote sensing of chlorophyll. Journal of plant physiology, 148(3-4), 494-500.	area	index	no

3	Yoder, B. J., & Pettigrew-Crosby, R. E. (1995). Predicting nitrogen and chlorophyll content and concentrations from reflectance spectra (400-2500 nm) at leaf and canopy scales. Remote Sensing of Environment, 53(3), 199–211. https://doi.org/10.1016/0034-4257(95)00135-N	mass/area	empirical	
4	Schlerf, M., Atzberger, C., Hill, J., Buddenbaum, H., Werner, W., & Schüler, G. (2010). Retrieval of chlorophyll and nitrogen in Norway spruce (Picea abies L. Karst.) using imaging spectroscopy. International Journal of Applied Earth Observation and Geoinformation, 12(1), 17–26. https://doi.org/10.1016/j.jag.2009.08.006	mass	empirical	
5	Carlson, K. M., Asner, G. P., Hughes, R. F., Ostertag, R., & Martin, R. E. (2007). Hyperspectral remote sensing of canopy biodiversity in Hawaiian lowland rainforests. Ecosystems, 10(4), 536–549. https://doi.org/10.1007/s10021-007-9041-z	area	empirical	
6	Asner, G. P., & Martin, R. E. (2008). Spectral and chemical analysis of tropical forests: Scaling from leaf to canopy levels. Remote Sensing of Environment, 112(10), 3958–3970. https://doi.org/10.1016/j.rse.2008.07.003	mass	empirical	
7	Richardson, A. D., Duigan, S. P., & Berlyn, G. P. (2002). An evaluation of noninvasive methods to estimate foliar chlorophyll content. New Phytologist, 153, 185–194.	area	index	
8	Asner, G. P., & Martin, R. E. (2009). Airborne spectranomics: Mapping canopy chemical and taxonomic diversity in tropical forests. Frontiers in Ecology and the Environment, 7(5), 269–276. https://doi.org/10.1890/070152	mass	empirical	
9	Zarco-Tejada, P. J., Miller, J. R., Morales, A., Berjón, A., & Agüera, J. (2004). Hyperspectral indices and model simulation for chlorophyll estimation in open-canopy tree crops. Remote sensing of environment, 90(4), 463-476.	area	RTM	
10	Zarco-Tejada, P. J., Miller, J. R., Harron, J., Hu, B., Noland, T. L., Goel, N., ... & Sampson, P. (2004). Needle chlorophyll content estimation through model inversion using hyperspectral data from boreal conifer forest canopies. Remote sensing of environment, 89(2), 189-199.	area	RTM	
11	Zarco-Tejada, P. J., Miller, J. R., Noland, T. L., Mohammed, G. H., & Sampson, P. H. (2001). Scaling-up and model inversion methods with narrowband optical indices for chlorophyll content estimation in closed forest canopies with hyperspectral data. IEEE Transactions on Geoscience and Remote Sensing, 39(7), 1491–1507. https://doi.org/10.1109/36.934080	area	RTM	
12	Berni, J. a J., Zarco-tejada, P. P. J., Suarez, L., Fereres, E., Member, S., & Suárez, L. (2009). Thermal and Narrowband Multispectral Remote Sensing for Vegetation Monitoring From an Unmanned Aerial Vehicle. IEEE Transactions on Geoscience and Remote Sensing, 47(3), 722–738. https://doi.org/10.1109/TGRS.2008.2010457	area	RTM	no
13	Sampson, P. H., Zarco-Tejada, P. J., Mohammed, G. H., Miller, J. R., & Noland, T. L. (2003). Hyperspectral Remote Sensing of Forest Condition in Tolerant Hardwoods. Forest Science, 49(3), 381–391.	area	RTM	

14	Zarco-Tejada, P. J., Miller, J. R., Harron, J., Hu, B., Noland, T. L., Goel, N., ... Sampson, P. (2004). Needle chlorophyll content estimation through model inversion using hyperspectral data from boreal conifer forest canopies. Remote Sensing of Environment, 89(2), 189–199. https://doi.org/10.1016/j.rse.2002.06.002	area	RTM	
15	Zarco-Tejada, P. J., Miller, J. R., Morales, A., Berjón, A., & Agüera, J. (2004). Hyperspectral indices and model simulation for chlorophyll estimation in open-canopy tree crops. Remote Sensing of Environment, 90(4), 463–476. https://doi.org/10.1016/j.rse.2004.01.017	area	RTM	
16	Darvishzadeh, R., Skidmore, A., Schlerf, M., & Atzberger, C. (2008). Inversion of a radiative transfer model for estimating vegetation LAI and chlorophyll in a heterogeneous grassland. Remote Sensing of Environment, 112(5), 2592-2604.	area	RTM	no
17	Haboudane, D., Miller, J. R., Tremblay, N., Zarco-Tejada, P. J., & Dextraze, L. (2002). Integrated narrow-band vegetation indices for prediction of crop chlorophyll content for application to precision agriculture. Remote sensing of environment, 81(2-3), 416-426.	area	index	no
18	Siebke, K., & Ball, M. C. (2009). Non-destructive measurement of chlorophyll b:a ratios and identification of photosynthetic pathways in grasses by reflectance spectroscopy. Functional Plant Biology, 36(11), 857–866. http://doi.org/10.1071/FP09201	area	index	no
19	Daughtry, C. (2000). Estimating Corn Leaf Chlorophyll Concentration from Leaf and Canopy Reflectance. Remote Sensing of Environment, 74(2), 229–239. https://doi.org/10.1016/S0034-4257(00)00113-9	area	RTM	no
20	Zhang, Y. (2007). Hyperspectral remote sensing algorithms for retrieving forest chlorophyll content, (September).	area	RTM	
21	Houborg, R., Anderson, M., & Daughtry, C. (2009). Utility of an image-based canopy reflectance modeling tool for remote estimation of LAI and leaf chlorophyll content at the field scale. Remote Sensing of Environment, 113(1), 259–274. https://doi.org/10.1016/j.rse.2008.09.014	area	RTM	
22	Ramoelo, A., Skidmore, A. K., Schlerf, M., Heitkönig, I. M. A., Mathieu, R., & Cho, M. A. (2013). Savanna grass nitrogen to phosphorous ratio estimation using field spectroscopy and the potential for estimation with imaging spectroscopy. International Journal of Applied Earth Observation and Geoinformation, 23(1), 334–343. https://doi.org/10.1016/j.jag.2012.10.008	area	index	
23	Schlemmera, M., Gitelson, A., Schepersa, J., Fergusona, R., Peng, Y., Shanahana, J., & Rundquist, D. (2013). Remote estimation of nitrogen and chlorophyll contents in maize at leaf and canopy levels. International Journal of Applied Earth Observation and Geoinformation, 25(1), 47–54. https://doi.org/10.1016/j.jag.2013.04.003	area	index	
24	Wu, C., Niu, Z., Tang, Q., Huang, W., Rivard, B., & Feng, J. (2009). Remote estimation of gross primary production in wheat using chlorophyll-related vegetation indices. Agricultural and Forest Meteorology, 149(6–7), 1015–1021. https://doi.org/10.1016/j.agrformet.2008.12.007	area	index	no

25	Clevers, J. G. P. W., & Kooistra, L. (2012). Using hyperspectral remote sensing data for retrieving canopy chlorophyll and nitrogen content. IEEE Journal of Selected Topics in Applied Earth Observations and Remote Sensing, 5(2), 574-583.	area	RTM	
26	Asner, G. P., Martin, R. E., Knapp, D. E., Tupayachi, R., Anderson, C., Carranza, L., ... Weiss, P. (2011). Spectroscopy of canopy chemicals in humid tropical forests. Remote Sensing of Environment, 115(12), 3587–3598. https://doi.org/10.1016/j.rse.2011.08.020	mass	empirical	
27	Asner, G. P., Martin, R. E., Ford, A. J., Metcalee, D. J., & Liddell, M. J. (2009). Leaf chemical and spectral diversity in Australian tropical forests. Ecological Applications, 19(1), 236–253. https://doi.org/10.1890/08-0023.1	mass	index	
28	Lin, C., Popescu, S. C., Huang, S. C., Chang, P. T., & Wen, H. L. (2015). A novel reflectance-based model for evaluating chlorophyll concentrations of fresh and water-stressed leaves. Biogeosciences, 12(1), 49-66.	mass	index	
29	Broge, N. H., & Leblanc, E. (2001). Comparing prediction power and stability of broadband and hyperspectral vegetation indices for estimation of green leaf area index and canopy chlorophyll density. Remote Sensing of Environment, 76(2), 156–172. https://doi.org/10.1016/S0034-4257(00)00197-8	area	index	no
30	Haboudane, D., Miller, J. R., Pattey, E., Zarco-Tejada, P. J., & Strachan, I. B. (2004). Hyperspectral vegetation indices and novel algorithms for predicting green LAI of crop canopies: Modeling and validation in the context of precision agriculture. Remote Sensing of Environment, 90(3), 337–352. http://doi.org/10.1016/j.rse.2003.12.013	area	index	no
31	Colombo, R., Meroni, M., Marchesi, A., Busetto, L., Rossini, M., Giardino, C., & Panigada, C. (2008). Estimation of leaf and canopy water content in poplar plantations by means of hyperspectral indices and inverse modeling. Remote Sensing of Environment, 112(4), 1820–1834. https://doi.org/10.1016/j.rse.2007.09.005	area	RTM	no
32	Blackburn, G. A. (2006). Hyperspectral remote sensing of plant pigments. Journal of Experimental Botany. 58(4), 855–867. https://doi.org/10.1093/jxb/erl123	mass	review	no
33	Jago, R. A., Cutler, M. E. J., & Curran, P. J. (1999). Estimating canopy chlorophyll concentration from field and airborne spectra. Remote Sensing of Environment, 68(3), 217–224. https://doi.org/10.1016/S0034-4257(98)00113-8	mass	index	
34	Meroni, M., Rossini, M., Picchi, V., Panigada, C., Cogliati, S., Nali, C., & Colombo, R. (2008). Assessing steady-state fluorescence and PRI from hyperspectral proximal sensing as early indicators of plant stress: The case of ozone exposure. Sensors, 8(3), 1740–1754. https://doi.org/10.3390/s8031740	mass	index	no
35	Ji-Yong, S., Xiao-Bo, Z., Jie-Wen, Z., Kai-Liang, W., Zheng-Wei, C., Xiao-Wei, H., ... Holmes, M. (2012). Non-destructive diagnostics of nitrogen deficiency by cucumber leaf chlorophyll distribution map based on near infrared hyperspectral imaging. Scientia Horticulturae, 138, 190–197. https://doi.org/10.1016/j.scienta.2012.02.024	mass	empirical	
36	Jetz, W., Cavender-Bares, J., Pavlick, R., Schimel, D., Davis, F. W., Asner, G. P., ... Ustin, S. L. (2016). Monitoring plant functional diversity from space. Nature Plants, 2(3), 16024. http://doi.org/10.1038/nplants.2016.24	mass	review	

37	Martin, R. E., Chadwick, K. D., Brodrick, P. G., Carranza-Jimenez, L., Vaughn, N. R., & Asner, G. P. (2018). An Approach for Foliar Trait Retrieval from Airborne Imaging Spectroscopy of Tropical Forests. Remote Sensing, 10(2), 199.	mass	empirical	
38	Atzberger, C., & Werner, W. (1998). Needle reflectance of healthy and diseased Spruce stands. 1st EARSeL Workshop on Imaging Spectroscopy, 1–20.	mass	index	no
39	Kattenborn, T., Fassnacht, F. E., Pierce, S., Lopatin, J., Grime, J. P., & Schmidtlein, S. (2017). Linking plant strategies and plant traits derived by radiative transfer modelling. Journal of Vegetation Science, 28(4), 717-727.	area	RTM	
40	Oppelt, N., & Mauser, W. (2004). Hyperspectral monitoring of physiological parameters of wheat during a vegetation period using AVIS data. International Journal of Remote Sensing, 25(1), 145–159. https://doi.org/10.1080/0143116031000115300	area/mass	index	
41	Pinar, A., & Curran, P. J. (1996). Technical note: Grass chlorophyll and the reflectance red edge. International Journal of Remote Sensing, 17(2), 351–357. https://doi.org/10.1080/01431169608949010	area/mass	empirical	
42	Asner, G. P., Martin, R. E., Keith, L. M., Heller, W. P., Hughes, M. A., Vaughn, N. R., … & Balzotti, C. (2018). A spectral mapping signature for the Rapid Ohia Death (ROD) pathogen in Hawaiian forests. Remote Sensing, 10(3). http://doi.org/10.3390/rs10030404	mass	empirical	

6 Synthesis

Optical remote sensing evolved as a promising tool to track earth's functional diversity, but the causal links between the functioning of plants and their reflectance have not yet been assessed in sufficient depth. Hence, the main focus and innovative point of this thesis is to link plant functioning and canopy reflectance through radiative transfer modelling. It was expected that this link will firstly improve our capabilities to understand and characterize differences in plant functioning and secondly advance operational monitoring of plant functioning. In this respect three primary research gaps were identified which are conclusively addressed in the following chapter. Finally, limitations and potentials for future research are discussed.

Can gradients of plant functioning and strategies be revealed by trait maps derived from an inversion of radiative transfer models?

Within this thesis trait maps derived from a RTM inversion were for the very first time linked to plant strategies (Chapter 2). Thereby, it was evinced that quantitative trait maps derived from an inversion of PROSAIL are indeed valuable proxies for plant functional gradients. More specifically, it was demonstrated that retrieved spatial patterns of SLA, chlorophyll content and LAI reflected patterns of plant strategies determined in-situ. The analysis was restricted to these traits due to the availability of validation data. Yet, it can be expected that the remaining traits incorporated in PROSAIL are also valuable functional proxies as indicated in Chapter 3 and 4. Previous studies already demonstrated that a wide spectrum of functional traits can be mapped with optical remote sensing (Ustin and Gamon 2010; Homolová et al. 2013; Jetz et al. 2016). However, a large part of these studies focused firstly on empirical models and secondly on traits which do not have an explicit relation to canopy reflectance such as lignin, nitrogen or phosporus content (Gillon et al. 1999; Fourty et al. 1996; Baret and Fourty 1997; Knyazikhin

et al. 2013b; Knyazikhin et al. 2013a). These two factors greatly restrain the transferability and robustness of such mapping procedures and hence its operationalization (Colombo et al. 2003; Grossman et al. 1996). In contrast, it is expected and underlined by the presented findings that RTM inversions have a high potential in view of operational mapping of plant traits and functions. This potential is predominantly determined by the increased transferability in various aspects:

The transferability of RTM inversions across species and vegetation types is highlighted as the traits space considered in RTM is explicitly linked to plant functioning (Chapter 4) and generally a coherence of functional traits across species, growth forms and biomes can be assumed (Grime et al. 1997; Reich 2014; Díaz et al. 2015).

Furthermore, RTM account for the bidirectional reflectance and inversion procedures can thus be applied and transferred to data sets with different acquisitions characteristics, such as varying sun and sensor angles. This is an important feature for large scale and multitemporal assessments of plant functioning, where remote sensing data typically features a high variation in sensor viewing angles and sun angles (Hilker et al. 2015).

The transferability is further enhanced as RTM inversions do not require in-situ data for calibration purposes, which greatly reduces the need for expensive field surveys. This advantage was particularly underlined by the presented trait retrieval based on airborne HyMap data for which spatially explicit calibration data (in-situ measured traits) was not available (Chapter 2). Yet, it should be emphasized that a validation of the inversion procedure is critical in order to test the robustness of the RTM implementation and the derived trait maps.

The output of RTM is readily transferable across spatial scales, as the incorporated traits can readily be scaled through the PROSAIL inherent LAI, which is a dimensionless quantity (leaf surface per surface area). For instance leaf pigment or leaf mass per area (LMA) can be scaled to absolute canopy contents [g/m^2] via multiplication with LAI (sensu Chapter 4).

Moreover, the trait space of RTM (e.g. chlorophyll content, ALA, LAI or fAPAR) is directly relevant and hence transferable to multiple fields of research and can be integrated in respective process based models. Examples include models of the biosphere/atmosphere exchange such as the Soil-Vegetation-Atmospher-Transfer model (SVAT, Inoue 2003), state of the art terrestrial

biosphere models (TBMs) such as the CMIP5 used in the framework of the IPCC (Jung et al. 2007; Houborg et al. 2015; Anav et al. 2013) or crop growth models (CGM, Machwitz et al. 2014).

Despite the described advantages, there are several challenges linked to RTM inversions. Generally, it can be assumed that a correct implementation of an RTM inversion is complex as it requires an in-depth understanding of the principles of radiative transfer modelling and the vegetation characteristics under study. This firstly includes choosing an appropriate RTM which balances the trade-off between representativeness of the vegetation canopies of interest and model complexity. Secondly, the inversion procedure has to be carefully designed to avoid ambiguous solutions of the inversion ('ill-posed problem', Combal et al. 2003; Baret and Buis 2008) and to ensure the robustness of the estimates. Yet, various strategies exists to reduce the ill-posing problem (see Atzberger et al. 2015; Darvishzadeh et al. 2011; Verrelst et al. 2014; Houborg et al. 2015). Another challenge are the generally increased computational requirements of RTM-based approaches (Dorigo et al. 2007), which however can be assumed to be further alleviated by ongoing advances in IT hardware.

Which plant traits affecting radiative transfer help to spectrally separate plants of different functioning?

In view of mapping plant functional gradients with both empirical and RTM-based mapping procedures it is important to consider which optical traits are causing the relevant spectral variation. The presented findings based on simulated canopy spectra (PROSAIL) of different plant strategies and growth forms (Chapter 3) revealed that especially the plant traits describing the canopy structure are causing the principal differences in reflectance among functional types. Leaf constituents have a significantly lower contribution to the spectral separation of plant functional types. Although leaf constituents vary considerably among plant functional types (Atkin et al. 2015), their effect on the canopy reflectance and thus their contribution to spectrally differentiate plant functional types is comparably low. It is thus important to recognize that the separability of plant functions through reflectance does not necessarily correspond to trait differences measured in the field, as these differences may not be remotely retrievable in

the first place. These results are striking as most prior scientific contributions attributed spectral variation across plant functional gradients to biochemical constituents (Asner and Martin 2009; Jetz et al. 2016). This is further questioned as traits incorporating the canopy structure (LAI, fAPAR, canopy foliage biomass) were shown to have a strong and causal correspondence to functional gradients (Chapter 4).

Thus, the presented findings indicate that the field of remote sensing of plant functioning and functional traits is still not completely understood. This can firstly be traced back to the difficulty to explicitly attribute spectral variations to individual plant traits and secondly to the fact that most knowledge emerged from case studies, which are typically limited in representatives, e.g. in terms of geographic extent, vegetation types or temporal variation (Van Cleemput et al. 2018). The presented thesis demonstrated that RTM-based simulations can be an important tool to overcome the limitations of case studies and to gain more universally valid insights on the interaction between plant functioning, plant traits and canopy reflectance (Chapter 3). Such simulations can be harnessed to trace back spectral differences to individual functional traits and to identify the spectral features that are important to characterize variations in plant functioning. Such mechanistic knowledge is essential for identifying the plant functions that are retrievable using optical remote sensing as well as for selecting and designing suitable sensors and robust algorithms.

What are the causal associations between optical plant traits and plant functioning and can these extend our understanding of plant functioning?

The plant traits incorporated in RTMs were initially implemented due to their physical relevance for the radiative transfer in plant canopies rather than due to ecological relevance. Yet, as the radiative transfer in plant canopies greatly determines the energy turnover and thus the metabolism of a plant, the respective optical traits are assumed to directly correspond to the primary functions and strategies of plants (Ustin and Gamon 2010).

Within this thesis the trait space of PROSAIL was for the very first time compared to established functional schemes, i.e. the Leaf Economic Spectrum and CSR plant strategies (Chapter 2 and 4). It was evidenced that the expression of these optical traits directly reflect leaf resource

investments, competition, life history and persistence, which implies that leaf and canopy traits are tailored to ensure an efficient energy generation under the local abiotic conditions and biotic interaction (e.g. competition for light). Yet, regarding leaf constituents careful consideration should be given to the scale at which a constituent is quantified. Leaf constituents can assessed per leaf area [µg/cm^2], leaf mass [g/g or %] or canopy basis [m^2/m^2]. It was shown that the scale at which a leaf constituent is quantified greatly affects its relation to plant functions (Chapter 4). With regard to leaf pigments, it was even evinced that pigments quantified as concentration [%] is a unsuitable metric for the remote sensing-based characterization of plant functional gradients (Chapter 5), despite its frequent use in the community (e.g. see Asner and Martin 2009; Jetz et al. 2016). For statistical and ecological reasons and due to the principles of radiative transfer leaf pigments should be quantified as absolute content [µg/cm^2] instead. Overall, it was demonstrated that optical traits can serve as alternative or addition to those traits which are commonly used as proxies for functional gradients. The fact that these traits are retrievable from optical remote sensing data emphasizes the potential of trait-based ecology to become a more applied science.

Moreover, the causal links identified between the assessed plant functional gradients, optical traits and canopy reflectance do not only evidence the potential of RTM for assessing these gradients, but they also substantiate their fundamental existence. This was firstly demonstrated as primary plant strategies measured in-situ showed a strong coherence to the trait maps derived from an inversion of PROSAIL (Chapter 2). Secondly, It was found that some optical traits even show a comparable or even stronger correlation to plant strategies than traits that are traditionally used as respective proxies (Chapter 4). It can therefore be concluded that canopy *reflectance follows function* (In compliance with the maxim of 20th-century design and architecture *form follows function* coined by Louis Sullivan), meaning that the function directly determines the canopy 'architecture' and its components (e.g. leafs characteristics). These in turn determine how light is scattered within and from the canopy. It is thus important to recognize that remote sensing offers not merely tools for spatially mapping earth's functional diversity, but it also offers a different perspective and metrics to understand and describe plant functioning and the underlying processes.

Potentials for future research

As demonstrated in the presented thesis linking plant functioning and canopy reflectance through radiative transfer models features multiple application domains (Fig. 6.1): Firstly, RTMs inversion are a highly transferable approach to produce spatial maps of traits which are valuable proxies of plant functioning. Secondly, RTMs-based simulations can overcome several limitations of case studies and can advance our mechanistic knowledge on plant functioning and reflectance which enables to develop and further improve sensors and algorithms. Thirdly, the optical traits incorporated in RTMs provide an alternate perspective and metrics to characterize differences in plant functioning and therefore can thus be an important supplement to traits commonly used in plant ecology.

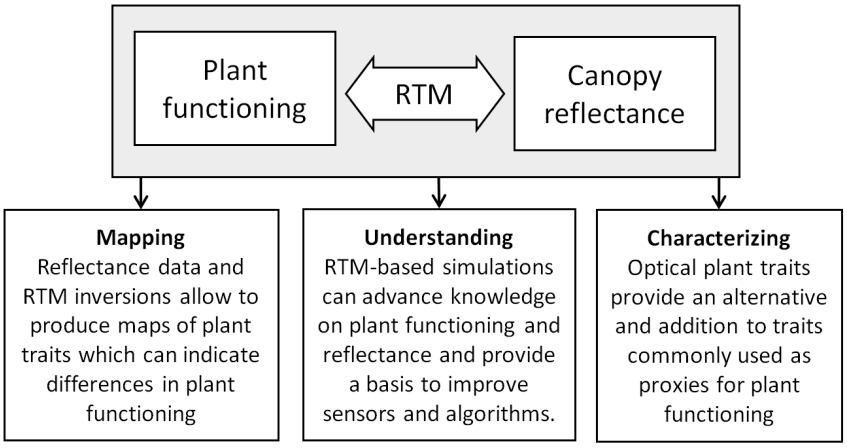

Figure 6.1: Merits of linking plant functioning and canopy reflectance with radiative transfer models.

In conjunction with the identified merits and potentials of bridging ecological theory with radiative transfer modelling there is a number of issues for further possible research:

The presented thesis focused on grassland species which have a comparably homogeneous canopy structure and therefore PROSAIL was used as RTM. In view of more complex canopies (composed of shrubs or trees) more sophisticated RTM such as FLIGHT (North 1996) or INFORM (Atzberger 2000) should be considered. These RTM incorporate additional traits affecting the spectral response of plant canopies, including crown characteristics and the overall canopy structure. In presence of trees and shrubs an inversion of these RTM is accordingly more likely to produce robust trait maps. However, an inversion of such RTM is more sophisticated,

as the increased complexity of the canopy structure requires the parametrization of additional plant traits (e.g. crown size, shape or density) increasing the ill-posed problem. Thus, incorporating prior-knowledge to e.g. narrow the possible trait range or to consider known relationships among traits becomes even more important. More complex RTM can also be harnessed in order to further understand which plant traits primarily contribute to the spectral variation within functional gradients. The simulation approach developed in the second study (Chapter 3) to assess the contribution of traits for the optical separation of PFT can be easily transferred to more complex RTM. Overall, it can be assumed that the additional traits describing the canopy structure implemented in these RTM show a strong coherence to plant functioning (Givnish 1984; Craine et al. 2001; Poorter et al. 2006; Niinemets 2010).

The data involved in this thesis involved a broad functional gradient. Yet, it can be expected that extending the functional spectrum, the number of species and their geographic representation will increase the generic validity of the observed relationships. In the field of plant ecology vast amounts of data which have been collected during the last decades are becoming more accessible through databases (e.g. TRY, Kattge et al. 2011; GLOPNET, Reich et al. 2007; LEDA, Kleyer et al. 2008). Until now only a few traits incorporated in RTM are available in these databases (predominantly in TRY), e.g. chlorophyll, SLA, LAI. For these traits there are only few observations which are mostly incomplete and not representative in terms of functional gradients and geographic coverage. Yet, the extension of such databases with trait observations relevant to RTM seems to be a promising step towards various research tasks, e.g. simulation-based sensitivity analysis to improve algorithms and sensor design, further identification of causal links between optical traits and plant functional gradients; or development of robust RTM inversion procedures towards global mapping products.

Overall, the present study focused on the primary functional gradients identified in plant ecology, such as resource investments, life history and strategies (introduced in chapter 1.1). These primary gradients thus reflect the bundled response of various individual functions (e.g. photosynthesis, reproduction or light preemption). In contrast, RTM inversions are also highly relevant to map specific plant functions. For instance in a joint study with the Institute for Environment and Sustainability (JRC, Ispra, Zarco-Tejada et al. 2018, *Nature Plants*) it was

demonstrated that leaf anthocyanin content retrieved from an inversion of PROSAIL-D was one of the most important functional traits to reveal infections of the bacteria *Xylella fastidiosa* in olive trees, where anthocyanin contents increased with increasing severity of the infection, demonstrating its function as pathogen defense. Moreover, it was shown that remotely sensed variations in functional traits including anthocyanin content reveal *Xylella fastidiosa* infections at very early stages before they were even visually detectable by professional plant pathologists.

As evidenced in chapter 2-4 canopy structural properties have a strong effect on the spectral variation of plant canopies and direcly relate to plant functioning. Thus, towards an operational mapping of plant functional traits and gradients the use of multi-angular observations (multiple spectral acquisitions within a short time interval) may be very promising, as the latter allows to convey the anisotrophy of the canopy reflectance and is therefore more likely to capture variation of the canopy structure (Chopping 2008; Widlowski et al. 2004). In this regard it is worth to note that the sensor of the EnMAP satellite can be tilted up to 30°. Likewise, the incorporation of SAR data is likely to improve the identification of differences in canopy structure (Schmidt et al. 2017). Especially the combination Sentinel-1 or TerraSAR-X with hyperspectral data from upcoming satellite-missions (EnMAP (Bachmann et al. 2015) or Hypsiri (Roberts et al. 2012; SHALOM (Ben-Dor et al. 2013); PRISMA (Stefano et al. 2013) is expected to be of high potential for mapping ecological gradients on a large scale, as both data types will be available with wide geographical coverage.

Bibliography

Aerts, R. and Berendse, F. (1988). The effect of increased nutrient availability on vegetation dynamics in wet heathlands. *Vegetatio*, 76(1-2):63–69.

Ali, a., Darvishzadeh, R., Skidmore, A. K., Duren, I.-V., Heiden, U., and Heurich, M. (2015). Prospect inversion for indirect estimation of leaf dry matter content and specific leaf area. *Proceedings of the 36th international symposium on remote sensing and environment, 11-15 May 2015, Berlin, Germany. ISPRS Archives, Vol XL-7/W3*, XL-7/W3(May):277–284.

Ali, A. M., Skidmore, A. K., Darvishzadeh, R., van Duren, I., Holzwarth, S., and Mueller, J. (2016). Retrieval of forest leaf functional traits from HySpex imagery using radiative transfer models and continuous wavelet analysis. *ISPRS Journal of Photogrammetry and Remote Sensing*, 122(December):68–80.

Allen, W. A., Gausman, H. W., Richardson, A. J., and Thomas, J. R. (1969). Interaction of isotropic light with a compact plant leaf. *JOSA*, 59(10):1376–1379.

Anav, A., Friedlingstein, P., Kidston, M., Bopp, L., Ciais, P., Cox, P., Jones, C., Jung, M., Myneni, R., and Zhu, Z. (2013). Evaluating the land and ocean components of the global carbon cycle in the cmip5 earth system models. *Journal of Climate*, 26(18):6801–6843.

Asam, S., Klein, D., and Dech, S. (2015). Estimation of grassland use intensities based on high spatial resolution lai time series. *The International Archives of Photogrammetry, Remote Sensing and Spatial Information Sciences*, 40(7):285.

Asner, G. and Martin, R. (2015). Spectroscopic Remote Sensing of Non-Structural Carbohydrates in Forest Canopies. *Remote Sensing*, 7(4):3526–3547.

Asner, G. P. and Martin, R. E. (2009). Airborne spectranomics: Mapping canopy chemical and taxonomic diversity in tropical forests. *Frontiers in Ecology and the Environment*, 7(5):269–276.

Asner, G. P., Scurlock, J. M. O., and Hicke, J. a. (2003). Global synthesis of leaf area index observations :. *Global Ecology & Biogeography*, 12(2003):191–205.

Atkin, O. K., Bloomfield, K. J., Reich, P. B., Tjoelker, M. G., Asner, G. P., Bonal, D., Bönisch, G., Bradford, M. G., Cernusak, L. A., Cosio, E. G., et al. (2015). Global variability in leaf respiration in relation to climate, plant functional types and leaf traits. *New Phytologist*, 206(2):614–636.

Atzberger, C. (2000). Development of an invertible forest reflectance model: The INFOR-model. In *A decade of trans-European remote sensing cooperation. Proceedings of the 20th EARSeL Symposium Dresden, Germany*, volume 14, pages 39–44.

Atzberger, C., Darvishzadeh, R., Immitzer, M., Schlerf, M., Skidmore, A., and le Maire, G. (2015). Comparative analysis of different retrieval methods for mapping grassland leaf area index using airborne imaging spectroscopy. *International Journal of Applied Earth Observation and Geoinformation*, 43:19–31.

Atzberger, C., Darvishzadeh, R., Schlerf, M., and Le Maire, G. (2013). Suitability and adaptation of prosail radiative transfer model for hyperspectral grassland studies. *Remote sensing letters*, 4(1):55–64.

Bachmann, M., Makarau, A., Segl, K., and Richter, R. (2015). Estimating the influence of spectral and radiometric calibration uncertainties on EnMAP data products-examples for ground reflectance retrieval and vegetation indices. *Remote Sensing*, 7(8):10689–10714.

Banskota, A., Wynne, R. H., Thomas, V. A., Serbin, S. P., Kayastha, N., Gastellu-Etchegorry, J. P., and Townsend, P. A. (2013). Investigating the utility of wavelet transforms for inverting a 3-D radiative transfer model using hyperspectral data to retrieve forest lai. *Remote Sensing*, 5(6):2639–2659.

Baret, F. and Buis, S. (2008). Estimating canopy characteristics from remote sensing observations: Review of methods and associated problems. In *Advances in land remote Sensing*, pages 173–201. Springer.

Baret, F., Clevers, J., and Steven, M. (1995). The robustness of canopy gap fraction estimates from red and near-infrared reflectances: A comparison of approaches. *Remote Sensing of Environment*, 54(2):141–151.

Baret, F. and Fourty, T. (1997). Radiometric estimates of nitrogen status of leaves and canopies. In *Diagnosis of the nitrogen status in crops*, pages 201–227. Springer.

Baret, F. and Guyot, G. (1991). Potentials and limits of vegetation indices for lai and apar assessment. *Remote sensing of environment*, 35(2-3):161–173.

Baret, F., Hagolle, O., Geiger, B., Bicheron, P., Miras, B., Huc, M., Berthelot, B., Niño, F., Weiss, M., Samain, O., et al. (2007). Lai, fapar and fcover cyclopes global products derived from vegetation: Part 1: Principles of the algorithm. *Remote sensing of environment*, 110(3):275–286.

Baret, F., Jacquemoud, S., Guyot, G., and Leprieur, C. (1992). Modeled analysis of the biophysical nature of spectral shifts and comparison with information content of broad bands. *Remote Sensing of Environment*, 41(2-3):133–142.

Ben-Dor, E., Kafri, A., and Varacalli, G. (2013). Shalom: Spaceborne hyperspectral applicative land and ocean mission: A joint project of asi–isa. In *Proceedings of the International Geoscience and Remote Sensing Symposium (IAGARSS'13), Melbourne, Australia*, volume 4.

Berger, K., Atzberger, C., Danner, M., D'Urso, G., Mauser, W., Vuolo, F., and Hank, T. (2018). Evaluation of the PROSAIL Model Capabilities for Future Hyperspectral Model Environments: A Review Study. *Remote Sensing*, 10(1):85.

Bini, L. M., Diniz-Filho, J. A. F., Rangel, T. F., Bastos, R. P., and Pinto, M. P. (2006). Challenging wallacean and linnean shortfalls: knowledge gradients and conservation planning in a biodiversity hotspot. *Diversity and distributions*, 12(5):475–482.

Björkman, O. (1981). Responses to different quantum flux densities. In *Physiological plant ecology I*, pages 57–107. Springer.

Blackburn, G. A. (2006). Hyperspectral remote sensing of plant pigments. *Journal of Experimental Botany*, 58(4):855–867.

Blackburn, G. A. and Ferwerda, J. G. (2008). Retrieval of chlorophyll concentration from leaf reflectance spectra using wavelet analysis. *Remote Sensing of Environment*, 112(4):1614–1632.

Bonan, G. B., Levis, S., Kergoat, L., and Oleson, K. W. (2002). Landscapes as patches of plant functional types: An integrating concept for climate and ecosystem models. *Global Biogeochemical Cycles*, 16(2):5–1.

Bondeau, A., Kicklighter, D. W., Kaduk, J., and Model, P. O. T. P. N. (1999). Comparing global models of terrestrial net primary productivity (npp): importance of vegetation structure on seasonal npp estimates. *Global Change Biology*, 5(S1):35–45.

Botha, E. J., Leblon, B., Zebarth, B., and Watmough, J. (2007). Non-destructive estimation of potato leaf chlorophyll from canopy hyperspectral reflectance using the inverted PROSAIL model. *International Journal of Applied Earth Observation and Geoinformation*, 9(4):360–374.

Bowyer, P. and Danson, F. (2004). Sensitivity of spectral reflectance to variation in live fuel moisture content at leaf and canopy level. *Remote Sensing of Environment*, 92(3):297–308.

Braun-Blanquet, J. et al. (1932). Plant sociology. the study of plant communities. *Plant sociology. The study of plant communities. First ed.*

Breiman, L. (2001). Random forests. *Machine learning*, 45(1):5–32.

Brito, D. (2010). Overcoming the linnean shortfall: data deficiency and biological survey priorities. *Basic and Applied Ecology*, 11(8):709–713.

Broge, N. H. and Leblanc, E. (2001). Comparing prediction power and stability of broadband and hyperspectral vegetation indices for estimation of green leaf area index and canopy chlorophyll density. *Remote sensing of environment*, 76(2):156–172.

Brown, A. and Macfadyen, A. (1969). Soil carbon dioxide output and small-scale vegetation pattern in a calluna heath. *Oikos*, pages 8–15.

Cao, K.-F. (2000). Leaf anatomy and chlorophyll content of 12 woody species in contrasting light conditions in a Bornean heath forest. *Canadian Journal of Botany*, 78(10):1245–1253.

Casas, A., Riaño, D., Ustin, S. L., Dennison, P., and Salas, J. (2014). Estimation of water-related biochemical and biophysical vegetation properties using multitemporal airborne hyperspectral data and its comparison to MODIS spectral response. *Remote Sensing of Environment*, 148:28–41.

Cerabolini, B., Pierce, S., Luzzaro, A., and Ossola, A. (2010a). Species evenness affects ecosystem processes in situ via diversity in the adaptive strategies of dominant species. *Plant Ecology*, 207(2):333–345.

Cerabolini, B., Pierce, S., Verginella, A., Brusa, G., Ceriani, R., and Armiraglio, S. (2016). Why are many anthropogenic agroecosystems particularly species-rich? *Plant Biosystems-An International Journal Dealing with all Aspects of Plant Biology*, 150(3):550–557.

Cerabolini, B. E. L., Brusa, G., Ceriani, R. M., de Andreis, R., Luzzaro, A., and Pierce, S. (2010b). Can CSR classification be generally applied outside Britain? *Plant Ecology*, 210(2):253–261.

Chambers, J. M. (1983). *Graphical Methods for Data Analysis: 0*. Chapman and Hall/CRC.

Cheng, T., Rivard, B., and Sanchez-Azofeifa, A. (2011). Spectroscopic determination of leaf water content using continuous wavelet analysis. *Remote Sensing of Environment*, 115(2):659–670.

Chopping, M. J. (2008). Terrestrial applications of multiangle remote sensing. In *Advances in Land Remote Sensing*, pages 95–144. Springer.

Close, D. C. and Beadle, C. L. (2003). The ecophysiology of foliar anthocyanin. *The Botanical Review*, 69(2):149–161.

Cocks, T., Jenssen, R., Stewart, A., Wilson, I., and Shields, T. (1998). The hymaptm airborne hyperspectral sensor: The system, calibration and performance. In *Proceedings of the 1st EARSeL workshop on Imaging Spectroscopy*, pages 37–42. EARSeL.

Colombo, R., Bellingeri, D., Fasolini, D., and Marino, C. M. (2003). Retrieval of leaf area index in different vegetation types using high resolution satellite data. *Remote Sensing of Environment*, 86(1):120–131.

Colombo, R., Meroni, M., Marchesi, A., Busetto, L., Rossini, M., Giardino, C., and Panigada, C. (2008). Estimation of leaf and canopy water content in poplar plantations by means of hyperspectral indices and inverse modeling. *Remote Sensing of Environment*, 112(4):1820–1834.

Combal, B., Baret, F., Weiss, M., Trubuil, A., Mace, D., Pragnere, A., Myneni, R., Knyazikhin, Y., and Wang, L. (2003). Retrieval of canopy biophysical variables from bidirectional reflectance: Using prior information to solve the ill-posed inverse problem. *Remote sensing of environment*, 84(1):1–15.

Craine, J. M., Froehle, J., Tilman, D. G., Wedin, D. A., Chapin, F. S., Craine, I., and Tilman, . D. G. (2001). The relationships among root and leaf traits of 76 grassland species and relative abundance along fertility and disturbance gradients. *Oikos*, 93(December 2015):274–285.

Curran, P. J. (1989). Remote sensing of foliar chemistry. *Remote sensing of environment*, 30(3):271–278.

Darvishzadeh, R., Atzberger, C., Skidmore, A., and Schlerf, M. (2011). Mapping grassland leaf area index with airborne hyperspectral imagery: A comparison study of statistical approaches and inversion of radiative transfer models. *ISPRS Journal of Photogrammetry and Remote Sensing*, 66(6):894–906.

Darvishzadeh, R., Skidmore, A., Schlerf, M., and Atzberger, C. (2008). Inversion of a radiative transfer model for estimating vegetation LAI and chlorophyll in a heterogeneous grassland. *Remote Sensing of Environment*, 112(5):2592–2604.

Darwin, C. and Wallace, A. (1858). On the tendency of species to form varieties; and on the perpetuation of varieties and species by natural means of selection. *Journal of the proceedings of the Linnean Society of London. Zoology*, 3(9):45–62.

de Beurs, K. M. and Henebry, G. M. (2005). Land surface phenology and temperature variation in the International Geosphere-Biosphere Program high-latitude transects. *Global Change Biology*, 11(5):779–790.

De Pury, D. and Farquhar, G. (1997). Simple scaling of photosynthesis from leaves to canopies without the errors of big-leaf models. *Plant, Cell & Environment*, 20(5):537–557.

Díaz, S. and Cabido, M. (1997). Plant functional types and ecosystem function in relation to global change. *Journal of vegetation science*, 8(4):463–474.

Diaz, S. and Cabido, M. (2001). Vive la difference: plant functional diversity matters to ecosystem processes. *Trends in ecology & evolution*, 16(11):646–655.

Díaz, S., Kattge, J., Cornelissen, J. H. C., Wright, I. J., Lavorel, S., Dray, S., Reu, B., Kleyer, M., Wirth, C., Prentice, I. C., Garnier, E., Bönisch, G., Westoby, M., Poorter, H., Reich, P. B., Moles, A. T., Dickie, J., Gillison, A. N., Zanne, A. E., Chave, J., Wright, S. J., Sheremet'ev, S. N., Jactel, H., Christopher, B., Cerabolini, B., Pierce, S., Shipley, B., Kirkup, D., Casanoves, F., Joswig, J. S., Günther, A., Falczuk, V., Rüger, N., Mahecha, M. D., and Gorné, L. D. (2015). The global spectrum of plant form and function. *Nature*, 529(7585):1–17.

Disney, M., Lewis, P., and Saich, P. (2006). 3d modelling of forest canopy structure for remote sensing simulations in the optical and microwave domains. *Remote Sensing of Environment*, 100(1):114–132.

Dorigo, W., Zurita-Milla, R., de Wit, A. J., Brazile, J., Singh, R., and Schaepman, M. E. (2007). A review on reflective remote sensing and data assimilation techniques for enhanced agroecosystem modeling. *International journal of applied earth observation and geoinformation*, 9(2):165–193.

Dormann, C. and Woodin, S. J. (2002). Climate change in the arctic: using plant functional types in a meta-analysis of field experiments. *Functional Ecology*, 16(1):4–17.

Dormann, C. F. and Skarpe, C. (2002). Flowering, growth and defence in the two sexes: Consequences of herbivore exclusion for Salix polaris. *Functional Ecology*, 16(5):649–656.

Duan, S.-B., Li, Z.-L., Wu, H., Tang, B.-H., Ma, L., Zhao, E., and Li, C. (2014). Inversion of the prosail model to estimate leaf area index of maize, potato, and sunflower fields from unmanned aerial vehicle hyperspectral data. *International Journal of Applied Earth Observation and Geoinformation*, 26:12–20.

Ehleringer, J. (1986). Modifications of solar radiation absorption patterns and implications for carbon gain at the leaf level. *On the economy of plant form and function*, pages 57–82.

Espinar, B., Blanc, P., Wald, L., Gschwind, B., Ménard, L., Wey, E., Thomas, C., and Saboret, L. (2012). HelioClim-3: a near-real time and long-term surface solar irradiance database. In *Workshop on" Remote Sensing Measurements for Renewable Energy"*.

Evans, J. and Poorter, H. (2001). Photosynthetic acclimation of plants to growth irradiance: the relative importance of specific leaf area and nitrogen partitioning in maximizing carbon gain. *Plant, Cell & Environment*, 24(8):755–767.

Evans, J. R. (1996). Developmental constraints on photosynthesis: effects of light and nutrition. In *Photosynthesis and the Environment*, pages 281–304. Springer.

Feilhauer, H., Doktor, D., Schmidtlein, S., and Skidmore, A. K. (2016). Mapping pollination types with remote sensing. *Journal of vegetation science*, 27(5):999–1011.

Feilhauer, H., Schmid, T., Faude, U., Sánchez-Carrillo, S., and Cirujano, S. (2018). Are remotely sensed traits suitable for ecological analysis? A case study of long-term drought effects on leaf mass per area of wetland vegetation. *Ecological Indicators*, 88(January):232–240.

Feilhauer, H., Somers, B., and van der Linden, S. (2017). Optical trait indicators for remote sensing of plant species composition: Predictive power and seasonal variability. *Ecological Indicators*, 73:825–833.

Feret, J.-B., François, C., Asner, G. P., Gitelson, A. A., Martin, R. E., Bidel, L. P., Ustin, S. L., Le Maire, G., and Jacquemoud, S. (2008). PROSPECT-4 and 5: Advances in the leaf optical properties model separating photosynthetic pigments. *Remote sensing of environment*, 112(6):3030–3043.

Féret, J.-B., François, C., Gitelson, A., Asner, G. P., Barry, K. M., Panigada, C., Richardson, A. D., and Jacquemoud, S. (2011). Optimizing spectral indices and chemometric analysis of leaf chemical properties using radiative transfer modeling. *Remote Sensing of Environment*, 115(10):2742–2750.

Feret, J.-B., Gitelson, A., Noble, S., and Jacquemoud, S. (2017). PROSPECT-D: Towards modeling leaf optical properties through a complete lifecycle. *Remote Sensing of Environment*, 193:204–215.

Field, C. B. (1991). Ecological scaling of carbon gain to stress and resource. *Response of plants to multiple stresses*, pages 35–65.

Fourty, T., Baret, F., Jacquemoud, S., Schmuck, G., and Verdebout, J. (1996). Leaf optical properties with explicit description of its biochemical composition: direct and inverse problems. *Remote sensing of Environment*, 56(2):104–117.

Friedl, M. A., Sulla-Menashe, D., Tan, B., Schneider, A., Ramankutty, N., Sibley, A., and Huang, X. (2010). Modis collection 5 global land cover: Algorithm refinements and characterization of new datasets. *Remote sensing of Environment*, 114(1):168–182.

Garbulsky, M. F., Peñuelas, J., Gamon, J., Inoue, Y., and Filella, I. (2011). The photochemical reflectance index (PRI) and the remote sensing of leaf, canopy and ecosystem radiation use efficiencies: A review and meta-analysis. *Remote Sensing of Environment*, 115(2):281–297.

Garnier, E. (1992). Growth analysis of congeneric annual and perennial grass species. *Journal of Ecology*, pages 665–675.

Garrigues, S., Lacaze, R., Baret, F., Morisette, J., Weiss, M., Nickeson, J., Fernandes, R., Plummer, S., Shabanov, N., Myneni, R., et al. (2008). Validation and intercomparison of global Leaf Area Index products derived from remote sensing data. *Journal of Geophysical Research: Biogeosciences*, 113(G2).

Gastellu-Etchegorry, J.-P., Demarez, V., Pinel, V., and Zagolski, F. (1996). Modeling radiative transfer in heterogeneous 3-D vegetation canopies. *Remote sensing of environment*, 58(2):131–156.

Gillon, D., Houssard, C., and Joffre, R. (1999). Using near-infrared reflectance spectroscopy to predict carbon, nitrogen and phosphorus content in heterogeneous plant material. *Oecologia*, 118(2):173–182.

Gitelson, A. A., Buschmann, C., and Lichtenthaler, H. K. (1998). Leaf chlorophyll fluorescence corrected for re-absorption by means of absorption and reflectance measurements. *Journal of Plant Physiology*, 152(2-3):283–296.

Gitelson, A. A. and Merzlyak, M. N. (1998). Remote sensing of chlorophyll concentration in higher plant leaves. *Advances in Space Research*, 22(5):689–692.

Givnish, T. (1984). Leaf and canopy adaptations in tropical forests. In *Physiological ecology of plants of the wet tropics*, pages 51–84. Springer.

Gond, V., de Pury, D. G., Veroustraete, F., and Ceulemans, R. (1999). Seasonal variations in leaf area index, leaf chlorophyll, and water content; scaling-up to estimate fapar and carbon balance in a multilayer, multispecies temperate forest. *Tree physiology*, 19(10):673–679.

Goward, S. N., Tucker, C. J., and Dye, D. G. (1985). North American vegetation patterns observed with the noaa-7 advanced very high resolution radiometer. *Vegetatio*, 64(1):3–14.

Grace, J. (1991). A clarification of the debate between Grime and Tilman. *Functional Ecology*, 5(5):583–587.

Grime, J., Thompson, K., Hunt, R., Hodgson, J., Cornelissen, J., Rorison, I., Hendry, G., Ashenden, T., Askew, A., Band, S., et al. (1997). Integrated screening validates primary axes of specialisation in plants. *Oikos*, pages 259–281.

Grime, J. P. (1974). Vegetation classification by reference to strategies. *Nature*, 250(5461):26.

Grime, J. P. (1977). Evidence for the existence of three primary strategies in plants and its relevance to ecological and evolutionary theory. *The American Naturalist*, 111(982):1169–1194.

Grime, J. P. (1988). The CSR model of primary plant strategies - origins, implications and tests. In *Plant evolutionary biology*, pages 371–393. Springer.

Grime, J. P. (2006). Trait convergence and trait divergence in herbaceous plant communities: mechanisms and consequences. *Journal of Vegetation Science*, 17(2):255–260.

Grime, J. P. and Pierce, S. (2012). *The evolutionary strategies that shape ecosystems*. John Wiley & Sons.

Grossman, Y. L., Ustin, S. L., Jacquemoud, S., Sanderson, E. W., Schmuck, G., and Verdebout, J. (1996). Critique of stepwise multiple linear regression for the extraction of leaf biochemistry information from leaf reflectance data. *Remote Sensing of Environment*, 56(3):182–193.

Guo, W., van Kleunen, M., Winter, M., Weigelt, P., Stein, A., Pierce, S., Pergl, J., Moser, D., Maurel, N., Lenzner, B., et al. (2018). The role of adaptive strategies in plant naturalization. *Ecology letters.*

Haboudane, D., Miller, J. R., Pattey, E., Zarco-Tejada, P. J., and Strachan, I. B. (2004). Hyperspectral vegetation indices and novel algorithms for predicting green lai of crop canopies: Modeling and validation in the context of precision agriculture. *Remote sensing of environment*, 90(3):337–352.

Haboudane, D., Miller, J. R., Tremblay, N., Zarco-Tejada, P. J., and Dextraze, L. (2002). Integrated narrow-band vegetation indices for prediction of crop chlorophyll content for application to precision agriculture. *Remote sensing of environment*, 81(2-3):416–426.

Haettenschwiler, S. and Vitousek, P. M. (2000). The role of polyphenols in terrestrial ecosystem nutrient cycling. *Trends in ecology & evolution*, 15(6):238–243.

Hallik, L., Kull, O., Nilson, T., and Peñuelas, J. (2009). Spectral reflectance of multispecies herbaceous and moss canopies in the boreal forest understory and open field. *Canadian Journal of Remote Sensing*, 35(5):474–485.

Hamilton, N. et al. (2016). ggtern: An extension to 'ggplot2', for the creation of ternary diagrams. *R package version*, 2(1).

Hikosaka, K. and Hirose, T. (1997). Leaf angle as a strategy for light competition: Optimal and evolutionarily stable light-extinction coefficient within a leaf canopy. *Ecoscience*, 4(4):501–507.

Hildebrandt, G. (1996). *Fernerkundung und Luftbildmessung: für Forstwirtschaft, Vegetationskartierung und Landschaftsökologie*. Wichmann.

Hilker, T., Coops, N. C., Wulder, M. A., Black, T. A., and Guy, R. D. (2008). The use of remote sensing in light use efficiency based models of gross primary production: A review of current status and future requirements. *Science of the Total Environment*, 404(2-3):411–423.

Hilker, T., Lyapustin, A. I., Hall, F. G., Myneni, R., Knyazikhin, Y., Wang, Y., Tucker, C. J., and Sellers, P. J. (2015). On the measurability of change in Amazon vegetation from MODIS. *Remote Sensing of Environment*, 166:233–242.

Hodgson, J., Wilson, P., Hunt, R., Grime, J., and Thompson, K. (1999). Allocating CSR plant functional types: a soft approach to a hard problem. *Oikos*, pages 282–294.

Homolová, L., Malenovský, Z., Clevers, J. G. P. W., García-Santos, G., and Schaepman, M. E. (2013). Review of optical-based remote sensing for plant trait mapping. *Ecological Complexity*, 15:1–16.

Hosgood, B., Jacquemoud, S., Andreoli, G., Verdebout, J., Pedrini, G., and Schmuck, G. (1995). Leaf optical properties experiment 93. *Joint Res. Center, Eur. Comm., Inst. Remote Sensing Applications, Ispra, Italy, Tech. Rep. EUR*, 16:095.

Houborg, R., Mccabe, M., Cescatti, A., Gao, F., Schull, M., and Gitelson, A. (2015). Remote Sensing of Environment Joint leaf chlorophyll content and leaf area index retrieval from Landsat data using a regularized model inversion system (REGFLEC). *Remote Sensing of Environment*, 159:203–221.

Huemmrich, K. F. (2013a). Simulations of Seasonal and Latitudinal Variations in Leaf Inclination Angle Distribution: Implications for Remote Sensing. *Advances in Remote Sensing*, 02(02):93–101.

Huemmrich, K. F. (2013b). Simulations of seasonal and latitudinal variations in leaf inclination angle distribution: Implications for remote sensing.

Inoue, Y. (2003). > synergy of remote sensing and modeling for estimating ecophysiological processes in plant production. *Plant Production Science*, 6(1):3–16.

Jacquemoud, S. (1993). Inversion of the PROSPECT + SAIL canopy reflectance model from AVIRIS equivalent spectra: theoretical study. *Remote sensing of environment*, 44(2-3):281–292.

Jacquemoud, S. and Baret, F. (1990). PROSPECT: A model of leaf optical properties spectra. *Remote Sensing of Environment*, 34(2):75–91.

Jacquemoud, S., Bidel, L., Francois, C., and Pavan, G. (2003a). Angers leaf optical properties database (2003). *Data set*.

Jacquemoud, S., Bidel, L., Francois, C., and Pavan, G. (2003b). Angers leaf optical properties database (2003). data set. available on-line [http://ecosis.org] from the ecological spectral information system (ecosis).

Jacquemoud, S., Ustin, S. L., Verdebout, J., Schmuck, G., Andreoli, G., and Hosgood, B. (1996). Estimating leaf biochemistry using the PROSPECT leaf optical properties model. *Remote Sensing of Environment*, 56(3):194–202.

Jacquemoud, S., Verhoef, W., Baret, F., Bacour, C., Zarco-Tejada, P. J., Asner, G. P., François, C., and Ustin, S. L. (2009). PROSPECT + SAIL models: A review of use for vegetation characterization. *Remote Sensing of Environment*, 113(SUPPL. 1):S56–S66.

Jetz, W., Cavender-Bares, J., Pavlick, R., Schimel, D., Davis, F. W., Asner, G. P., Guralnick, R., Kattge, J., Latimer, A. M., Moorcroft, P., Schaepman, M. E., Schildhauer, M. P., Schneider, F. D., Schrodt, F., Stahl, U., and Ustin, S. L. (2016). Monitoring plant functional diversity from space. *Nature Plants*, 2(3):16024.

Jung, M., Vetter, M., Herold, M., Churkina, G., Reichstein, M., Zaehle, S., Ciais, P., Viovy, N., Bondeau, A., Chen, Y., et al. (2007). Uncertainties of modeling gross primary productivity over europe: A systematic study on the effects of using different drivers and terrestrial biosphere models. *Global Biogeochemical Cycles*, 21(4).

Kattenborn, T., Fassnacht, F. E., Pierce, S., Lopatin, J., Grime, J. P., and Schmidtlein, S. (2017). Linking plant strategies and plant traits derived by radiative transfer modelling. *Journal of Vegetation Science*, 28(4):717–727.

Kattenborn, T., Fassnacht, F. E., and Schmidtlein, S. (2018). Differentiating plant functional types using reflectance: which traits make the difference? *Remote Sensing in Ecology and Conservation*, pages 1–15.

Kattenborn, T., Maack, J., Faßnacht, F., Enßle, F., Ermert, J., and Koch, B. (2015). Mapping forest biomass from space–fusion of hyperspectral eo1-hyperion data and tandem-x and worldview-2 canopy height models. *International Journal of Applied Earth Observation and Geoinformation*, 35:359–367.

Kattge, J., Diaz, S., Lavorel, S., Prentice, I. C., Leadley, P., Bönisch, G., Garnier, E., Westoby, M., Reich, P. B., Wright, I. J., et al. (2011). Try–a global database of plant traits. *Global change biology*, 17(9):2905–2935.

Kelemen, A., Török, P., Valkó, O., Miglécz, T., and Tóthmérész, B. (2013). Mechanisms shaping plant biomass and species richness: plant strategies and litter effect in alkali and loess grasslands. *Journal of Vegetation Science*, 24(6):1195–1203.

Klančnik, K., Vogel-Mikuš, K., and Gaberščik, A. (2014). Silicified structures affect leaf optical properties in grasses and sedge. *Journal of Photochemistry and Photobiology B: Biology*, 130:1–10.

Kleyer, M., Bekker, R., Knevel, I., Bakker, J., Thompson, K., Sonnenschein, M., Poschlod, P., Van Groenendael, J., Klimeš, L., Klimešová, J., et al. (2008). The leda traitbase: a database of life-history traits of the northwest European flora. *Journal of Ecology*, 96(6):1266–1274.

Knyazikhin, Y., Lewis, P., Disney, M. I., Stenberg, P., Mottus, M., Rautianinen, M., Kaufmann, R. K., Marshak, A., Schull, M. A., Carmona, P. L., et al. (2013a). Decoupling contributions from canopy structure and leaf optics is critical for remote sensing leaf biochemistry (reply to Townsend, et al.).

Knyazikhin, Y., Schull, M. A., Stenberg, P., Mõttus, M., Rautiainen, M., Yang, Y., Marshak, A., Latorre Carmona, P., Kaufmann, R. K., Lewis, P., Disney, M. I., Vanderbilt, V., Davis, A. B., Baret, F., Jacquemoud, S., Lyapustin, A., and Myneni, R. B. (2013b). Hyperspectral remote sensing of foliar nitrogen content. *Proceedings of the National Academy of Sciences of the United States of America*, 110(3):E185–92.

Kokaly, R. F., Asner, G. P., Ollinger, S. V., Martin, M. E., and Wessman, C. A. (2009). Characterizing canopy biochemistry from imaging spectroscopy and its application to ecosystem studies. *Remote Sensing of Environment*, 113(SUPPL. 1):S78–S91.

Kötz, B., Schaepman, M., Morsdorf, F., Bowyer, P., Itten, K., and Allgöwer, B. (2004). Radiative transfer modeling within a heterogeneous canopy for estimation of forest fire fuel properties. *Remote Sensing of Environment*, 92(3):332–344.

Kucharik, C. J., Foley, J. A., Delire, C., Fisher, V. A., Coe, M. T., Lenters, J. D., Young-Molling, C., Ramankutty, N., Norman, J. M., and Gower, S. T. (2000). Testing the performance of a

dynamic global ecosystem model: water balance, carbon balance, and vegetation structure. *Global Biogeochemical Cycles*, 14(3):795–825.

Kühn, I., Durka, W., and Klotz, S. (2004). Biolflor: a new plant-trait database as a tool for plant invasion ecology. *Diversity and Distributions*, 10(5/6):363–365.

Kunstler, G., Falster, D., Coomes, D. A., Hui, F., Kooyman, R. M., Laughlin, D. C., Poorter, L., Vanderwel, M., Vieilledent, G., Wright, S. J., Aiba, M., Baraloto, C., Caspersen, J., Cornelissen, J. H. C., Gourlet-Fleury, S., Hanewinkel, M., Herault, B., Kattge, J., Kurokawa, H., Onoda, Y., Peñuelas, J., Poorter, H., Uriarte, M., Richardson, S., Ruiz-Benito, P., Sun, I. F., Ståhl, G., Swenson, N. G., Thompson, J., Westerlund, B., Wirth, C., Zavala, M. A., Zeng, H., Zimmerman, J. K., Zimmermann, N. E., and Westoby, M. (2016). Plant functional traits have globally consistent effects on competition. *Nature*, 529(7585):204–207.

Kuusk, A. (1991). The hot spot effect in plant canopy reflectance. In *Photon-Vegetation Interactions*, pages 139–159. Springer.

Labate, D., Ceccherini, M., Cisbani, A., De Cosmo, V., Galeazzi, C., Giunti, L., Melozzi, M., Pieraccini, S., and Stagi, M. (2009). The PRISMA payload optomechanical design, a high performance instrument for a new hyperspectral mission. *Acta Astronautica*, 65(9-10):1429–1436.

Larcher, W. (2003). *Physiological plant ecology: ecophysiology and stress physiology of functional groups*. Springer Science & Business Media.

Latifi, H., Fassnacht, F., and Koch, B. (2012). Forest structure modeling with combined airborne hyperspectral and LiDAR data. *Remote Sensing of Environment*, 121:10–25.

Laurent, V. C., Verhoef, W., Clevers, J. G., and Schaepman, M. E. (2011). Inversion of a coupled canopy–atmosphere model using multi-angular top-of-atmosphere radiance data: A forest case study. *Remote Sensing of Environment*, 115(10):2603–2612.

Lavorel, S. and Garnier, É. (2002). Predicting changes in community composition and ecosystem functioning from plant traits: revisiting the holy grail. *Functional ecology*, 16(5):545–556.

Lavorel, S., McIntyre, S., Landsberg, J., and Forbes, T. D. (1997). Plant functional classifications: From general groups to specific groups based on response to disturbance. *Trends in Ecology and Evolution*, 12(12):474–478.

Lawlor, D. W. and Cornic, G. (2002). Photosynthetic carbon assimilation and associated metabolism in relation to water deficits in higher plants. *Plant, cell & environment*, 25(2):275–294.

Le Maire, G., Francois, C., and Dufrene, E. (2004). Towards universal broad leaf chlorophyll indices using prospect simulated database and hyperspectral reflectance measurements. *Remote sensing of environment*, 89(1):1–28.

Leitão, P. J., Schwieder, M., Pötzschner, F., Pinto, J. R., Teixeira, A. M., Pedroni, F., Sanchez, M., Rogass, C., van der Linden, S., Bustamante, M. M., et al. (2018). From sample to pixel: multi-scale remote sensing data for upscaling aboveground carbon data in heterogeneous landscapes. *Ecosphere*, 9(8):e02298.

Li, D., Cheng, T., Jia, M., Zhou, K., Lu, N., Yao, X., Tian, Y., Zhu, Y., and Cao, W. (2018). PROCWT: Coupling PROSPECT with continuous wavelet transform to improve the retrieval of foliar chemistry from leaf bidirectional reflectance spectra. *Remote Sensing of Environment*, 206(November 2017):1–14.

Lichtenthaler, H. K. (1987). [34] chlorophylls and carotenoids: pigments of photosynthetic biomembranes. In *Methods in enzymology*, volume 148, pages 350–382. Elsevier.

Lloyd, J., Bloomfield, K., Domingues, T. F., and Farquhar, G. D. (2013). Photosynthetically relevant foliar traits correlating better on a mass vs an area basis: of ecophysiological relevance or just a case of mathematical imperatives and statistical quicksand? *New Phytologist*, 199(2):311–321.

MacArthur, R. H., Diamond, J. M., and Karr, J. R. (1972). Density compensation in island faunas. *Ecology*, 53(2):330–342.

Machwitz, M., Giustarini, L., Bossung, C., Frantz, D., Schlerf, M., Lilienthal, H., Wandera, L., Matgen, P., Hoffmann, L., and Udelhoven, T. (2014). Enhanced biomass prediction by assimilating satellite data into a crop growth model. *Environmental modelling & software*, 62:437–453.

McCune, B., Grace, J. B., and Urban, D. L. (2002). *Analysis of ecological communities*, volume 28. MjM software design Gleneden Beach, OR.

McGill, B. J., Enquist, B. J., Weiher, E., and Westoby, M. (2006). Rebuilding community ecology from functional traits. *Trends in ecology & evolution*, 21(4):178–185.

Medlyn, B., Badeck, F.-W., De Pury, D., Barton, C., Broadmeadow, M., Ceulemans, R., De Angelis, P., Forstreuter, M., Jach, M., Kellomäki, S., et al. (1999). Effects of elevated [co2] on photosynthesis in european forest species: a meta-analysis of model parameters. *Plant, Cell & Environment*, 22(12):1475–1495.

Meroni, M., Colombo, R., and Panigada, C. (2004). Inversion of a radiative transfer model with hyperspectral observations for LAI mapping in poplar plantations. *Remote sensing of environment*, 92(2):195–206.

Middleton, E. M., Cheng, Y. B., Hilker, T., Black, T. A., Krishnan, P., Coops, N. C., and Huemmrich, K. F. (2009). Linking foliage spectral responses to canopy-level ecosystem photosynthetic light-use efficiency at a douglas-fir forest in canada. *Canadian Journal of Remote Sensing*, 35(2):166–188.

Mielke, J. and Paul, W. (1991). The application of multivariate permutation methods based on distance functions in the earth sciences. *Earth-Science Reviews*, 31(1):55–71.

Müller-linow, M., Pinto-espinosa, F., Scharr, H., and Rascher, U. (2015). The leaf angle distribution of natural plant populations : assessing the canopy with a novel software tool. pages 1–16.

Myneni, R. B., Hoffman, S., Knyazikhin, Y., Privette, J., Glassy, J., Tian, Y., Wang, Y., Song, X., Zhang, Y., Smith, G., et al. (2002). Global products of vegetation leaf area and fraction absorbed par from year one of modis data. *Remote sensing of environment*, 83(1-2):214–231.

Nelson, N. and Yocum, C. F. (2006). Structure and function of photosystems I and II. *Annu. Rev. Plant Biol.*, 57:521–565.

Niinemets, Ü. (2010). A review of light interception in plant stands from leaf to canopy in different plant functional types and in species with varying shade tolerance. *Ecological Research*, 25(4):693–714.

Niinemets, Ü. and Valladares, F. (2004). Photosynthetic acclimation to simultaneous and interacting environmental stresses along natural light gradients: optimality and constraints. *Plant Biology*, 6(03):254–268.

Niklas, K. J. (1994). *Plant allometry: the scaling of form and process*. University of Chicago Press.

North, P. R. (1996). Three-dimensional forest light interaction model using a Monte Carlo method. *Geoscience and Remote Sensing, IEEE Transactions on*, 34(4):946–956.

Ollinger, S. V. (2011). Sources of variability in canopy reflectance and the convergent properties of plants. *New Phytologist*, 189(2):375–394.

Ommen, O., Donnelly, A., Vanhoutvin, S., Van Oijen, M., and Manderscheid, R. (1999). Chlorophyll content of spring wheat flag leaves grown under elevated co2 concentrations and other environmental stresses within the 'espace-wheat'project. *European Journal of Agronomy*, 10(3-4):197–203.

Oppelt, N. and Mauser, W. (2004). Hyperspectral monitoring of physiological parameters of wheat during a vegetation period using AVIS data. *International Journal of Remote Sensing*, 25(1):145–159.

Osnas, J. L., Lichstein, J. W., Reich, P. B., and Pacala, S. W. (2013). Global leaf trait relationships: mass, area, and the leaf economics spectrum. *Science*, 340(6133):741–744.

Osnas, J. L. D., Katabuchi, M., Kitajima, K., Wright, S. J., Reich, P. B., Van Bael, S. A., Kraft, N. J. B., Samaniego, M. J., Pacala, S. W., and Lichstein, J. W. (2018). Divergent drivers of leaf trait variation within species, among species, and among functional groups. *Proceedings of the National Academy of Sciences*, 115(21):5480–5485.

Paganini, M., Leidner, A. K., Geller, G., Turner, W., and Wegmann, M. (2016). The role of space agencies in remotely sensed essential biodiversity variables. *Remote Sensing in Ecology and Conservation*, 2(3):132–140.

Peng, Y., Gitelson, A. A., Keydan, G., Rundquist, D. C., and Moses, W. (2011). Remote estimation of gross primary production in maize and support for a new paradigm based on total crop chlorophyll content. *Remote Sensing of Environment*, 115(4):978–989.

Pérez-Harguindeguy, N., Diaz, S., Garnier, E., Lavorel, S., Poorter, H., Jaureguiberry, P., Bret-Harte, M. S., Cornwell, W. K., Craine, J. M., Gurvich, D. E., Urcelay, C., Veneklaas, E. J., Reich, P. B., Poorter, L., Wright, I. J., Etc., Ray, P., Etc., Díaz, S., Lavorel, S., Poorter, H., Jaureguiberry, P., Bret-Harte, M. S., Cornwell, W. K., Craine, J. M., Gurvich, D. E., Urcelay, C., Veneklaas, E. J., Reich, P. B., Poorter, L., Wright, I. J., Ray, P., Enrico, L., Pausas, J. G., de Vos, A. C., Buchmann, N., Funes, G., Quétier, F., Hodgson, J. G., Thompson, K., Morgan,

H. D., ter Steege, H., van der Heijden, M. G. A., Sack, L., Blonder, B., Poschlod, P., Vaieretti, M. V., Conti, G., Staver, A. C., Aquino, S., and Cornelissen, J. H. C. (2013). New Handbook for standardized measurment of plant functional traits worldwide. *Australian Journal of Botany*, 61(34):167–234.

Pettorelli, N., Wegmann, M., Skidmore, A., Mücher, S., Dawson, T. P., Fernandez, M., Lucas, R., Schaepman, M. E., Wang, T., O'Connor, B., Jongman, R. H., Kempeneers, P., Sonnenschein, R., Leidner, A. K., Böhm, M., He, K. S., Nagendra, H., Dubois, G., Fatoyinbo, T., Hansen, M. C., Paganini, M., de Klerk, H. M., Asner, G. P., Kerr, J. T., Estes, A. B., Schmeller, D. S., Heiden, U., Rocchini, D., Pereira, H. M., Turak, E., Fernandez, N., Lausch, A., Cho, M. A., Alcaraz-Segura, D., McGeoch, M. A., Turner, W., Mueller, A., St-Louis, V., Penner, J., Vihervaara, P., Belward, A., Reyers, B., and Geller, G. N. (2016). Framing the concept of satellite remote sensing essential biodiversity variables: challenges and future directions. *Remote Sensing in Ecology and Conservation*, (March):n/a–n/a.

Pianka, E. R. (1970). On r-and k-selection. *The American Naturalist*, 104(940):592–597.

Pierce, S., Brusa, G., Vagge, I., and Cerabolini, B. E. L. (2013). Allocating CSR plant functional types: The use of leaf economics and size traits to classify woody and herbaceous vascular plants. *Functional Ecology*, 27(4):1002–1010.

Pierce, S. and Cerabolini, B. (2018). Plant economics and size trait spectra are both explained by one theory. *The Plant Press, Milan*.

Pierce, S., Negreiros, D., Cerabolini, B. E. L., Kattge, J., Díaz, S., Kleyer, M., Shipley, B., Wright, S. J., Soudzilovskaia, N. A., Onipchenko, V. G., van Bodegom, P. M., Frenette-Dussault, C., Weiher, E., Pinho, B. X., Cornelissen, J. H. C., Grime, J. P., Thompson, K., Hunt, R., Wilson, P. J., Buffa, G., Nyakunga, O. C., Reich, P. B., Caccianiga, M., Mangili, F., Ceriani, R. M., Luzzaro, A., Brusa, G., Siefert, A., Barbosa, N. P. U., Chapin, F. S., Cornwell, W. K., Fang, J., Fernandes, G. W., Garnier, E., Le Stradic, S., Peñuelas, J., Melo, F. P. L., Slaviero, A., Tabarelli, M., and Tampucci, D. (2017). A global method for calculating plant CSR ecological strategies applied across biomes world-wide. *Functional Ecology*, 31(2):444–457.

Pons, T., Lambers, H., and Chapin III, F. (1998). Plant physiological ecology.

Poorter, H. and Garnier, E. (1999). Ecological significance of inherent variation in relative growth rate and its components. *Handbook of functional plant ecology*, 20:81–120.

Poorter, H., Niinemets, Ü., Poorter, L., Wright, I. J., and Villar, R. (2009). Causes and consequences of variation in leaf mass per area (lma): a meta-analysis. *New phytologist*, 182(3):565–588.

Poorter, L., Bongers, L., and Bongers, F. (2006). Architecture of 54 moist forest tree species: traits, trade-offs, and functional groups. *Ecology*, 87(5):1289–1301.

Rathcke, B. and Lacey, E. P. (1985). Phenological patterns of terrestrial plants. *Annual Review of Ecology and Systematics*, 16(1):179–214.

Raunkiaer, C. (1934). *The life forms of plants and statistical plant geography*. Oxford: Clarendon Press.

Reich, P. B. (2014). The world-wide 'fast-slow' plant economics spectrum: A traits manifesto. *Journal of Ecology*, 102(2):275–301.

Reich, P. B., Walters, M. B., and Ellsworth, D. S. (1997). From tropics to tundra: Global convergence in plant functioning. *Proceedings of the National Academy of Sciences*, 94(25):13730–13734.

Reich, P. B., Wright, I. J., and Lusk, C. H. (2007). Predicting leaf physiology from simple plant and climate attributes: a global glopnet analysis. *Ecological Applications*, 17(7):1982–1988.

Reichstein, M., Bahn, M., Mahecha, M. D., Kattge, J., and Baldocchi, D. D. (2014). Linking plant and ecosystem functional biogeography. *Proceedings of the National Academy of Sciences*, 111(38):13697–13702.

Richter, K., Atzberger, C., Vuolo, F., Weihs, P., and D'Urso, G. (2009). Experimental assessment of the Sentinel-2 band setting for RTM-based LAI retrieval of sugar beet and maize. *Canadian Journal of Remote Sensing*, 35(3):230–247.

Rivera, J. P., Verrelst, J., Leonenko, G., and Moreno, J. (2013). Multiple cost functions and regularization options for improved retrieval of leaf chlorophyll content and LAI through inversion of the PROSAIL model. *Remote Sensing*, 5(7):3280–3304.

Roberts, D. A., Quattrochi, D. A., Hulley, G. C., Hook, S. J., and Green, R. O. (2012). Synergies between vswir and tir data for the urban environment: An evaluation of the potential for the hyperspectral infrared imager (hyspiri) decadal survey mission. *Remote Sensing of Environment*, 117:83–101.

Root, R. B. (1967). The niche exploitation pattern of the blue-gray gnatcatcher. *Ecological monographs*, 37(4):317–350.

Ryu, Y., Sonnentag, O., Nilson, T., Vargas, R., Kobayashi, H., Wenk, R., and Baldocchi, D. D. (2010). How to quantify tree leaf area index in an open savanna ecosystem: a multi-instrument and multi-model approach. *Agricultural and Forest Meteorology*, 150(1):63–76.

Schaepman, M. E., Ustin, S. L., Plaza, A. J., Painter, T. H., Verrelst, J., and Liang, S. (2009). Earth system science related imaging spectroscopy—an assessment. *Remote Sensing of Environment*, 113:S123–S137.

Schlerf, M., Atzberger, C., and Hill, J. (2005). Remote sensing of forest biophysical variables using hymap imaging spectrometer data. *Remote Sensing of Environment*, 95(2):177–194.

Schmidt, J., Fassnacht, F. E., Förster, M., and Schmidtlein, S. (2017). Synergetic use of sentinel-1 and sentinel-2 for assessments of heathland conservation status. *Remote Sensing in Ecology and Conservation*.

Schmidtlein, S. (2005). Imaging spectroscopy as a tool for mapping Ellenberg indicator values. *Journal of Applied Ecology*, 42(5):966–974.

Schmidtlein, S., Feilhauer, H., and Bruelheide, H. (2012). Mapping plant strategy types using remote sensing. *Journal of Vegetation Science*, 23(3):395–405.

Schweiger, A. K., Schütz, M., Risch, A. C., Kneubühler, M., Haller, R., and Schaepman, M. E. (2017). How to predict plant functional types using imaging spectroscopy: Linking vegetation community traits, plant functional types and spectral response. *Methods in Ecology and Evolution*, 8(1):86–95.

Sellers, P., Dickinson, R., Randall, D., Betts, A., Hall, F., Berry, J., Collatz, G., Denning, A., Mooney, H., Nobre, C., et al. (1997). Modeling the exchanges of energy, water, and carbon between continents and the atmosphere. *Science*, 275(5299):502–509.

Si, Y., Schlerf, M., Zurita-Milla, R., Skidmore, A., and Wang, T. (2012). Mapping spatio-temporal variation of grassland quantity and quality using meris data and the prosail model. *Remote Sensing of Environment*, 121:415–425.

Sitch, S., Smith, B., Prentice, I. C., Arneth, A., Bondeau, A., Cramer, W., Kaplan, J., Levis, S., Lucht, W., Sykes, M. T., et al. (2003). Evaluation of ecosystem dynamics, plant geography and terrestrial carbon cycling in the LPJ dynamic global vegetation model. *Global Change Biology*, 9(2):161–185.

Skidmore, A. K. and Pettorelli, N. (2015). Agree on biodiversity metrics to track from space: ecologists and space agencies must forge a global monitoring strategy. *Nature*, 523(7561):403–406.

Smith, B., Prentice, I. C., and Sykes, M. T. (2001). Representation of vegetation dynamics in the modelling of terrestrial ecosystems: comparing two contrasting approaches within european climate space. *Global Ecology and Biogeography*, 10(6):621–637.

Smith, T. M., Smith, T. M., Shugart, H. H., and Woodward, F. (1997). *Plant functional types: their relevance to ecosystem properties and global change*, volume 1. Cambridge University Press.

Stefano, P., Angelo, P., Simone, P., Filomena, R., Federico, S., Tiziana, S., Umberto, A., Vincenzo, C., Acito, N., Marco, D., et al. (2013). The prisma hyperspectral mission: Science activities and opportunities for agriculture and land monitoring. In *Geoscience and Remote Sensing Symposium (IGARSS), 2013 IEEE International*, pages 4558–4561. IEEE.

Stuffler, T., Kaufmann, C., Hofer, S., Förster, K., Schreier, G., Müller, A., Eckardt, A., Bach, H., Penne, B., Benz, U., et al. (2007). The enmap hyperspectral imager - an advanced optical payload for future applications in earth observation programmes. *Acta Astronautica*, 61(1-6):115–120.

Terashima, I. and Hikosaka, K. (1995). Comparative ecophysiology of leaf and canopy photosynthesis. *Plant, Cell & Environment*, 18(10):1111–1128.

Tilman, D. (1985). The resource-ratio hypothesis of plant succession. *The American Naturalist*, 125(6):827–852.

Tilman, D. (1988). *Plant strategies and the dynamics and structure of plant communities*. Princeton University Press.

Tjoelker, M., Craine, J. M., Wedin, D., Reich, P. B., and Tilman, D. (2005). Linking leaf and root trait syndromes among 39 grassland and savannah species. *New Phytologist*, 167(2):493–508.

Trombetti, M., Riaño, D., Rubio, M., Cheng, Y., and Ustin, S. (2008). Multi-temporal vegetation canopy water content retrieval and interpretation using artificial neural networks for the continental usa. *Remote Sensing of Environment*, 112(1):203–215.

Tucker, C. J. and Sellers, P. J. (1986). Satellite remote sensing of primary production. *International Journal of Remote Sensing*, 7(11):1395–1416.

Turner, W. (2014). Sensing biodiversity. *Science*, 346(6207):301–302.

Ustin, S. L. and Gamon, J. A. (2010). Remote sensing of plant functional types. *New Phytologist*, 186(4):795–816.

van Bodegom, P. M., Douma, J. C., and Verheijen, L. M. (2014). A fully traits-based approach to modeling global vegetation distribution. *Proceedings of the National Academy of Sciences*, 111(38):13733–13738.

Van Cleemput, E., Vanierschot, L., Fernández-Castilla, B., Honnay, O., and Somers, B. (2018). The functional characterization of grass-and shrubland ecosystems using hyperspectral remote sensing: trends, accuracy and moderating variables. *Remote Sensing of Environment*, 209:747–763.

Verhoef, W. (1985). Earth observation modeling based on layer scattering matrices. *Remote Sensing of Environment*, 17(2):165–178.

Verhoef, W. and Bach, H. (2007). Coupled soil-leaf-canopy and atmosphere radiative transfer modeling to simulate hyperspectral multi-angular surface reflectance and TOA radiance data. *Remote Sensing of Environment*, 109(2):166–182.

Verrelst, J., Dethier, S., Rivera, J. P., Muñoz-Marí, J., Camps-Valls, G., and Moreno, J. (2016). Active learning methods for efficient hybrid biophysical variable retrieval. *IEEE Geoscience and Remote Sensing Letters*, 13(7):1012–1016.

Verrelst, J., Rivera, J. P., Leonenko, G., Alonso, L., and Moreno, J. (2014). Optimizing lut-based rtm inversion for semiautomatic mapping of crop biophysical parameters from sentinel-2 and-3 data: Role of cost functions. *IEEE Transactions on Geoscience and Remote Sensing*, 52(1):257–269.

Violle, C., Reich, P. B., Pacala, S. W., Enquist, B. J., and Kattge, J. (2014). The emergence and promise of functional biogeography. *Proceedings of the National Academy of Sciences*, 111(38):13690–13696.

Vohland, M. and Jarmer, T. (2008). Estimating structural and biochemical parameters for grassland from spectroradiometer data by radiative transfer modelling (prospect+ sail). *International Journal of Remote Sensing*, 29(1):191–209.

Vohland, M., Mader, S., and Dorigo, W. (2010). Applying different inversion techniques to retrieve stand variables of summer barley with prospect+ sail. *International Journal of Applied Earth Observation and Geoinformation*, 12(2):71–80.

von Humboldt, A. (1806). *Ideen zu einer Physiognomik der Gewächse*. Cotta, Tübingen.

Vuolo, F., Neugebauer, N., Bolognesi, S. F., Atzberger, C., and D'Urso, G. (2013). Estimation of leaf area index using DEIMOS-1 data: Application and transferability of a semi-empirical relationship between two agricultural areas. *Remote sensing*, 5(3):1274–1291.

Weiher, E., van der Werf, A., Thompson, K., Roderick, M., Garnier, E., and Eriksson, O. (1999). Challenging Theophrastus: A common core list of plant traits for functional ecology. *Journal of Vegetation Science*, 10(5):609–620.

Weiss, M., Baret, F., Myneni, R., Pragnère, A., and Knyazikhin, Y. (2000). Investigation of a model inversion technique to estimate canopy biophysical variables from spectral and directional reflectance data. *Agronomie*, 20(1):3–22.

West, B. J. and Shlesinger, M. (1990). The noise in natural phenomena. *American Scientist*, 78(1):40–45.

Westoby, M. (1998). A leaf-height-seed (LHS) plant ecology strategy scheme. *Plant and Soil*, 199(2):213–227.

White, M. A., de Beurs, K. M., Didan, K., Inouye, D. W., Richardson, A. D., Jensen, O. P., O'KEEFE, J., Zhang, G., Nemani, R. R., van Leeuwen, W. J., et al. (2009). Intercomparison, interpretation, and assessment of spring phenology in north america estimated from remote sensing for 1982–2006. *Global Change Biology*, 15(10):2335–2359.

Widlowski, J., Pinty, B., Gobron, N., Verstraete, M., Diner, D., and Davis, A. (2004). Canopy structure parameters derived from multi-angular remote sensing data for terrestrial carbon studies. *Climatic Change*, 67(2-3):403–415.

Widlowski, J.-L., Taberner, M., Pinty, B., Bruniquel-Pinel, V., Disney, M., Fernandes, R., Gastellu-Etchegorry, J.-P., Gobron, N., Kuusk, A., Lavergne, T., et al. (2007). Third radiation transfer model intercomparison (RAMI) exercise: Documenting progress in canopy reflectance models. *Journal of Geophysical Research: Atmospheres*, 112(D9).

Wood, S. N. (2003). Thin plate regression splines. *Journal of the Royal Statistical Society: Series B (Statistical Methodology)*, 65(1):95–114.

Wright, I. J., Reich, P. B., Westoby, M., Ackerly, D. D., Baruch, Z., Bongers, F., Cavender-Bares, J., Chapin, T., Cornelissen, J. H. C., Diemer, M., Flexas, J., Garnier, E., Groom, P. K., Gulias, J., Hikosaka, K., Lamont, B. B., Lee, T., Lee, W., Lusk, C., Midgley, J. J., Navas, M.-L., Niinemets, U., Oleksyn, J., Osada, N., Poorter, H., Poot, P., Prior, L., Pyankov, V. I., Roumet, C., Thomas, S. C., Tjoelker, M. G., Veneklaas, E. J., and Villar, R. (2004). The worldwide leaf economics spectrum. *Nature*, 428(6985):821–827.

Wullschleger, S. D., Epstein, H. E., Box, E. O., Euskirchen, E. S., Goswami, S., Iversen, C. M., Kattge, J., Norby, R. J., van Bodegom, P. M., and Xu, X. (2014). Plant functional types in earth system models: past experiences and future directions for application of dynamic vegetation models in high-latitude ecosystems. *Annals of botany*, 114(1):1–16.

Zarco-Tejada, P., Camino, C., Beck, P., Calderon, R., Hornero, A., Hernández-Clemente, R., Kattenborn, T., Montes-Borrego, M., Susca, L., Morelli, M., et al. (2018). Previsual symptoms of Xylella fastidiosa infection revealed in spectral plant-trait alterations. *Nature Plants*, page 1.

Zarco-Tejada, P., Miller, J., Morales, A., Berjón, A., and Agüera, J. (2004). Hyperspectral indices and model simulation for chlorophyll estimation in open-canopy tree crops. *Remote sensing of environment*, 90(4):463–476.

Zarco-Tejada, P., Rueda, C., and Ustin, S. (2003). Water content estimation in vegetation with MODIS reflectance data and model inversion methods. *Remote Sensing of Environment*, 85(1):109–124.

Zarco-Tejada, P. J., Miller, J. R., Noland, T. L., Mohammed, G. H., and Sampson, P. H. (2001). Scaling-up and model inversion methods with narrowband optical indices for chlorophyll content estimation in closed forest canopies with hyperspectral data. *IEEE Transactions on Geoscience and Remote Sensing*, 39(7):1491–1507.

Zheng, G. and Moskal, L. M. (2009). Retrieving Leaf Area Index (LAI) Using Remote Sensing: Theories, Methods and Sensors. *Sensors (Basel, Switzerland)*, 9(4):2719–45.

A Appendices

Appendix 1

Appendix 1.1: Compilation of plant traits for the validation of the estimated plant traits derived from the PROSAIL inversion

The implemented inversion procedure was analysed regarding its plausibility. Therefore, the estimates derived from the inversion of PROSAIL were compared to available field measurements of relevant vegetation types or species. Apart from relevant literature we also consulted the TRY-database (Kattge et al. 2011). Data was available for LAI, Cab, Car and SLA and is listed in Table A.1. The values are predominantly given as range (min - max) and if possible the average value (x) was added. In a few cases only average values or single measurements were available

Appendix 2

Appendix 2.1: Inversion of PROSPECT-D for the retrieval of chlorophyll content, carotenoid content, brown pigment content and the mesophyll structure coefficient

As a compromise between robustness and computation speed a look-up-table size of 100,000 was selected. The value ranges of each trait for the generation of the LUT is shown in Table A3. Leaf reflectance was simulated using PROSPECT-D (Feret et al. 2017). Previous studies demonstrated that wavelet analysis improves the parameter retrieval of RTM inversions (Blackburn and Ferwerda 2008; Cheng et al. 2011; Ali et al. 2015). Wavelet analysis decomposes the hyperspectral signature into frequency components at different spectral scales, which facilitates

the retrieval of the spectral features. Thus, the simulated LUT spectra with the closest correspondence to the ASD spectra were identified using continuous wavelet transformations. The wavelets were calculated using the R-package 'wmtsa' (settings: number of scales, i.e. wavelets = 8, scale range = 1 to 350). The wavelets of scale 1 to 2 were excluded as these primarily represent noise and artefacts and only the wavelets 3 to 8 were used in the analysis. To identify the closest match between the wavelet transformations of LUT and ASD spectra the RMSE was used as cost function. The final estimates for each trait were derived by selecting the 20 LUT entries which resulted in the smallest RMSE. As proposed by Vohland et al. (2010) the trait values of these LUT entries where weighted according to their RMSE value and subsequently averaged.

The validation of the above described inversion procedure was performed using the ANGERS leaf optical properties database, which was acquired in 2003 at INRA, France (Jacquemoud et al. 2003b). The data base contains 276 leaf reflectance spectra (400-2450nm) for 43 different species as well as reference values of inter alia chlorophyll (a+b) content [µg/cm^2], carotenoid content [µg/cm^2] and mesophyll structure coefficient. After applying the inversion on the leaf spectra the accuracy of the trait was assessed using the r^2 and NRMSE (see Tab. A.3). A validation of the estimated brown pigment content was not possible, since the ANGERS dataset does not contain respective reference values. However, the relatively accurate retrieval of chlorophyll content, carotenoid content and the mesophyll structure coefficient indicate the overall robustness of the inversion procedure.

Table A.2: The range of each parameter for the inversion of leaf spectra using PROSPECT-D.

PROSPECT-D parameter/ Trait	**Abbrev.**	**Min**	**Max**
Chlorophyll content [µg/cm^2]	Cab	1	110
Carotenoid content [µg/cm^2]	Car	1	26
Mesophyll structure coefficient [ ]	N	1	2.8
Dry matter content [g/cm^2]	Cm	0.0015	0.033
water content [g/cm^2]	Cw	0.004	0.055
Brown pigment content [ ]	Cbrown	0.0	0.4

Table A.3: Validation of the PROSPECT inversion procedure for chlorophyll content, carotenoid content and mesophyll structure coefficient using the ANGERS leaf optical properties database.

PROSPECT-D parameter/ Trait	**r^2**	**NRMSE [%]**
Chlorophyll content [µg/cm^2]	0.91	7.91
Carotenoid content [µg/cm^2]	0.66	15.1
Mesophyll structure coefficient [ ]	0.77	11.6

We carried out an additional validation of the chlorophyll and carotenoids retrieval using UV-VIS spectroscopy as described in Lichtenthaler (1987). Due to resource constrains this procedure could only be performed for a single date and 20 samples of 9 different species. We compared the chlorophyll and carotenoid contents determined this way to the respective contents retrieved from the above described inversion (PROSPECT-D) procedure. The r^2 and NMRSE [%] between inverted and reference pigment content was 0.85 and 10.5% for chlorophyll and 0.7 and 15% for carotenoids.

Appendix 2.2: Statistical summary of the sampled plant traits

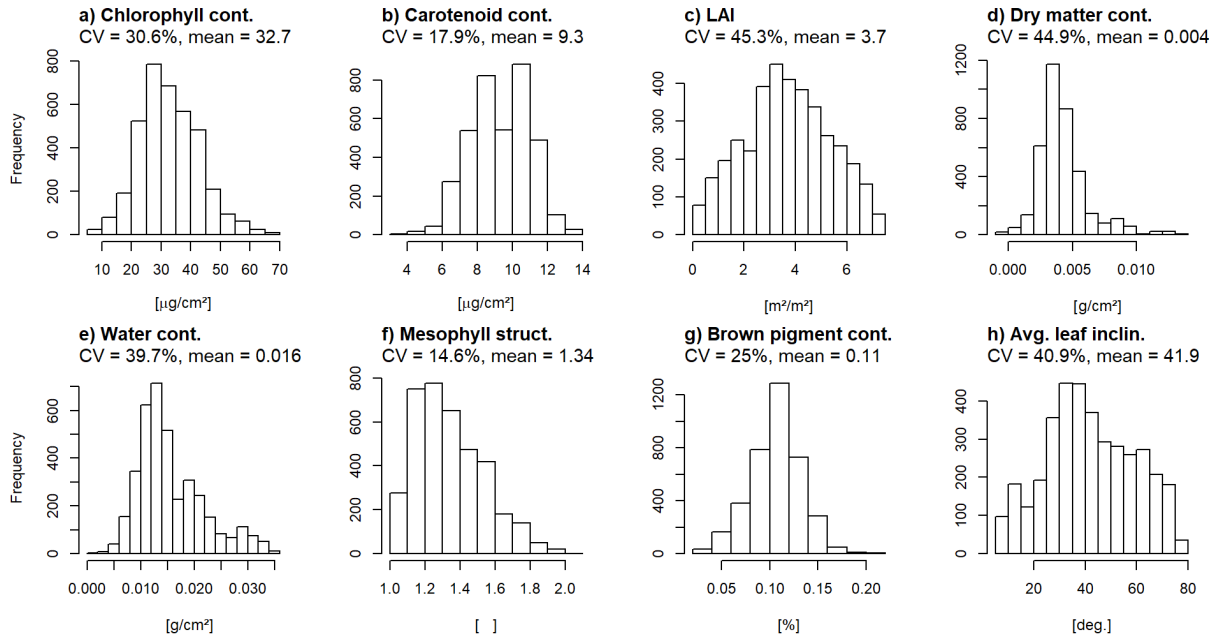

Figure A.1: Histograms of the sampled trait values that were used as input for PROSAIL to simulate canopy reflectance. The histograms, mean and coefficient of variation (CV) are based on the trait values across all species.

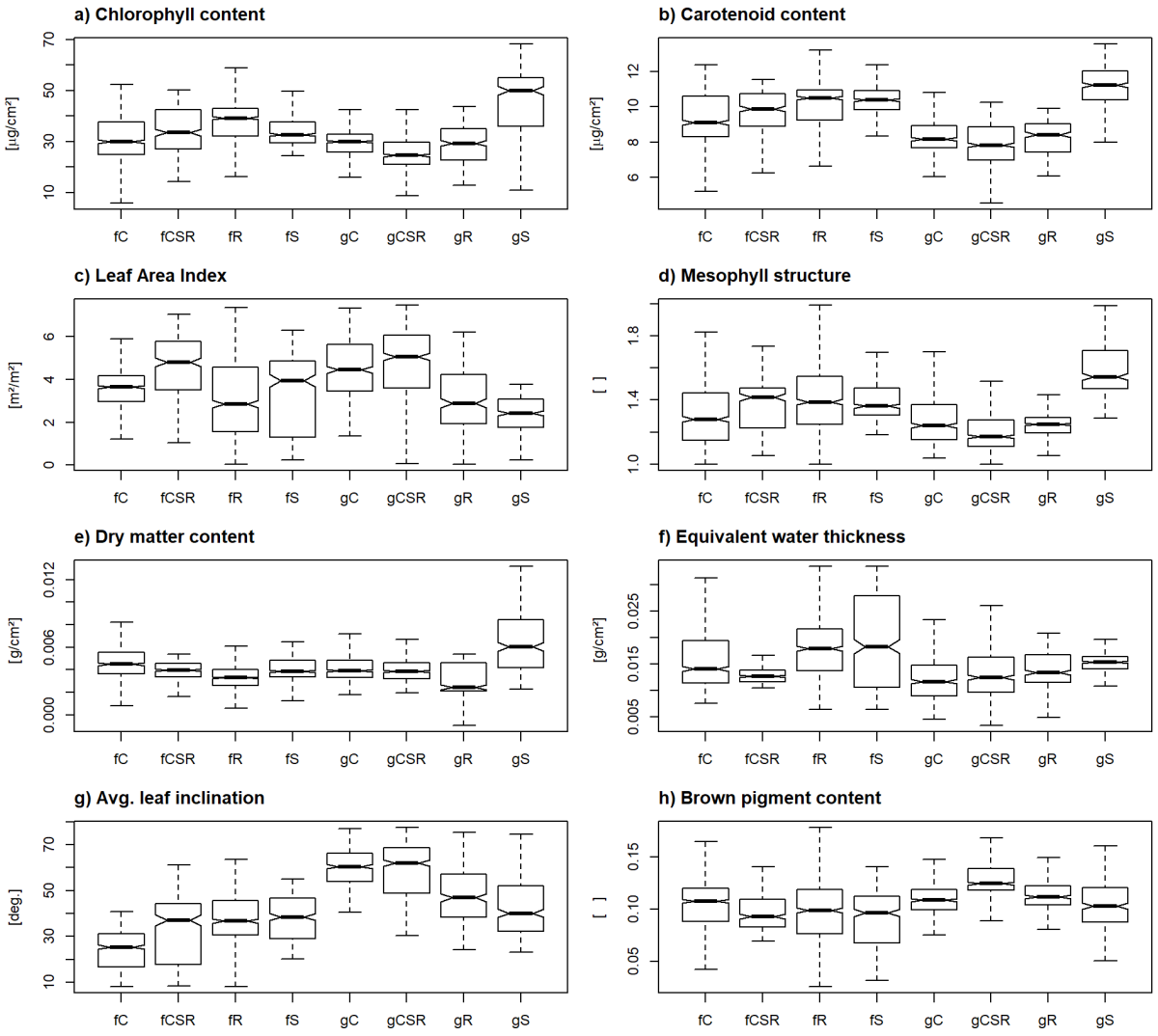

Figure A.2: Sampled trait values for each PFT that were used as input for PROSAIL to simulate canopy reflectance. Notches have been added to each bar to indicate significant differences among classes (Chambers 1983). The full names of the PFT classes are given in Tab. 3.1.

Appendix 2.3: Pre-processing of the trait data

For smoothing of the time series, we calculated median trait values for each individual species (4 repetitions per species) and time-step. Subsequently the phenology of each species was modelled using a quadratic regression (second order) on the species specific median values, which were found to be well suited to model phenology of herbaceous vegetation in temperate climates (de Beurs and Henebry 2005). The applicability of this procedure was further justified by a Saphiro-Wilk-Test on the residuals, which indicated that 169 of the 175 quadratic regression models complied with a normality of the distribution ($p < 0.001$).

Out of these trait expressions we randomly generated trait combinations for each PFT (in total 1,000 combinations for each PFT). For the respective species belonging to that PFT and its phenological state, we sampled trait expressions from a range defined by the median absolute deviation (MAD) of the fitted quadratic regression. For instance the sampling of competitive graminoids (gC, compare Fig. 3.1) was based on 1) selecting a species which belongs to competitive graminoids, 2) randomly selecting a point in the time series (phenological state) where all traits values are to be sampled and 3) sampling a value for each trait at this time step within the trait and species specific plasticity. The plasticity of the species-specific leaf inclination distribution, which was only assessed once, was considered by drawing samples around the median of the species leaf angle measurements in a range defined by the species-specific MAD.

Appendix 2.4: Generation of radiometric noise

1/f-noise was individually generated for each spectrum (R-function TK95, Package 'RobPer'). The frequency (f) was randomly sampled from 0 (white noise) to 2 (brown noise). The generated noise vector was scaled to the standard radiometric uncertainty expected for EnMAP (Bachmann et al. 2015), i.e. 0.2%-0.1% reflectance in the VIS (400-749 nm), 0.5%-2% in the NIR (750-1399) nm and 0.25%-1.5% in the SWIR (1400-2500 nm), and subsequently added to the simulated spectra.

Appendix 3

Appendix 3.1: Inversion of PROSPECT-D for the retrieval of chlorophyll$_{area}$, carotenoid$_{area}$, anthocyannin$_{area}$, Cbrown and N$_{meso}$

As a compromise between robustness and computation speed we selected a look-up-table size of 100,000. The range of each trait for the generation of the LUT is shown in Table A.2. We simulated spectra using PROSPECT-D (Feret et al. 2017). Previous studies demonstrated that wavelet analysis improves the parameter retrieval of RTM inversions (Blackburn and Ferwerda

2008; Cheng et al. 2011; Ali et al. 2015). Wavelet analysis decomposes the hyperspectral signature into frequency components at different spectral scales, which facilitates the retrieval of the spectral features. Thus, we identified the simulated LUT spectra with the closest correspondence to the ASD spectra using continuous wavelet transformations. The wavelets were calculated using the R-package 'wmtsa' (settings: number of scales, i.e. wavelets = 8, scale range = 1 to 350). We excluded the wavelets of scale 1 to 3 as these primarily represent noise and artefacts and only used the wavelets 4 to 8 in the analysis. To identify the closest match between the wavelet transformations of LUT and ASD spectra we used the RMSE as cost function. We derived the final estimates for each trait by selecting the 20 LUT entries which resulted in the smallest RMSE. As proposed by (Vohland et al. 2010) we weighted and subsequently averaged the trait values of these LUT entries according to their RMSE value. We validated the above described inversion procedure using the ANGERS leaf optical properties database, which was acquired in 2003 at INRA, France (Jacquemoud et al. 2003b). The data base contains 276 leaf reflectance spectra (400-2450nm) for 43 different species as well as reference values of inter alia chlorophyll (a+b) content [µg/cm^2], carotenoid content [µg/cm^2] and N_{meso}. After applying the inversion on the leaf spectra the accuracy of the trait was assessed using the R^2 and NRMSE (see Tab. A.5) A validation of the estimated brown pigment content was not possible, since the LOPEX dataset does not contain respective reference values. However, the relatively accurate retrieval of chlorophyll content, carotenoid content and the mesophyll structure coefficient indicate the overall robustness of the inversion procedure.

Table A.4: The range of each parameter for the inversion of leaf spectra using PROSPECT-D.

PROSPECT-D parameter/ Trait	**Abbrev.**	**Min**	**Max**
Chlorophyll content [µg/cm^2]	Cab_{area}	1	110
Carotenoid content [µg/cm^2]	Car_{area}	1	26
Anthocyannin content [µg/cm^2]	Ant_{area}	0.1	4
Mesophyll structure coefficient [ ]	N_{meso}	1	2.8
Dry matter content [g/cm^2]	Cm	0.0015	0.033
Water content [g/cm^2]	Cw	0.004	0.055
Brown pigment content [ ]	Cbrown	0.0	0.4

Table A.5: Validation of the PROSPECT inversion procedure for chlorophyll$_{area}$, carotenoid$_{area}$ and N_{meso} coefficient using the ANGERS leaf optical properties database.

PROSPECT-D parameter/ Trait	**r^2**	**NRMSE [%]**
Chlorophyll content [µg/cm^2]	0.91	7.91
Carotenoid content [µg/cm^2]	0.66	15.1
Mesophyll structure coefficient [ ]	0.77	11.6

Appendix 3.2: Statistical summary of the measured traits implemented in PROSAIL and derivates thereof

Table A.6: Statistical summary of the measured traits implemented in PROSAIL and derivates.

Trait [unit]	**min**	**max**	**mean**	**median**	**sd**
ALA [°]	11.325	70.115	42.847	43.252	15.86
LAI [m^2/m^2]	1.096	8.758	5.311	5.428	1.79
LMA [g/cm^2]	1.759	8.923	4.319	4.097	1.658
EWT [g/cm^2]	0.009	0.046	0.016	0.014	0.007
LDMC [%]	0.102	0.379	0.216	0.217	0.061
Cab$_{area}$ [µg/cm^2]	19.73	54.505	32.349	30.376	8.022
Car$_{area}$ [µg/cm^2]	6.695	12.188	9.256	8.944	1.39
Ant$_{area}$ [µg/cm^2]	0.716	2.188	1.241	1.249	0.325
LMA$_{canopy}$ [g/m^2]	40.023	510.496	220.278	200.566	100.776
EWT$_{canopy}$ [g/m^2]	0.012	0.239	0.082	0.072	0.044
Cab$_{mass}$ [%]	3.854	28.041	9.493	8.111	4.904
Car$_{mass}$ [%]	1.024	7.12	2.716	2.432	1.279
Ant$_{mass}$ [%]	0.123	1.197	0.371	0.353	0.209
fAPAR [%]	0.595	0.967	0.933	0.956	0.066
APAR$_{cum}$ [kWh/m^2]	2.34	23.802	14.997	15.822	5.446
Cbown [-]	0.047	0.137	0.107	0.109	0.021
N_{meso} [-]	1.107	1.723	1.343	1.302	0.178

Appendix 3.3: Derivation of fAPAR and APAR$_{cum}$

For each species we simulated fAPAR using the radiative transfer model PROSAIL parametrized with the retrieved trait expressions. fAPAR was calculated based on the method provided in (Verhoef and Bach 2007) and the following formula:

$$\mathrm{fAPAR} = \frac{1}{24}\sum_{\Theta=1}^{24}\frac{\sum_{400}^{700}\alpha_{s_\Theta} * E_{sun_\Theta} + \alpha_{d_\Theta} * E_{sky_\Theta}}{\sum_{400}^{700} E_{sun_\Theta} + E_{sky_\Theta}} \quad \text{eqn A3-1}$$

$$\alpha_s = 1 - r_{sd} - \tau_{sd} - \tau_{ss} \quad \text{eqn A3-2}$$

$$\alpha_d = 1 - r_{sd} - \tau_{dd} \quad \text{eqn A3-3}$$

where E_{sun} is the solar irradiance at ground level, E_{sky} is the sky irradiance at ground level, rsd is the soil surface reflectance, τsd is the directional-hemispherical transmittance for solar flux, τss is the direct transmittance for solar flux and τdd is the bi-hemispherical transmittance. For simplicity fAPAR was integrated for the course of a day in central Germany (01st August, Lat. 48°, Long. 8°). $APAR_{cum}$ was derived from fAPAR, photosynthetic active radiation (PAR) [kWh/m^2] and the number of growing days for each cultivated species. Hourly PAR values were derived from the default radiation albedos (E_{sun} and E_{sky}) in PROSAIL (400-700 nm) scaled with averaged direct and diffuse radiation for April-October (2016, Lat. 48°, Long. 8°) assessed from Helios-3 archives (Espinar et al. 2012).

$$\mathrm{APAR_{cum}} = d_{growth} * \sum_{\Theta=1}^{24} \mathrm{fAPAR}_\Theta * (\mathrm{PAR}_{sun_\Theta} + \mathrm{PAR}_{sky_\Theta}) \quad \text{eqn A3-4}$$

where d_{growth} is the number of growing days, θ is the sun angle at a given hour of the day, PAR_{sun_θ} and PAR_{sky_θ} are the direct and diffuse photosynthetic active radiation, respectively.

Appendix 3.4: Species and traits considered in the LES analysis

Aegopodium podagraria, Anthyllis vulneraria, Anthoxanthum odoratum, Alopecurus pratensis, Arctium lappa, Arrhenatherum elatius, Calamagrostis epigejos, Campanula rotundifolia, Centaurium erythraea, Cirsium acaule, Cirsium arvense, Geranium pretense, Geranium robertianum, Festuca ovina, Holcus lanatus, Molinia caerulea, Nardus stricta, Phalaris arundinaceae, Plantago major, Poa annua, Trifolium pretense, Trisetum flavescens, Stellaria media, Succisa pratensis, Urtica dioica

Appendix 3.5: Correlation of optical plant traits and the Leaf Economic Spectrum

Table A.7: The correlation (Pearson's r) between each optical trait and the Leaf Economic Spectrum

Trait	**r trait~LES**	**p-value**
ALA	-0.21	0.308
LAI	0.07	0.752
LMA	-0.68	0.000
EWT	-0.31	0.131
LDMC	-0.28	0.178
Cab_{area}	-0.45	0.023
Car_{area}	-0.44	0.028
Ant_{area}	-0.00	0.992
LMA_{canopy}	-0.36	0.079
EWT_{canopy}	-0.22	0.293
Cab_{mass}	0.42	0.037
Car_{mass}	0.53	0.006
Ant_{mass}	0.52	0.008
fAPAR	0.04	0.841
$APAR_{cum}$	0.23	0.258
Cbrown	0.32	0.114
N_{meso}	-0.4	0.046

Appendix 3.6: Relationship of optical traits and CSR plant strategies

Table A.8: Adjusted R^2 and p-values of the relationship between the CSR feature space and plant traits derived using generalized additive models for all species (n=45), graminoids (n=19) and forbs (n=26).

Trait	R^2_{adj} all	p all	R^2_{adj} grass	p grass	R^2_{adj} forb	p forb
ALA	-0.06	0.891	-0.34	0.844	0.33	0.216
LAI	0.36	0.001	0.6	0.055	0.45	0.018
LMA	0.42	0.000	0.73	0.008	0.48	0.013
EWT	-0.14	0.928	0.01	0.567	-0.12	0.962
LDMC	0.43	0.003	0.34	0.025	0.4	0.003
Cab_{area}	0.2	0.088	0.52	0.006	0.29	0.088
Car_{area}	0.11	0.159	0.41	0.68	0.22	0.147
Ant_{area}	0.19	0.048	0.4	0.092	0.22	0.146
LMA_{canopy}	0.43	0.000	0.39	0.018	0.4	0.031
EWT_{canopy}	0.02	0.401	0.07	0.433	-0.06	0.69
Cab_{mass}	0.57	0.000	0.47	0.074	0.67	0.000
Car_{mass}	0.55	0.000	0.47	0.074	0.67	0.002
Ant_{mass}	0.37	0.003	0.41	0.134	0.44	0.031
Cbrown	-0.9	0.777	0.46	0.107	-0.08	0.791
N_{meso}	0.08	0.101	0.29	0.045	-0.09	0.919
fAPAR	0.37	0.002	0.68	0.017	0.63	0.001
$APAR_{cum}$	0.57	0.000	0.57	0.001	0.57	0.000

Appendix 3.7: N_{meso} and Cbrown gradients across graminoid growth forms

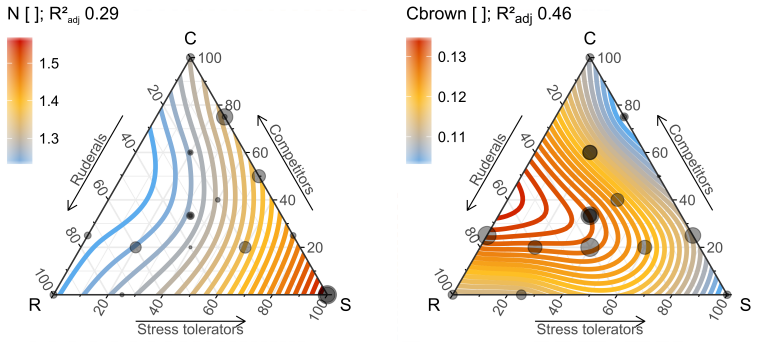

Figure A.3: Distribution of mesophyll thickness (N_{meso}) and Brown pigment content (Cbrown) across graminoid CSR strategies based on GAM extrapolations. Observations are displayed as transparent grey dots with a size proportional to the respective trait.

Appendix 3.8: Null model of $pigment_{mass}$ vs CSR plant strategies

The information content of $pigment_{mass}$ was assessed using a null model, that involved random sampling of $pigment_{area}$ values within the range of the in-situ measurements, which were subsequently mass-normalized (divided by LMA). As shown in Figure A.4 the resulting artificial $pigment_{mass}$ values and their relation to CSR plant strategies show a great correspondence to the actual values of $pigment_{mass}$, indicating that $pigments_{mass}$ primarily reflects variation in LMA.

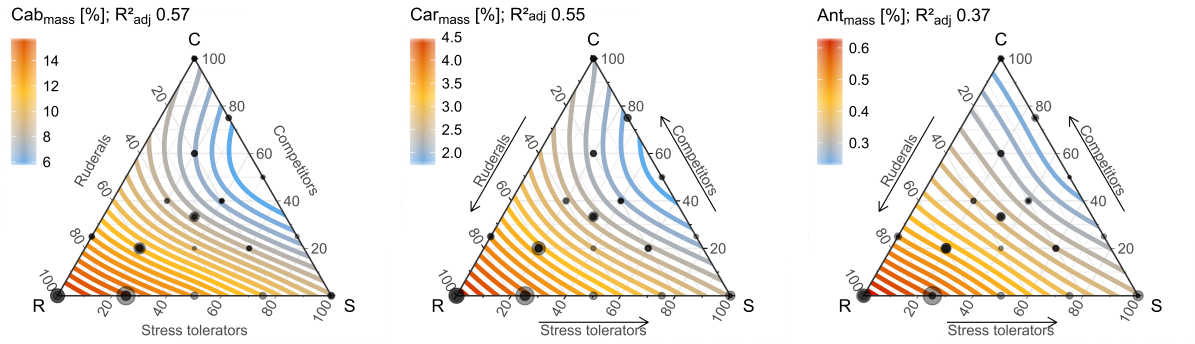

Figure A.4: Distribution of $pigments_{mass}$ across CSR strategies (graminoids and forbs) based on GAM extrapolations. Observations are displayed as transparent grey dots with a size proportional to the respective trait.

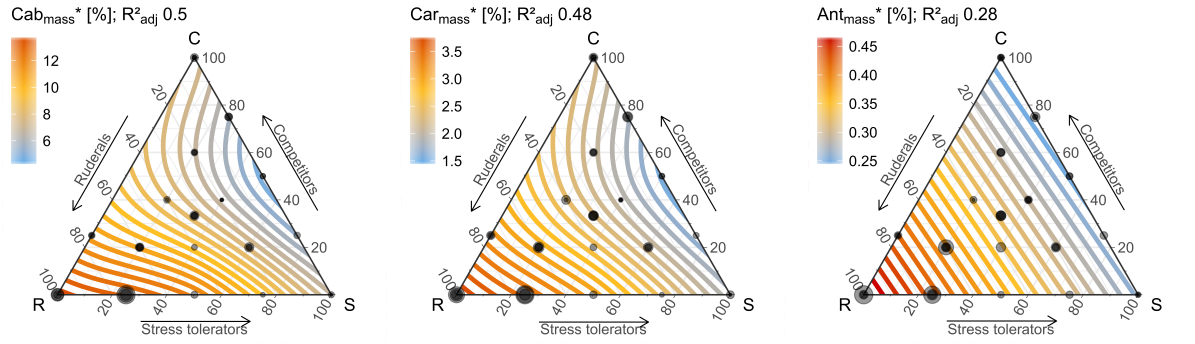

Figure A.5: Distribution of $pigments_{mass}$ derived from the null model across CSR strategies (graminoids and forbs) based on GAM extrapolations. Observations are displayed as transparent grey dots with a size proportional to the respective trait.

Appendix 3.9: Null model of $pigment_{mass}$ vs Leaf Economic Spectrum

The information content of $pigments_{mass}$ was assessed using a null model, that involved random sampling of $pigments_{area}$ values within the range of the in-situ measurements, which

were subsequently mass-normalized (divided by LMA). As shown in figure A.6 the resulting $pigments_{mass}$ values and its relation to the LES show a great correspondence to the actual values of $pigments_{mass}$, indicating that $pigments_{mass}$ primarily reflects variation in LMA.

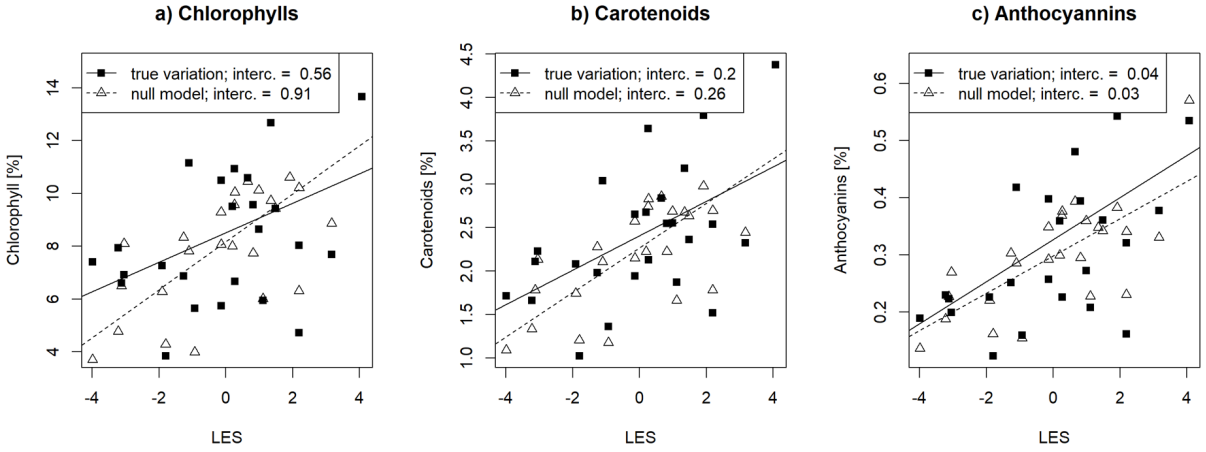

Figure A.6: The relation of original and artificial (null-model) $pigment_{mass}$ values towards the Leaf Economic Spectrum.

Table A.1: Plant traits for the validation of the estimated plant traits derived from the PROSAIL inversion

Parameter	**LAI [m^2/m^2]**	**Cab [$\mu g/cm^2$]**	**SLA [m^2/kg]**
Natural grassland		29.1-60.8 (Klančnik et al. 2014)	12.5 - 22.2
Semi natural grassland	2.9-5.4 (Vohland and Jarmer 2008); 0.4-6.8, 3.06 (x) (Si et al. 2012); 1.5-7.4, 3.6 (x) (Asam et al. (2015))	31.3-39.0 (Vohland and Jarmer 2008); 14.6-37.3 (Si et al. 2012)	
Herbs		12.8-36.1 (Hallik et al. 2009)	11.8 - 20 (Poorter et al. (2009))
Sedges		55.9 (x) (Klančnik et al. 2014)	
Spring wheat		41.9-65.3 (Ommen et al. 1999)	
Swamps / marhes / meadows	3.6-7.0 (Larcher 2003)	30.0 (x) (Larcher 2003)	
Herbs / grassland	0.7-7.5, 2.9 (x) (Cao 2000)	18.9-40.9, 28.7 (x) (Darvishzadeh et al. 2011)	5.1-8.7 (Poorter et al. 2009)
Heathland	0.9-5.0 (Aerts and Berendse 1988)		
Calluna vulgaris			5.8-24.9, 11.9 (x) (Aerts and Berendse 1988)
Calluna vulgaris, pioneer		27.0-27.9 (Brown and Macfadyen 1969)	
Calluna vulgaris, mature		46.1-50.6 (Brown and Macfadyen 1969)	
Trichophorum caespitosum			15.6 (x) (Kleyer et al. 2008)
Molinia caerulea	2.1 (Gond et al. 1999)	3.0-25.5, 16.7 (x) (Medlyn et al. 1999); ; 42.1 (Kattge et al. 2011) 12-25 (Gond et al. 1999)	7.8-30.9, 19.5 (x) (Aerts and Berendse 1988) 7.8-30.9, 19.5 (x) (Aerts and Berendse 1988)
Phragmites australis		42.1 (Kattge et al. 2011); 12-25 (Gond et al. 1999)	7.7-24.9, 14.4 (x) (Medlyn et al. 1999)

Eidesstattliche Versicherung

Eidesstattliche Versicherung gemäß § 6 Abs. 1 Ziff. 4 der Promotionsordnung des Karlsruher Instituts für Technologie für die Fakultät für Bauingenieur-, Geo- und Umweltwissenschaften

1. Bei der eingereichten Dissertation zu dem Thema Linking Canopy Reflectance and Plant Functioning through Canopy Radiative Transfer Models handelt es sich um meine eigenständig erbrachte Leistung.

2. Ich habe nur die angegebenen Quellen und Hilfsmittel benutzt und mich keiner unzulässigen Hilfe Dritter bedient. Insbesondere habe ich wörtlich oder sinngemäß aus anderen Werken übernommene Inhalte als solche kenntlich gemacht.

3. Die Arbeit oder Teile davon habe ich wie folgt/ bislang nicht* an einer Hochschule des In- oder Auslands als Bestandteil einer Prüfungs- oder Qualifikationsleistung vorgelegt.

Titel der Arbeit: *Linking Canopy Reflectance and Plant Functioning through Canopy Radiative Transfer Models*

Hochschule und Jahr: *Karlsruher Institute für Technologie, 2018*

Art der Prüfungs- oder Qualifikationsleistung: *Dissertation*

4. Die Richtigkeit der vorstehenden Erklärungen bestätige ich.

5. Die Bedeutung der eidesstattlichen Versicherung und die strafrechtlichen Folgen einer unrichtigen oder unvollständigen eidesstattlichen Versicherung sind mir bekannt.

Ich versichere an Eides statt, dass ich nach bestem Wissen die reine Wahrheit erklärt und nichts verschwiegen habe.

Ort und Datum Unterschrift

Eidesstattliche Versicherung

Belehrung

Die Universitäten in Baden-Württemberg verlangen eine Eidesstattliche Versicherung über die Eigenständigkeit der erbrachten wissenschaftlichen Leistungen, um sich glaubhaft zu versichern, dass der Promovend die wissenschaftlichen Leistungen eigenständig erbracht hat.

Weil der Gesetzgeber der Eidesstattlichen Versicherung eine besondere Bedeutung beimisst und sie erhebliche Folgen haben kann, hat der Gesetzgeber die Abgabe einer falschen eidesstattlichen Versicherung unter Strafe gestellt. Bei vorsätzlicher (also wissentlicher) Abgabe einer falschen Erklärung droht eine Freiheitsstrafe bis zu drei Jahren oder eine Geldstrafe.

Eine fahrlässige Abgabe (also Abgabe, obwohl Sie hätten erkennen müssen, dass die Erklärung nicht den Tatsachen entspricht) kann eine Freiheitsstrafe bis zu einem Jahr oder eine Geldstrafe nach sich ziehen.

Die entsprechenden Strafvorschriften sind in § 156 StGB (falsche Versicherung an Eides Statt)und in § 161 StGB (fahrlässiger Falscheid, fahrlässige falsche Versicherung an Eides Statt) wiedergegeben.

§ 156 StGB: Falsche Versicherung an Eides Statt
Wer vor einer zur Abnahme einer Versicherung an Eides Statt zuständigen Behörde eine solche Versicherung falsch abgibt oder unter Berufung auf eine solche Versicherung falsch aussagt, wird mit Freiheitsstrafe bis zu drei Jahren oder mit Geldstrafe bestraft.

§ 161 StGB: Fahrlässiger Falscheid, fahrlässige falsche Versicherung an Eides Statt
Abs. 1: Wenn eine der in den § 154 bis 156 bezeichneten Handlungen aus Fahrlässigkeit begangen worden ist, so tritt Freiheitsstrafe bis zu einem Jahr oder Geldstrafe ein. Abs. 2: Straflosigkeit tritt ein, wenn der Täter die falsche Angabe rechtzeitig berichtigt. Die Vorschriften des § 158 Abs. 2 und 3 gelten entsprechend.

Ort und Datum Unterschrift